OFFICE OF CIVILIAN RADIOACTIVE WASTE MANAGEMENT
SPECIAL INSTRUCTION SHEET

1. QA: QA

Complete Only Applicable Items

This is a placeholder page for records that cannot be scanned or microfilmed

2. Record Date	3. Accession Number
09/28/2000	MOL.20001016.0008
4. Author Name(s)	**5. Author Organization**
HARLAN W. STOCKMAN	N/A

6. Title
IN-DRIFT ACCUMULATION OF FISSLE MATERIAL FROM WASTE PACKAGE CONTAINING PLUTONIUM DISPOSITION WASTE FORMS

7. Document Number(s)	8. Version
CAL-EDC-GS-000001	REV. 00
9. Document Type	**10. Medium**
REPORT	OPTIC/PAPER

11. Access Control Code
PUB

12. Traceability Designator
DC #22013

13. Comments
THIS IS A ONE-OF-A-KIND DOCUMENT DUE TO THE COLORED GRAPHS ENCLOSED AND CAN BE LOCATED THROUGH THE RPC

OFFICE OF CIVILIAN RADIOACTIVE WASTE MANAGEMENT
CALCULATION COVER SHEET

1. QA: QA
Page: 1 Of: 53

2. Calculation Title
In-Drift Accumulation of Fissile Material from Waste Packages Containing Plutonium Disposition Waste Forms

3. Document Identifier (including Revision Number)
CAL-EDC-GS-000001 REV 00

4. Total Attachments	5. Attachment Numbers – Number of pages in each
2	I-16, II-(2 compact disks)

	Print Name	Signature	Date
6. Originator	Harlan W. Stockman Susan LeStrange	Peter Gottlieb (for Harlan Stockman) Peter Gottlieb (for Susan LeStrange)	9/13/00
7. Checker	Terry Steinborn		9/13/00
8. Lead	Peter Gottlieb	Peter Gottlieb	9/28/2000

9. Remarks

Revision History

10. Revision No.	11. Description of Revision
REV 00	Initial Issue

CONTENTS

Page

FIGURES

Page

TABLES

Page

1. PURPOSE

The objective of this calculation is to provide estimates of the amount of fissile material flowing out of the waste package (source term) and the accumulation of fissile elements (U and Pu) in a crushed-tuff invert. These calculations provide input for the analysis of repository impacts of the Pu-ceramic waste forms. In particular, the source term results are used as input to the far-field accumulation calculation reported in Ref. 51, and the in-drift accumulation results are used as inputs for the criticality calculations reported in Ref. 2. The results are also summarized and interpreted in Ref. 52.

The scope of this calculation is the waste package (WP) Viability Assessment (VA) design, which consists of an outer corrosion-allowance material (CAM) and an inner corrosion-resistant material (CRM). This design is used in this calculation in order to be consistent with earlier Pu-ceramic degradation calculations (Ref. 15). The impact of the new Enhanced Design Alternative-II (EDA-II) design on the results will be addressed in a subsequent report. The design of the invert (a leveling foundation, which creates a level surface of the drift floor and supports the WP mounting structure) is consistent with the EDA-II design. The invert will be composed of crushed stone and a steel support structure (Ref. 17).

The scope of this calculation is also defined by the nominal degradation scenario, which involves the breach of the WP (Section 10.5.1.2, Ref. 48), followed by the influx of water. Water in the WP may, in time, gradually leach the fissile components and neutron absorbers out of the ceramic waste forms. Thus, the water in the WP may become laden with dissolved actinides (e.g., Pu and U), and may eventually overflow or leak from the WP. Once the water leaves the WP, it may encounter the invert, in which the actinides may reprecipitate. Several factors could induce reprecipitation; these factors include: the high surface area of the crushed stone, and the presence of reactive components in the stone (such as calcium and silica); the contrasting chemistry of water trapped in the pores of the invert; and the possible presence of reducing materials in the support structure. This calculation estimates the amounts of Pu and U that may accumulate in the invert as a consequence of chemical precipitation.

The degradation scenario is consistent with the overall degradation analysis methodology outlined in Section 3.1 of the Disposal Criticality Analysis Methodology Topical Report (Ref. 47). Specifically, the scenario NF-1b of Figure 3-2a of that document prescribes the processes analyzed in this calculation. The only difference is that the present calculation extends the possibilities of in-drift interacting materials to include incompletely oxidized iron, which was not a major constituent of the drift at the time the Topical Report was written.

This calculation was prepared in accordance with the administrative procedure AP-3.12Q, *Calculations*, Ref. 53. It was specifically requested and guided by the development plan TDP-DDC-MD-000001 (Ref. 54, items 4 and 5).

2. METHOD

The first step of the method of this calculation consists of using a geochemistry code to calculate the concentration of fissile elements in the solution inside the waste package as these elements are released from the degrading waste form. The second step uses the concentration of fissile elements in the solution flowing out of the waste package as the source term for geochemistry calculations of the precipitation of these fissile elements in the drift.

The EQ6 code (Section 4.1) was used to perform reaction path runs that simulate the reaction of water with components of a WP, and subsequent reaction of the water with a crushed-tuff invert. The 7.2bLV version can simulate decay of ^{239}Pu to ^{235}U, and the code can pass a time-varying solution composition from one reaction path run to a successive run. The code retains the solid-centered flow-through (SCFT) mode developed in the previous Addendum to EQ6 (Ref. 14).

The User's Manual for 7.2bLV (Ref. 49, Sections 2.2 through 2.4 and Appendices A through C) provides a detailed example that is very similar to the EQ6 runs described in this calculation. The process is shown schematically in Figure 2-1. It should be noted that the nominal output files from the two runs (reflecting the two steps in the methodology) have identical names, because they represent the use of the same program, although in different ways. These files are always renamed by the postprocessor so that the individual case runs are always distinct.

Each run represents a physical portion of space, referred to as a cell. All the cells use the SCFT mode, so that a drop of water entering the "top" of one cell displaces an equal volume of water out the "bottom" of the cell. That displaced drop then enters the second cell, where it displaces an equal volume out the bottom of the second cell. Each cell contains reactants that are initially out of equilibrium with the solids in the cell; in the WP cell, these reactants include the steels, high-level waste (HLW) glass, and the Pu-ceramic disks. The incremental addition of these reactants by EQ6, and consequent reaction with the aqueous phase, simulates the corrosion of the WP components. In the invert, the reactants include the tuff minerals, and (in some runs) rust from the partially-oxidized steel support structure. The reactants in the WP and invert systems degrade by constant rates, or by rates that incorporate a pH-dependent, transition state theory (TST) formalism (Section 3.3.3 in Ref. 46).

This calculation used version 7.2bLV (Ref. 22) of EQ6 (Refs. 44, 23, 45, and 46). This code will hereafter be referred to as EQ6 and "7.2bLV;" the latter nomenclature will be used when the discussion utilizes methodologies unique to this specific version.

The tight coupling achieved by passing a time-varying solution from the WP cell to the invert cell obviates the need to assume a single "worst case" composition for water percolating through the invert.

Throughout this calculation, **`bold courier`** type is used to indicate file names, program or macro variables, and input parameters in EQ6. The output files from the individual cases are listed in the two compact disks (CDs) of Attachment II. The control of the electronic

management of data was evaluated in accordance with AP-SV.1Q, *Control of the Electronic Management of Information* (Ref. 58). The evaluation (Ref. 20) determined that current work processes and procedures are adequate for the control of electronic management of data for this activity.

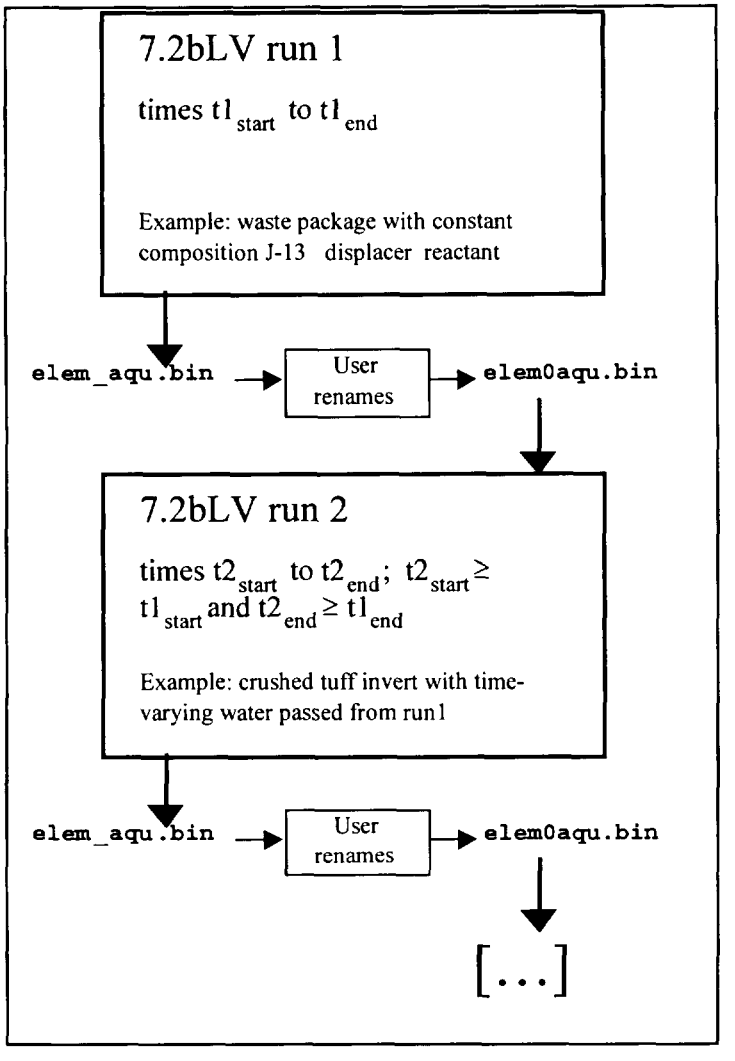

Figure 2-1. Coupling of 7.2bLV Runs

3. ASSUMPTIONS

All assumptions are used throughout Section 5 and Section 6.

3.1 It is assumed that an aqueous solution fills all voids within WPs, and that the solutions that drip into the WP will have a composition approximating that of the J-13 well water for ~106 years. The basis for the first part of this assumption is that it provides the maximum degradation rate for each reactant with the potential for the fastest flushing of the neutron absorber from the WP, and is thereby conservative. The basis for the second part of the assumption is that the groundwater composition is controlled largely by transport through the host rock, over pathways of hundreds of meters, and the host rock composition is not expected to change substantially over 106 years. For a few thousand years after waste emplacement, the composition may differ because of perturbations resulting from reactions with engineered materials and from the thermal pulse. These perturbations are not taken into account in this calculation because the CAM and CRM are not expected to breach until after that perturbed period. Therefore, the early perturbation is not relevant to the calculations reported in this document. See Assumption 3.3. The concentration of the major constituents of J-13 well water is given in Ref. 57; the concentration of Li, B, and PO4 is given in Table 4.2 of Ref. 29; and, the concentration of Fe, Mn, and Al is given in Table 5-4 of Ref. 15. (The J-13-like compositions are hereafter referred to as "in-dripping water", or "J-13-like water," rather than "J-13 well water", to distinguish the idealized compositions from actual well water samples.)

3.2 The assumption that the water entering the WP can be approximated by the J-13-like water implicitly assumes that the in-dripping water will have only a minimal contact, if any at all, with undegraded metal in the corrosion allowance barrier. The basis for the assumption is that the water will move sufficiently rapidly through openings in the WP barriers such that its residence time in the corroded barrier will be too short for significant reaction to occur, and the corrosion products lining the cracks should consist primarily of inert Fe oxides. In addition, recent evaluations of codisposal WPs show that degradation of the WP materials (specifically, HLW and steel) overwhelms the native chemistry of the in-dripping water (Figures 5-2 through 5-20 of Ref. 11 show pH variations of 3 to 10 in WP). Thus, even though the chemistry of the infiltrating water may vary substantially, the effects of the variations will likely be insignificant in a WP that undergoes significant alteration. An evaluation of the effects of varying in-dripping water chemistry is given in Section 5.3.2 of Ref. 15.

3.3 In most calculations, it is assumed that water may circulate sufficiently freely in the partially degraded WP that all degraded solid products may react with each other through the aqueous solution medium. The basis for this assumption is that this provides one bound for the extent of chemical interactions within the WP. An analysis of the plausibility of this assumption is given in Section 6.3.

3.4 It is assumed that the calculations can satisfactorily be simulated with the thermodynamic database containing data for a temperature of 25 °C. The basis for this assumption is that

even though the initial breach may occur when the WP contents are at temperatures ≥ 50 °C (Ref. 24, Figures 3-22 and 3-24), at times > 25,000 years, the WP temperatures are likely to be closer to 25 °C.

3.5 In most calculations, it is assumed that chromium and molybdenum will oxidize fully to chromate (or dichromate) and molybdate, respectively. The basis of the assumption is the body of available thermodynamic data (the data0.p0a file in the accompanying electronic media, Attachment II, Disk 1, "databases" folder), which indicates that in the presence of air the chromium and molybdenum would both oxidize to the VI valence state. Laboratory observation of the corrosion of Cr- and Mo-containing steels and alloys, however, indicates that any such oxidation would be extremely slow. In fact, oxidation to the VI state may not occur at a significant rate with respect to the time frame of interest, or there may exist stable Cr(III) or Cr(VI) solids (not present in the EQ3/6 thermodynamic database) that substantially lower aqueous Cr concentration. For the present analyses, the assumption is made that over the times of concern the oxidation will occur.

3.6 It is assumed that the CRM of the WP will react so slowly with the infiltrating water (and the water already in the WP) as to have negligible effect on the chemistry. The bases for this assumption consist of the facts that the CRM is fabricated from an extremely durable Ni-W-Mo alloy, which corrodes very slowly compared (1) to other reactants in the WP and (2) to the rate at which soluble corrosion products will likely be flushed out of the WP.

3.7 In most calculations, it is assumed that the gases in solution in the waste package will remain in equilibrium with the ambient atmosphere outside the waste package. The basis for this assumption is that under the assumed conditions, in which water freely enters the waste package and circulates within it, there will be little to prevent extensive prolonged contact between the solution inside the waste package and the atmosphere outside the waste package. Under the assumed equilibrium condition, the partial pressure of CO_2 will exert important controls on the pH and carbonate concentration in the solution and hence on the solubility of uranium, gadolinium, and other elements.

3.8 It is assumed that all solids generated by the degradation calculations (step 1 of the methodology) are initially deposited inside the WP and remain in place until the geochemistry code predicts their re-dissolution (as a consequence of changed in-package water chemistry). The basis for this assumption is that such solids are likely to be filtered by debris in the waste package and retained therein.

3.9 It is assumed that the corrosion rates used in this calculation encompass rates for microbially assisted degradation, and that the degradation rates will not be controlled principally by bacteria. The bases for this assumption are (1) steel corrosion rates measured under environmental conditions inherently include exposure to bacteria, and (2) the low levels or lack of organic nutrients available for bacterial corrosion will limit the involvement of bacteria. It is assumed that bacteria act as catalysts, particularly for processes such as the reduction of sulfate, but this catalytic effect is not expected to change significantly the types of solids formed in the WP.

3.10 In most WP calculations, it is assumed that O_2 and other gases are well-mixed and are transported throughout the WP by convective circulation. The bases for this assumption are: the analysis in Ref. 7 (Att. VI); and the fact that the assumption is generally conservative, causing actinides to reach the most soluble oxidation state. The plausibility of the assumption, and proof of conservatism, are discussed in Section 6.3.

3.11 For any WP components that were described as "304" stainless steel, without indication of the carbon grade, the alloy was assumed to be the low-carbon equivalent. The basis of this assumption is that, in general, the carbon in the steel is totally insignificant compared to the carbon supplied by the fixed CO_2 fugacity of the EQ3/6 calculation, and to the constant influx of carbonate via the in-dripping water.

3.12 It is assumed that the thermodynamic behavior of hafnium (Hf) can be treated as if it were zirconium (Zr). The basis of this assumption is the extreme similarity of the chemical behaviors of the two elements. Thermodynamic data for many important Hf solids and aqueous species are lacking, thus Zr was substituted for Hf in the calculation.

3.13 It is assumed that the invert will be composed of crushed tuff ballast, with 10% to 100% of its pore spaces filled with water. This assumption is based on Ref. 17 (p. 6-47). Crushed tuff is a conservative choice with respect to reactions that precipitate U-silicates, or involve conversion of Ca-silicates to calcium carbonate; 10% irreducible saturation is consistent with poorly sorted sands and gravels (Ref. 3, Figure 9.4.9).

3.14 It is assumed that the invert will contain a steel support structure. The basis of this assumption is implicit in Ref. 17.

3.15 It is assumed that the depth of the invert is in the range of 60.6 to 80.6 cm. The basis for the greater depth is Ref. 16. The lesser depth was suggested in Ref. 41 (DTN: SN9908T0872799.004, File name: indriftgeom_rev01.doc). However, the exact depth does not seem fixed at this stage. This calculation used 72 cm, which was the planned depth at the commencement of this study. For this study, the depth of the invert is of principal interest for determining the mineral surface area and effective residence time of the fluid. The results in Section 6-1 show that the accumulation is not particularly sensitive to these factors.

3.16 It is assumed that the crushed tuff consists of grains having diameter of approximately 1 cm. The basis of this assumption is that the material is referred to as "ballast" in Ref. 17 (p. 6-47) and the term ballast is normally used to describe crushed stone (that is, "ballast" is not commonly used to describe fine sand). In addition, the *Water Diversion Model* (Ref. 19, p. 9) assumed a size ranging from 0.200 to 0.475 cm for the crushed tuff in the invert. The grain size affects the surface area of tuff exposed to percolating solutions, and the default surface area was conservatively multiplied by a factor of 10 to 100 to increase likelihood of actinide precipitation in the tuff.

3.17 For purposes of calculating the accumulation of fissile material on the magnetite in the drift, it is assumed that all of the iron in the drift (in EBS materials) will be available as magnetite when any fissile material begins flowing out of the waste package. The basis of this assumption is that it is conservative. If any of the in-drift iron were completely oxidized to hematite by the time of flow out of the waste package, there would be less available for reducing the fissile material in solution, and there would be less precipitation of fissile material.

3.18 It is assumed that the crushed tuff ballast in the invert has a porosity of 0.35. The basis of the assumption is that Ref. 3, Figure 9.4.9, gives ~30 to 40% for average sorting, from sand to cobbles.

3.19 It is assumed that the crushed tuff ballast in the invert has a tortuosity (τ) equal to 2. The basis for this assumption is Ref. 3, p. 111, which recommends $\tau \sim 1/0.56$ to $1/0.8$. We conservatively pick high $\tau \sim 2$ to slow the rate of oxygen access and enhance actinide precipitation by reduction.

3.20 It is assumed that the concentrations of the minor constituents of J-13 well water can be adequately represented by values for Li, B, and PO_4 taken from Reference 29, Table 4.2; values for Al, Fe, and Mn in equilibrium with diaspore, pyrolusite, and goethite, respectively; and the values for the trace elements, Cr and Mo, set to a molality of 10^{-16}. The rationale for this assumption is that even if the chemistry of the infiltrating water varies substantially, the effects of such variations will likely be insignificant for WPs that undergo significant degradation. An evaluation of the effects of varying the chemistry of the water dripping into a WP is given in Section 5.3.2 of Ref. 15.

4. USE OF COMPUTER SOFTWARE AND MODELS

4.1 SOFTWARE

Software name: EQ3/6
Software version/revision number(s): 7.2b, 7.2bLV
Software tracking number(s): STN: 10075-7.2bLV-00
Computer type(s): Standard PC
Operating platform: Windows
Location: Civilian Radioactive Waste Management System Management and Operating Contractor (CRWMS M&O), tag # 115815

The EQ3/6 7.2b package was obtained from Configuration Management (CM). The version 7.2bLV of EQ6 was developed by the originator under software activity plan 10075-SAP-7.2bLV-00, the validation and test report (VTR, Ref. 22) was reviewed and approved, and a compact disc (CD) with the software was submitted to CM.

The software was appropriate for the application. EQ6 7.2bLV is the only version of EQ6 capable of incorporating radioactive decay, and is the only version capable of passing time-varying aqueous compositions from run to run. The calculation inputs include several EQ6 database files with the file extensions "p0*", described in Section 5.1.1, and other EQ6 input files specific to different WP degradation scenarios with the extension "6i". There are several types of EQ6 output files, and they are not all important for the purpose of this calculation. The EQ6 input and output files pertinent to this calculation are described further in Section 5 and can be found on the CDs in Attachment II.

The software was used within its range of validation. However, some runs simulated periods of high ionic strength (1 to ~4). While EQ6 is capable of handling high ionic strengths, there is no Yucca Mountain Site Characterization Project (YMP)-qualified thermodynamic database with corrections for high ionic strength. To address this issue, several sensitivity tests were performed using other thermodynamic databases that have corrections for high ionic strength. The calculations relating to these tests are described in Sections 5.1.2 where it is shown that calculations at high ionic strength with the YMP database will overestimate the solubility of Pu and U, which will be conservative with respect to external accumulations of these elements. The external accumulation results from this calculation are used in other documents (Refs. 2 and 52).

4.2 SOFTWARE ROUTINES

Spreadsheet analyses were performed with Microsoft Excel 97 SR-2, installed on a PC running Microsoft Windows 95. The specific spreadsheets, used for results reported in this document, are included in the electronic media (Attachment II, Disk 1, "Excel" folder). These spreadsheets contain all the equations used and are sufficiently annotated that the correctness of all calculations can be directly verified. The spreadsheets have been verified and documented according to the procedure AP-SI.1Q, *Software Management* (Ref. 55). Formulas used are listed in the spreadsheets and have been checked where used and found to be identical.

Some plots were made with the program PP (Ref. 40), which is included in the electronic media (Attachment II, Disk 1, "pp" folder). PP is exempt from the requirements of AP-SI.1Q, *Software Management* (Ref. 55). Section 2.1.5 of the procedure states: "Software used solely for visual display or graphical representation of data which is used in a product which is checked and approved in accordance with applicable procedures and meets stated acceptance criteria is exempt."

4.3 MODELS

None used. This calculation is based on the conceptual model discussed in Section 3.1 of Ref. 47, as mentioned in Section 1 of this report.

5. CALCULATION

5.1 THERMODYNAMIC CONSTRAINTS

5.1.1 Databases

Most recent calculations of WP degradation (e.g., Ref. 15) have used a composite thermodynamic database called **data0.nuc.R8**, derived from the **data0.skb** and other databases provided by Lawrence Livermore National Laboratory (LLNL). The U.S. Department of Energy (DOE) is currently determining the path for acceptance of the EQ6 databases, and a single **data0.ymp** will be issued, drawing heavily on the recommendations from Ref. 30. In addition, the U.S. Nuclear Regulatory Commission (NRC) has identified several thermodynamic database issues that require resolution, including the appropriate stability constants for U-silicates, the identity of the phase that controls Pu solubility, and the stability of "colloidal" $Pu(OH)_4$ (Ref. 33, pp. 38, 70, 73, and 86). To determine the sensitivity of the WP calculations to choice of database, and to anticipate the recommendations of the DOE and NRC, several databases were defined for this calculation. The nomenclature and distinctions among the databases, and the motivations for their construction are given below.

data0.p0a is essentially the same as the database **data0.nuc.R8a**, used in Ref. 15. In particular, the database retains the older thermodynamic data for uranium silicates such as soddyite and haiweeite. The rare earth data are taken from the SKB dataset (Ref. 39); these rare earth data will be used in **data0.ymp**. The molar volumes for trevorite, pyrolusite, baddelyite, and zircon were estimated using densities from Ref. 37 (pp. 46-47, 500, 624-625, 689-690). Several pseudo-minerals were added to the database to allow use of TST reactants for HLW glass and Pu-ceramic, and to allow upper limits to be placed on the fugacities of gases that are allowed to "drift" in certain EQ6 calculations. The entries added for these pseudo-minerals are placeholders, with no numerical significance, and do not require qualification.

data0.p0c is comprised of the standard EQ3/6 **data0.com**, plus the rare earth constants from the SKB database. However, it lacks some of the actinide species found in **data0.p0a**. The purpose of this database is to test the sensitivity of the accumulation calculations to the actinide carbonate species.

data0.p0n is like **data0.p0a**, but adds a pseudo-mineral, **GlassNp** to model HLW in which the UO_2 is completely replaced with NpO_2. This database is used only to estimate (by comparison with runs based on **data0.p0a**) the amount of accumulated U that originates from the HLW glass, vs. the Pu-ceramic.

data0.p0s is based on **data0.p0a**, except the data for several U silicates (soddyite, haiweeite, uranophane, and sodium boltwoodite) have been replaced with the data from Ref. 50.

data0.p0t and **data0.p0u** are identical to **data0.p0s**, except the $\hat{a}_i$ parameters (referred to as **azer0** in EQ6 databases and defined in Section 5.1.2) for some actinide carbonate complexes have been changed to obtain better agreement with solubility experiments, as explained in Section 5.1.2.

All the databases are included on the electronic media accompanying this calculation (Attachment II, Disk 1, "databases" folder). The header of each database gives a detailed change history. For this calculation, the database used in an EQ6 run is always identified by the 4th character in the ***.6i** file name, which corresponds to the last character in the database name. For example, run **Pe2a1231.6i** used **data0.p0a**. For the remainder of this document, the databases are denoted by the three letters of the extension (e.g., **data0.p0a** = p0a).

5.1.2 Ionic Strength Artifacts

Thermodynamic calculations require the use of activities of dissolved substances, rather than simply their concentrations. (The conversion is done by multiplying the concentrations by activity coefficients.) Several factors affect the value of the activity coefficient, notably the charge on the ion, the total local electrostatic field in the solution (taken into account by means of the ionic strength, and interactions among ions). In very dilute solutions, only the charging effects need to be taken into account. At higher concentrations the ionic interactions and ion-solvent (water) interactions become of major importance and are much more difficult to calculate.

For all WP runs with slow water fluence and high glass degradation rates, EQ6 will calculate high ionic strengths. For example, in the **Pe1a1231** source term, ionic strengths exceed 2.0 for a period of ~10^4 years, with a brief peak at ~3.7 molal. EQ6 itself can deal with high ionic strengths, given a Pitzer-type thermodynamic database. However, no Pitzer database exists that is sufficiently complete to allow modeling of WP degradation, and the B-dot corrections (Ref. 45, pp. 39-42) for ionic strength, which are used in the current calculation, are of limited accuracy above ionic strengths of ~1 molal. Thus it is important to understand how use of the B-dot correction will affect the calculated solubility of actinides.

The B-dot equation is an approximation used to calculate the activity coefficients, which indirectly affect the calculated solubilities. The activity coefficient γ_i is defined as:

$$a_i = m_i \cdot \gamma_i \qquad \text{(Eq. 1)}$$

where a_i is the thermodynamic activity of the ith species in terms of molality, and m_i is the actual molal concentration of the species. The activity is an idealized concentration; the solubility products in the thermodynamic databases are actually formulated in terms of activities, not concentrations. For some highly charged species, the B-dot method grossly underestimates γ_i, so the activities are underestimated as well, and the code is less likely to predict the saturation of the aqueous phase with a U or Pu solid, for example.

The B-dot correction is based on the equation (Ref. 45, pp. 39-42):

$$\log_{10}\gamma_i = -\frac{A_\gamma \cdot z_i^2 \sqrt{I}}{1 + \mathring{a}_i \cdot B_\gamma \sqrt{I}} + \dot{B} \cdot I \qquad \text{(Eq. 2)}$$

where I is the ionic strength, z_i is the charge on the ith species, and A_γ, B_γ and $\dot{B}$ are fixed parameters. For most neutral species, EQ6 does not use the B-dot equation, but rather simply sets $\log_{10}\gamma$ to 0. The $\mathring{a}_i$ parameter is the "hard core" radius of the species, and is supposed in some sense to include the waters of hydration. In the thermodynamic databases used in this study, the $\mathring{a}_i$ for well-characterized species have been selected to give reasonably good corrections. However, many actinide species have been assigned the default setting of 4 Å (the value for the Na^+, Cl^- pair); this value is inaccurate for large complexes such as $(UO_2)_3(CO_3)_6^{6-}$, $PuO_2(CO_3)_3^{4-}$, and $UO_2(CO_3)_3^{4-}$; these latter species are significant, because under the alkaline conditions predicted for dissolution of glass waste forms, the carbonate complexes tend to dominate the calculated solubility. Choosing more realistic $\mathring{a}_i$ can improve the quality of the corrections for large molecules substantially, as shown below.

An alternative to the B-dot equation is the specific interaction theory (SIT; Ref. 28):

$$\log_{10}\gamma_i = -\frac{A \cdot z_i^2 \sqrt{I}}{1 + B \cdot \sqrt{I}} + \sum_{n \neq i} \varepsilon_{in} m_{in} \qquad \text{(Eq. 3)}$$

where A and B are fixed parameters, and ε_{in} is the specific interaction parameter between species i and species $n \neq i$. The summation is generally taken over species in solution that have non-zero charges, and only over species whose charge is opposite in sign to the charge on the ith species. The SIT approach is reputed to be good up to ionic strengths of 4. In comparing equations 1 through 3, one sees that the SIT approach has more flexibility than B-dot for the 2nd term on the right side, and less for the 1st term; the latter poses a problem for some highly charged species. The SIT approach requires substantially more experimental information than the B-dot equation. The SIT interaction parameters (ε) are usually given in terms of molarity, and a strict comparison with molal EQ3/6 calculations requires a correction for the solution density; however, the correction is small compared to the error in ε at $I < 3$.

Figure 5-1 (taken from spreadsheet **bdot.xls**) shows how the choice of **azer0** affects the calculated B-dot activity coefficient, for ions with charge of –2 and –4. Clearly the spread is much greater for the more highly charged species. The plot also shows the curve for the SIT correction for $UO_2(CO_3)_3^{4-}$. Note that by choosing **azer0** = 4.85 for the B-dot correction, the B-dot and SIT estimates are extremely close over most of the ionic strength range.

However, the SIT corrections for individual speces are not to be used in isolation. The SIT correction for $UO_2(CO_3)_3^{4-}$ depends heavily on the ε assumed for UO_2^{++}, and that value is not well-known. A stronger measure of accuracy comes from a comparison against experimental results. The only suitable experimental data are given by Grenthe et al. (Ref. 27, Table 1);

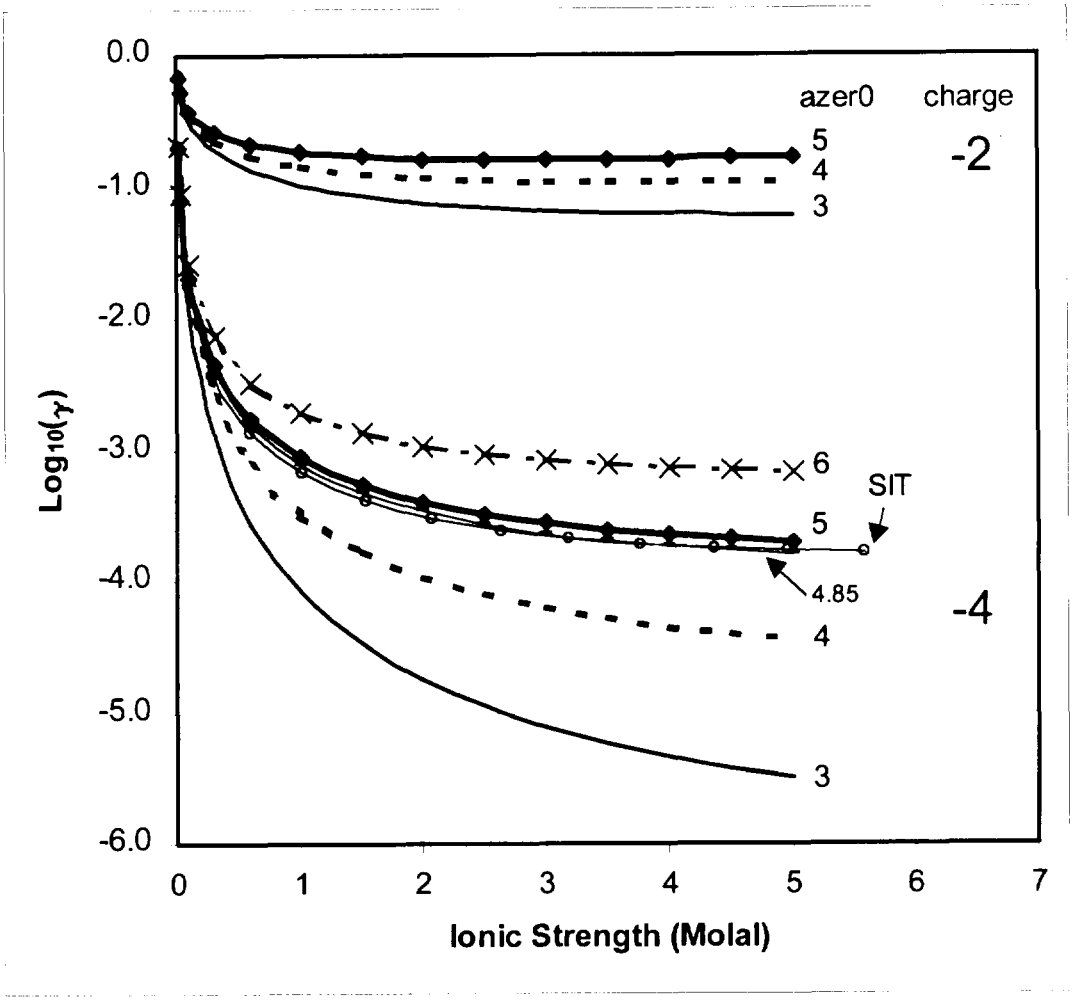

NOTE: B-dot with azer0=4.85 matches SIT for $UO_2(CO_3)_3^{4-}$; reference spreadsheet is `bdot.xls`.

Figure 5-1. Comparison of SIT and B-Dot Activity Coefficient (γ) Calculations

these experiments were performed at an ionic strength of ~3 molal, which is similar to the maximum ionic strength seen in the EQ6 calculations. However, the experiments are somewhat extreme, since they employ CO_2 pressures of ~0.1 bars, or 10^2 times the default fCO_2 estimated for the repository. Thus the experiments tend to overestimate the formation of carbonate complexes. In addition, most of the experiments are for low pH; the experiments at pH > 5 are of greatest interest for the WP modeling.

Figures 5-2 through 5-4 below compare experimental results (Ref. 27) against EQ6 calculations (the calculations are associated with the EQ6 `U_carb*.*` files in the electronic distribution [Attachment II, Disk 1, "ionic strength" folder]). The default `azer0` values (Figure 5-2) yield gross overestimation of the total solubility of U. Even with the `azer0` used in Figure 5-3, the total U solubility is overestimated by at least an order of magnitude in the

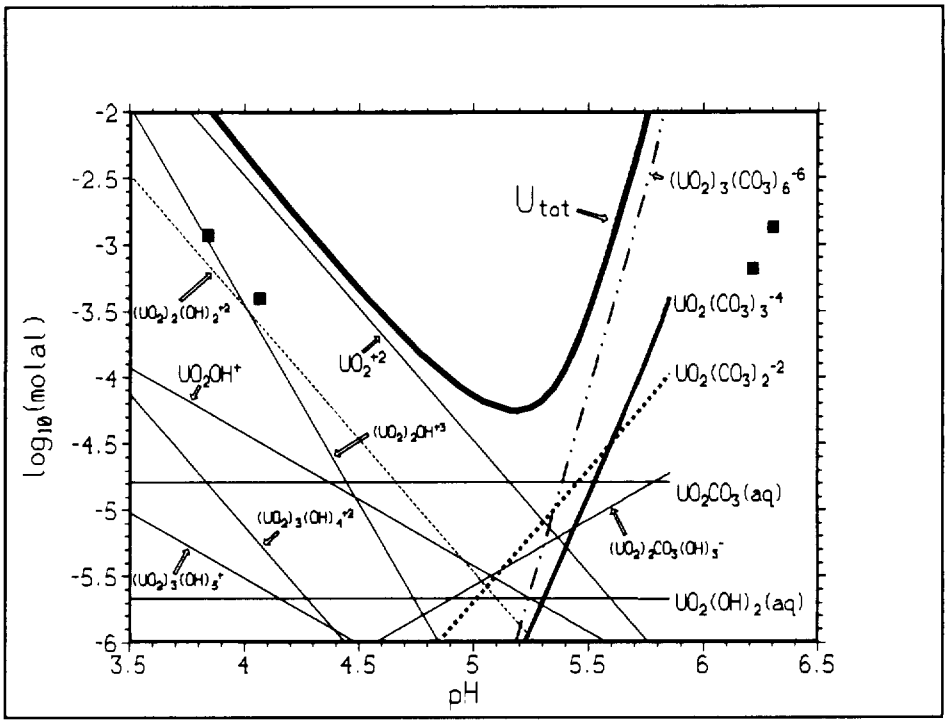

NOTE: azer0=4.0 for $UO_2(CO_3)_3^{4-}$ and $(UO_2)_3(CO_3)_6^{6-}$

Figure 5-2. Comparison of Experiments (Squares) and EQ6 Calculations (Lines), for Database p0a

high-pH leg of the curve. With the **azer0** used in Figure 5-4, the total U solubility is still overestimated by at least a half-order of magnitude.

Thus, it is possible that the thermodynamic databases used in this study will cause significant overestimation of actinide solubility in solutions where the speciation is dominated by highly charged carbonate complexes. Perhaps more significant, these databases may overestimate actinide precipitation when the solutions are diluted, since the activity coefficient will increase artificially as the ionic strength is reduced. However, as shown in Section 6, the differences among calculations performed with the different databases, but otherwise similar conditions, are remarkably small.

5.1.3 $Pu(OH)_4$ Solubility

Most EQ6 calculations were performed with formation of PuO_2 suppressed, and the $\log_{10}K$ (stability constant, in the thermodynamic database) of $Pu(OH)_4$ reduced by 4 units, via the EQ6 **augmentk** input file parameter. This section develops the justification for this default value. As will be shown in Section 6.1, the accumulation calculations are rather insensitive to the choice of $\log_{10}K$ for the Pu solids.

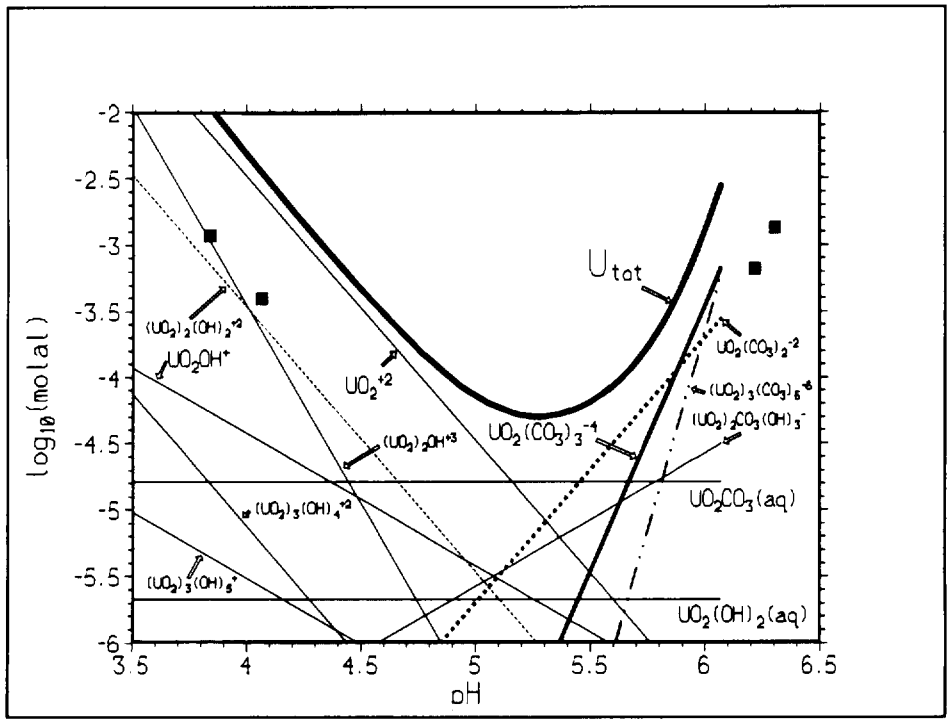

NOTE: azero=4.85 for $UO_2(CO_3)_3^{4-}$ and azero=6.0 for $(UO_2)_3(CO_3)_6^{6-}$

Figure 5-3. Comparison of Experiments (Squares) and EQ6 Calculations (Lines), for Database p0t

Figure 5-5 compares the Pu solubilities found by Wilson and Bruton (Ref. 43) for dissolution of spent fuel (exposed to air, over several years), with several EQ6 calculations. The template for the calculations in Figure 5-5 is the standard EQ6 test file **j13wsf.6i**; this test file simulates the reaction of 100 g of spent UO_2 fuel into J-13-like water at $\log_{10}(f(CO_2)) = -3.5$. In all runs for this figure, the test file was modified by changing the "closed system" option to "titration" (the input files are included in the electronic distribution [Attachment II, Disk 1, "J13" folder] and are named **j13wsf*.6i**). For the upper EQ6 curve in the figure, formation of PuO_2 was suppressed and the **augmentk** option was used to decrease the $\log_{10}K$ of $Pu(OH)_4$ by 4 units; this choice results is rather good agreement with the experimental results. This observation is consistent with the long-term (3.6 year) experiments of Rai and Ryan (Ref. 35); those experiments showed $\log_{10}$(solubility of Pu) intermediate between solubilities of freshly-precipitated $Pu(OH)_4$ (=$PuO_2 \cdot 2H_2O$) and annealed PuO_2.

The figure also compares results using the p0c database with those from the p0a database. The **j13wsf.6i** run was performed with each database for the PuO_2-allowed calculations (lower curves in Figure 5-5). The results of the two databases are nearly indistinguishable.

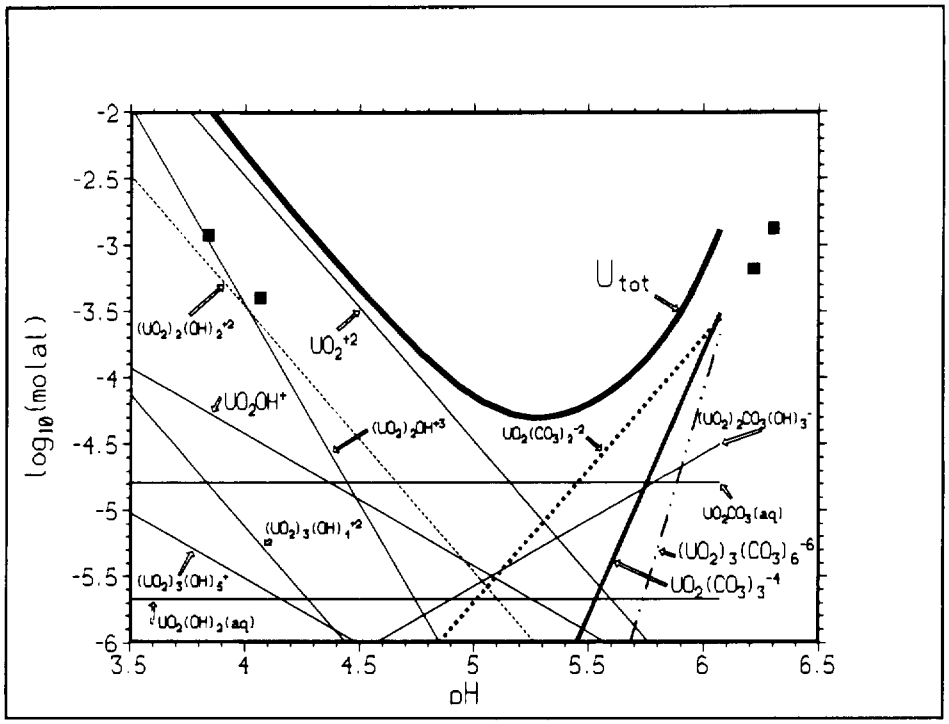

NOTE: **azer0**=5.5 for $UO_2(CO_3)_3^{4-}$ and **azer0**=6.5 for $(UO_2)_3(CO_3)_6^{6-}$

Figure 5-4. Comparison of Experiments (Squares) and EQ6 Calculations (Lines), for Database p0u

5.2 WP DEGRADATION SCENARIOS

5.2.1 The Bathtub Scenario

For the WP, SCFT calculations represent a bathtub "scenario," in which water constantly drips into the package, mixes thoroughly with the water already resident in the package, then exits the package with a rate equal to the drip rate. This scenario is equivalent to a constantly stirred tank reactor, or the single mixing cell employed in the Viability Assessment (VA) (Ref. 9, Section 6.5).

An alternative scenario involves a WP in which water drips through an unsaturated mix of degraded and partially degraded components, so that the total amount of fluid water in the package, at any time, is small. In such a system, there can be extreme variability encountered by a packet of water that moves through the WP. For example, a water drop that first encounters degraded glass may experience a very high pH and relatively oxidizing conditions; if the drop then passes through a breached, steel-clad fuel element, the water may experience acid conditions and local reducing environments. To calculate the chemistry in such a drip-through system, the reaction code must be spatially gridded. A one-dimensional gridding is possible with EQ6 v7.2bLV, but the computer runs are lengthy, and arbitrary decisions must be

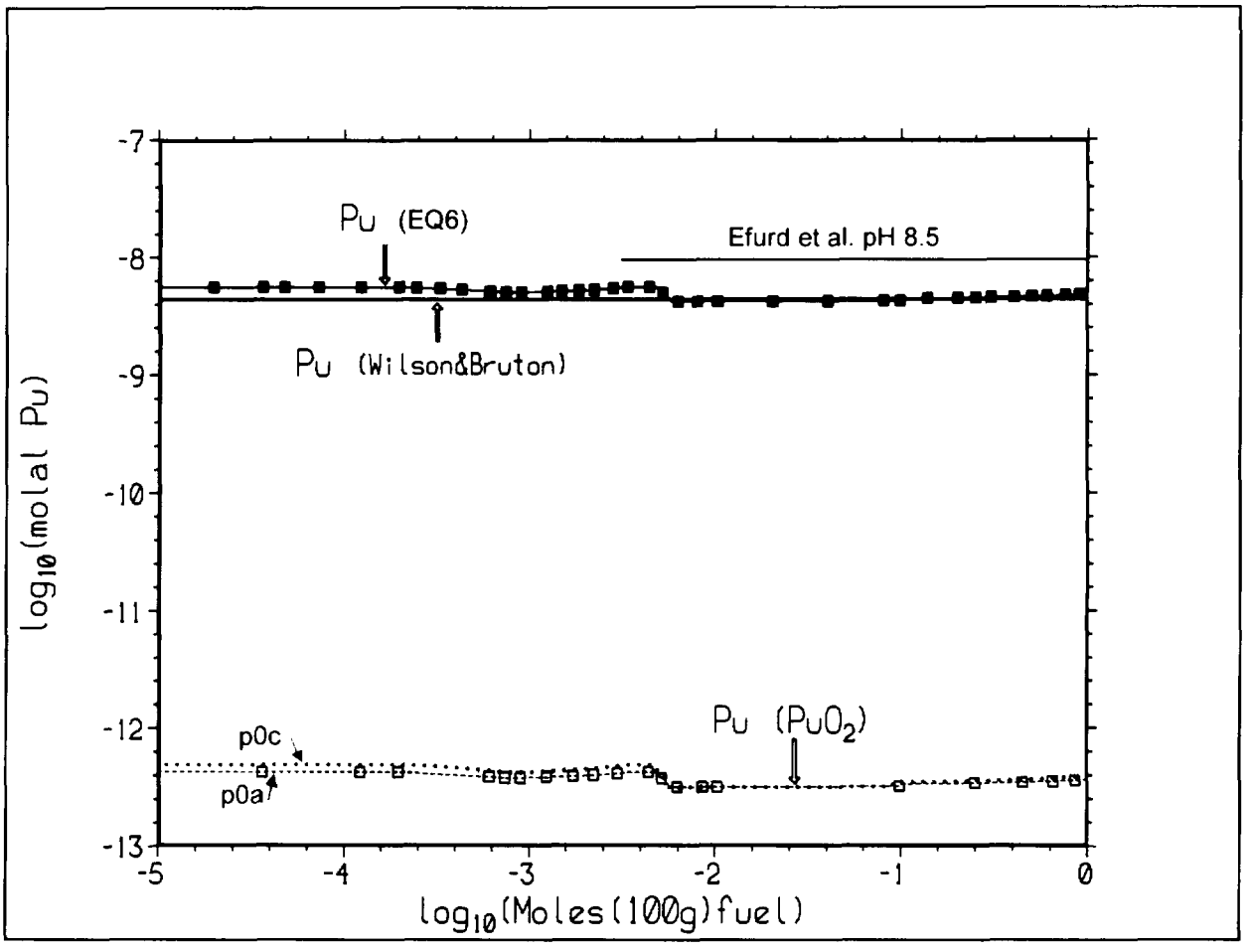

NOTE: Upper curves: EQ6 calculation, with filled squares, used database p0a with PuO_2 suppressed and $Pu(OH)_4$ $\log_{10}(K)$ lowered by 4 units. Lower curves: in runs with solubility controlled by PuO_2, p0c (dotted) and p0a (dashed) give similar results. For EQ6 calculations, pH ~8.5 and $\log_{10}(fCO_2) = -3.5$; Efurd et al. [Ref. 25] used pH=8.5 and $\log_{10}(fCO_2) \sim -3.2$. Wilson&Bruton is experimental data from Table 3 in Ref. 43.

Figure 5-5. Comparison of Experiments and EQ6 Calculations for "Spent Fuel" in J-13-Like Water

made about the sequencing of the cells (grid elements). In addition, a VA sensitivity analysis (Ref. 9, Section 6.6.1) showed that multiple-cell models yielded lower overall release than models that employed a single mixing cell, due to transport limitations.The bathtub scenario is used for all the SCFT runs described in this calculation. There are two justifications for this scenario, apart from its simplicity. Both justifications begin with the observation that an aqueous phase, containing dissolved radionuclides, must leave the package before it becomes of consequence to the external criticality calculations. First, the VA calculations (Ref. 10, Figure 5-61) suggest that the probability of a WP breach is low, and the probability of more than one breach in a WP is much lower still. With the new drip shield designs, the breach probabilities become even more remote. Therefore, a breached package will likely have only one entry point for influx of water; if that entry point is on the lower 180° arc of the package, water will not be able to drip into the package, and will not accumulate. If the entry point is on the top, water will accumulate in at least half the package, until the package is breached again

internally or externally. The worst WP source terms discussed in this calculation (in terms of accumulation of a critical mass in the invert) lose most U and Pu within the first few thousand years post-breach, in a period of high pH. Second, the bathtub scenario generally maximizes the loss of fissile materials, because the constant dilution lowers the chance that the aqueous solution will reach the solubility limits for the U and Pu solids.

5.2.2 Oxidation State in the WP

In most runs performed in this calculation (and all those reported in Table 6-1), the materials in the WP were assumed (Assumption 3.7) to be at equilibrium with ambient fO_2 (~0.2 bars). As discussed in Assumption 3.7, such oxidizing conditions are conservative for estimating actinide loss from the WP, as the higher oxidation states of the actinides form soluble, stable carbonate complexes. In a drip-through scenario, in which only a thin film of water wets the bulk of the WP components at any given time, oxidizing conditions may indeed prevail. However, in the bathtub scenario, a combination of rapid degradation of waste forms and widespread oxidizing conditions is inherently unrealistic. When degradation rates are high, the EQ6 calculation quickly produces large volumes of degradation products (typically enough to fill ~20% of the void space in $\sim 2 \times 10^2$ y, or ~50% in 5×10^3 y). The EQ6 volume estimates do not include the abundant porosity found in alteration clays and rusts. Thus if degradation rates are high, the degrading WP materials should be mantled with substantial diffusive boundary layers. Consequently, the delivery of oxygen to undegraded waste will be controlled by diffusion in water (a very slow process), not by convective overturn. Section 6-3 provides estimates of the effects of boundary-layer diffusion on the solubilities of actinides in the WP, and on the eventual accumulation of actinides in the invert.

5.2.3 Choice of WP Source Term Scenarios

The choice of WP source term scenarios was based on Table 6-1 in Ref. 15. The highest Pu losses were found for scenarios that involved slow water fluences (0.0015 m^3/y) and very fast Pu-ceramic degradation rates. Case 8 of that study (file root name **p00_1231**) produced the highest Pu loss, ~29.94%. Of scenarios with more moderate fleunces (0.015 m^3/y), Case 10 of that study (file root name **p00_1222**) produced the highest Pu loss (1.8%). These two scenarios were selected as potential source terms; that is, they were selected to provide a time-varying aqueous composition that would leave the WP, and percolate through the crushed tuff invert. However, because the factors that determine conservatism are different for external and internal criticality, the WP calculations were rerun. Changes made to the WP calculations are described in Section 5.3; the most significant of these changes are the incorporation of pH-dependent rates for HLW (Section 5.3.1.1), and the use, in some calculations, of the new LLNL Pu-ceramic corrosion results (Section 5.3.1.2). In addition, the baseline solubility-controlling solid was taken as $Pu(OH)_4$ (with the stability constant lowered 4 orders, as described in Section 5.1.3), instead of PuO_2. The change in Pu-controlling phases was made because experiments typically show Pu solubilities much higher than that of PuO_2 (Section 5.1.3). While the choice of PuO_2 is conservative for internal criticality studies (as it lessens the likelihood of Pu leaving the package), this choice is certainly not conservative for external dose calculations, and is not obviously conservative for external criticality. All the new WP source

terms are included in the electronic media accompanying this calculation (Attachment II); as described in Section 5.7, the source term used for any accumulation calculation (that is, the calculations reported in Table 6-1) is easily identified from the invert output files.

Figure 5-6 demonstrates the differences among source terms used for this and a previous study (Ref. 15 and Ref. 18). The runs **Pe0a1231**, **Pe1a1222**, and **P00_1231** use the Pu-ceramic rates from the previous study (Ref. 15, Table 5-3); the run **Pw2a1231** uses the newer, lower ceramic rates described in Section 5.3.1.2. The **Pe1a1222** case uses a comparatively high Pu-ceramic degradation rate (the average rate of Ref. 15, Table 5-3, $\sim 10^{-14}$ mols/($cm^2 \cdot s$)), but because it is flushed rapidly (water fluence of 0.015 m^3/y, versus 0.0015 m^3/y for the other three), the ionic strength and pH remain moderate, so aqueous Pu-carbonate complexes are less stable. Thus the aqueous Pu concentrations are lower for **Pe1a1222** than for the cases **Pe1a1231** and **Pw2a1231**. (Note that in Figure 5-6 and all subsequent figures and tables the time refers to time after breach.)

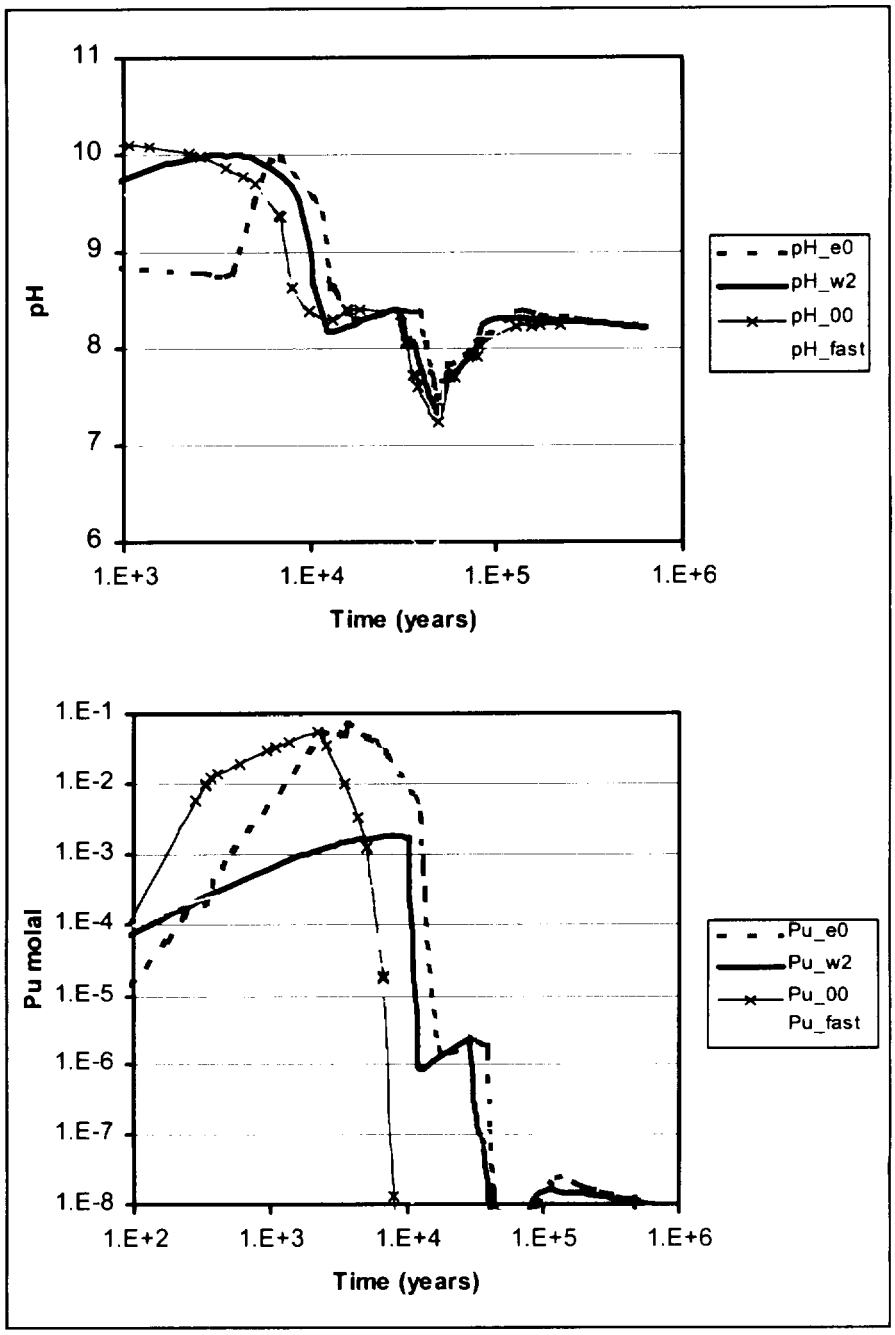

NOTE: In the keys, the endings correspond to the root names as follows:
_00 corresponds to P00_1231 (Ref. 15, Case 8);
_e0 corresponds to Pe0a1231 (like P00_1231, but pH-dependent glass rate);
_w2 corresponds to Pw2a1231 (like Pe0a1231, but slightly lower ceramic rate); and
_fast corresponds to Pe1a1222 (like Pe0a1231, but much slower ceramic rate and higher water fluence).

Figure 5-6. Comparison of pH vs. Time and Aqueous Pu vs. Time for Four Source Terms

5.3 MATERIALS COMPOSITIONS AND RATES

5.3.1 Compositions and Rates of WP Materials

The compositions and degradation rates for steels were taken directly from Table 5-1 of Ref. 15, and the basic compositions of the HLW glass and Pu-ceramic were taken from Tables 5-2 and 5-3 of Ref. 15. The J-13-like in-dripping water composition was taken from Table 5-4 of Ref. 15, and is essentially the composition given in Reference 57 (DTN: MO0006J13WTRCM.000) and Table 4.2 of Reference 29 .

Several minor changes were made to these basic compositions to increase the efficiency of the calculations and to decrease the EQ6 run time. Principally, minor elements in the HLW glass, and other package materials compositions were removed or merged with chemically similar elements (e.g., Li was merged with Na in the glass composition). For the J-13-like water composition, Li was removed as it constitutes only $\sim 10^{-3}$ of the alkali metal (Na + K) content of the in-dripping water. The simplified J-13-like water composition is given in file **J13nc30p.3i**, and the simplified composition of the glass is given in Table 5-1, and the details of the conversion are given in **Glass_rates_110999.xls** in the electronic media (Attachment II, Disk 1, folder "Excel"). Reference 56 is the source of the original glass composition. The simplification of the HLW glass composition allows the material to be entered as an EQ6 TST reactant via the database p0a entry **GlassSRL**. As was shown in Sections 5.3.2 and 5.3.3 of Ref. 15, EQ6 estimates of Pu and U loss from the WP are not greatly affected by substantial variations in the compositions of the HLW glass and J-13-like water.

5.3.1.1 HLW Corrosion Rates

Two pH-dependent rate abstractions were tested for the HLW. The first, used in all calculations reported in Table 6-1, is the VA abstraction (Ref. 9, Section 6.3.3); the second, used only here as a comparison and for corroborative evidence, is the AMR HLW glass abstraction (Ref. 21). For both, the "high" rate was chosen to correspond to 50 °C. The conversion of the HLW rate parameters into EQ6 parameters is given in spreadsheets **Glass_rates_110999.xls** and **Ebert_glass.xls**. The EQ6 input file, which uses the Analysis Model Report (AMR) HLW glass abstraction (Ref. 21) is provided in Attachment II (Disk 1, "Ebert glass" folder).

Figure 5-7 compares the results of two source term calculations that use the two different abstractions. Both produce similar peak ionic strengths, pH and U and Pu contents. Therefore the single VA abstraction was used for the remainder of this work.

Table 5-1. Simplified Glass Composition

Element	Mols [a]	Comment
O	2.7666	
U	0.008	
Np	0	Merged with U (~0.1% of actinides,ceramic Np overwhelms)
Pu	0	Merged with U (Pu ~1% actinides, ceramic Pu overwhelms glass Pu).
Ba	0.0011	
Al	0.0883	
S	0.0041	
Ca	0.0166	
P	0.0005	
Cr	0	Merged with Al (overwhelmed by steel Cr; Cr_2O_3 similar to Al_2O_3)
Ni	0	Merged with Fe
Pb	0	Merged with Ba (both form insoluble $CrO_4^=$ compounds in EQ6 runs)
Si	0.7945	
Ti	0	Merged with Si (overwhelmed by ceramic Ti; TiO_2 similar to SiO_2)
B	0.298	
Li	0	Merged with Na
F	0.0017	
Cu	0	Merged with Fe
Fe	0.1762	
K	0.0768	
Mg	0.0341	
Mn	0	Merged with Fe
Na	0.5901	
Cl	0	Removed (overwhelmed by Cl in in-dripping water)

NOTE: [a] Moles constrained to yield 100g / "mol" glass for EQ6 reactant.

5.3.1.2 Pu-ceramic Rates

At the beginning of this study, the only published degradation rates, for the Pu-ceramic, came from Ref. 32. At that time, the ceramic dissolution experiments, run by LLNL, were incomplete, and temperature and pH effects were estimated with extreme conservatism. Because of this uncertainty, a set of "low," "average," and "high" Pu-ceramic rates were chosen for Ref. 15 (Table 5-3); this set of Pu-ceramic rates is hereafter referred to as the "older" rates. Since completion of the work in Ref. 15, Shaw (Ref. 38, Section 6) published pH-dependent rates for Pu-ceramic; these "newer" rates include much more experimental work (Figure 5-8). In particular, the newer rates show less temperature- and pH-dependence than was previously estimated in Ref. 32. The older ceramic rates are used in comparatively few runs for the present calculation. For example, in Table 6-1, only the code 3 runs used the older "average" rate from (Ref. 15, Table 5-3). WP runs that used the older rates can generally be

distinguished as having an **e** for the second character of the root file name. The corresponding invert runs can be distinguished by having a **t** for the second character of the root file name.

Most of the runs reported in this calculation are based on the newer LLNL data. The 50 °C rates for radiation-damaged ceramic (Ref. 38, Section 6) were chosen as the baseline "high" degradation rate, since temperatures over 50 °C are not expected after the WPs breach (Ref. 24, Figure 3-24). LLNL suggested (Ref. 38, Section 6) a conservative factor 30 multiplier for radiation damage, and that value was applied to the 50 °C rates. Ref. 38 (Table 6.1) provides an abstraction of pH dependence that was implemented in EQ6 for this calculation. The conversion of the LLNL abstraction to EQ6 parameters is performed in spreadsheet **Invert_EQ6_122299.xls**, sheet '**Pu-ceram_pH**', in the electronic media (Attachment II). A corresponding Pu-ceramic pseudo-mineral was placed in the thermodynamic databases. WP runs with the newer rates are generally distinguished by having the letter **w** as the second character of the root file name; the corresponding invert runs have the letter **x** for the second character.

However, for runs with the newer rates, the pH dependence was abandoned in favor of a simpler, constant rate. There are several motivations behind this simplification. First, EQ6 7.2bLV can model radioactive decay in reactants, but only if the reactants are not defined as minerals; this is a fundamental limitation of EQ6, since the code enforces strict preservation of stoichiometry, and arbitrary radioactive decay (e.g., ^{133}Xe to ^{133}Cs) violates stoichiometry (this restriction applies only to the reactants; decay is properly handled in the minerals that precipitate as part of the equilibrium system, because the equilibrium system is updated at every step). EQ6 can use pH-dependent rates for "minerals" only, so if the ceramic is to have a pH-dependent rate, its ^{239}Pu cannot be be decayed to ^{235}U; this restriction is quite serious for calculations that simulate times to several ^{239}Pu halflives. Second, use of the constant Pu-ceramic rate improves the speed and stability of the EQ6 calculations. Third, it was determined that a constant rate of 8×10^{-15} mols/(cm^2·s) and the pH-dependent rate produced extremely similar results, as can be seen in Figure 5-9. In part, the similarity is due to the fact that the pH-dependence in the LLNL abstraction is quite shallow in the pH range of 8 to 10. (This constant rate was estimated from **Pw1a1231.6o** [Attachment II, Disk 1, "WP 1,2,4,5,8,10" folder]; sampling rates out to 3.5×10^4 y [when Pu concentration drops to 10^{-7} molal] yields an average rate of $\sim7\times10^{-15}$; sampling only points on the high-Pu peak between 2×10^2 and 1.3×10^4 y yields an average of $\sim8\times10^{-15}$ mol/(cm^2·s). The total variation in the rate in this period is less than a factor of 2. See **Rate_avg_Pw1a1231.xls** in the electronic media, Attachment II). Fourth, in comparing the LLNL pH-dependent abstraction to the 50 °C experimental rates (Figure 5-8), it is apparent that there is a factor ~3 uncertainty for the pH range of interest ($8 \leq pH \leq 10$), and that the abstraction overestimates both the experimental rates and the slope of the pH dependence. Therefore, selection of an extremely precise value from the LLNL abstraction is not justified. A sensitivity study was performed on the effect of varying the rate by factors of 5, 10, and 100 above the baseline value, and is reported in group 9 of Table 6-1.

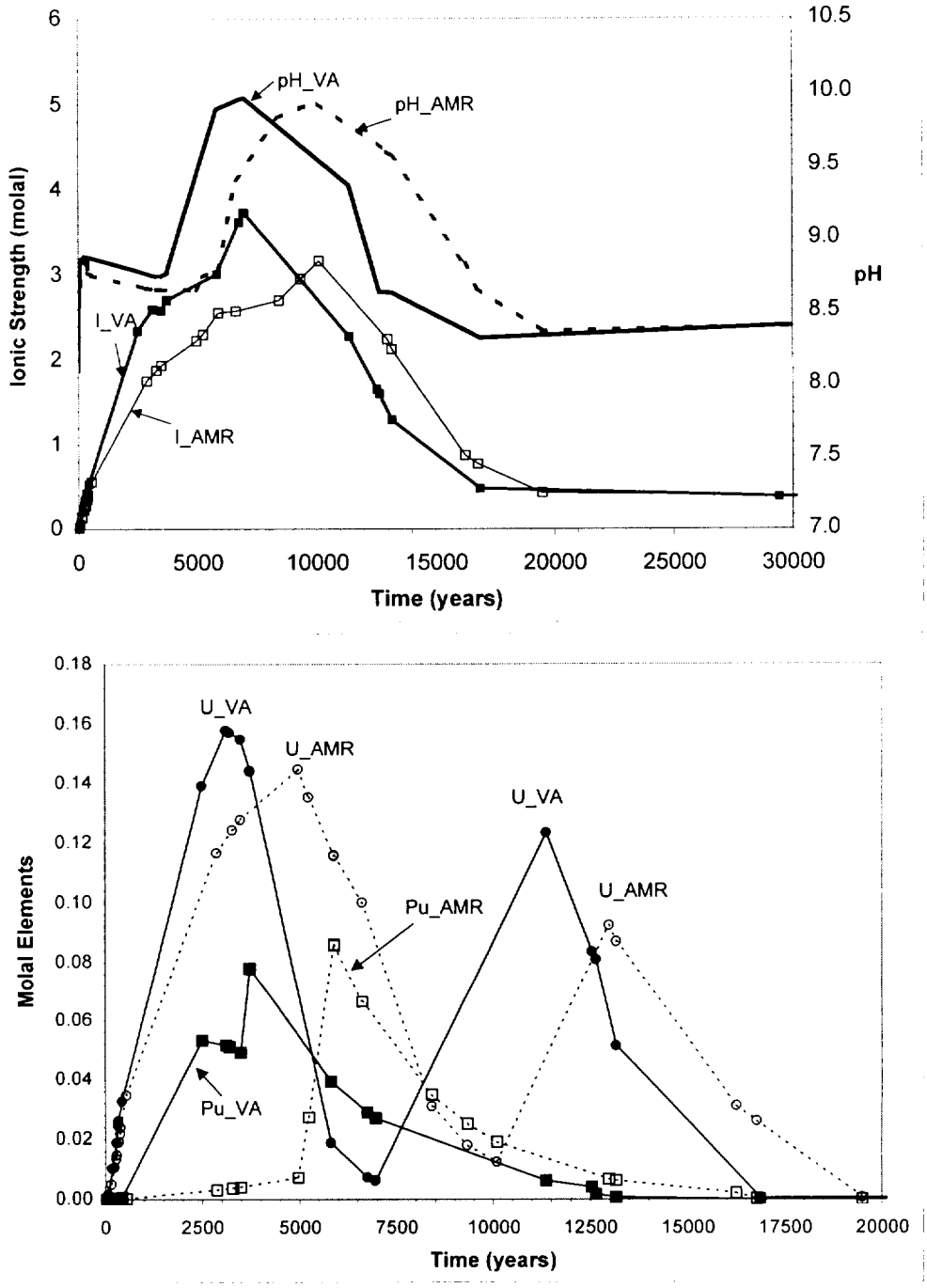

NOTE: WP runs Pe1a1231 [VA model, filled symbols and unbroken lines] and PeEa1231 [AMR model, open symbols and dashed lines]

Figure 5-7. Effect of VA vs. AMR Glass Models

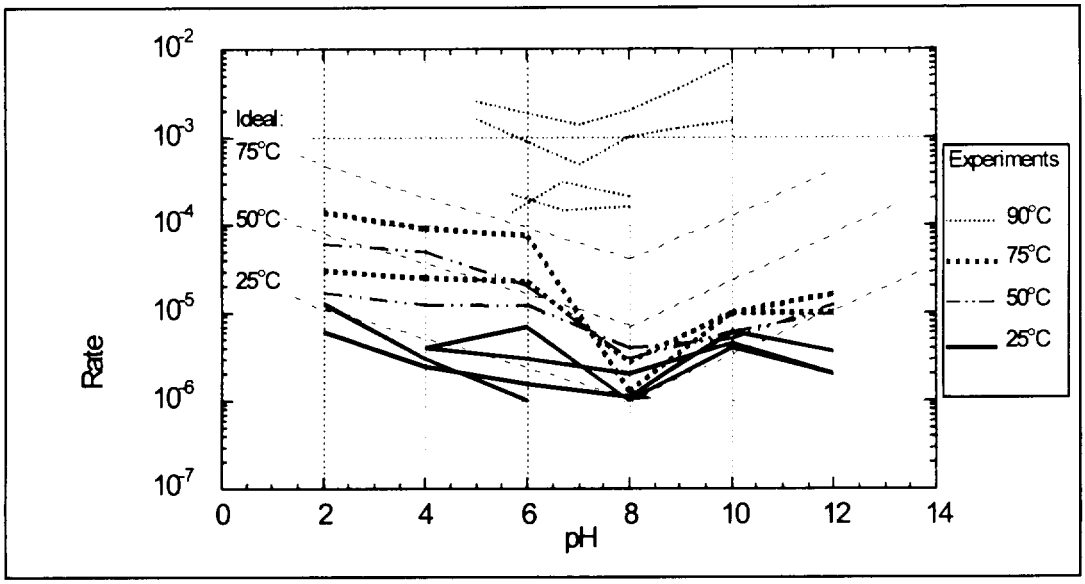

NOTE: Rate is in g/m^2/day. Data for all tests of pyrochlore-based composite ceramics, and single-phase zirconolite and pyrochlore (Ref. 38, Figure 6.1). The thin, dashed "Ideal" lines (for 25, 50, and 75 °C) give LLNL model.)

Figure 5-8. Normalized Rates for Single-Pass Flow Test

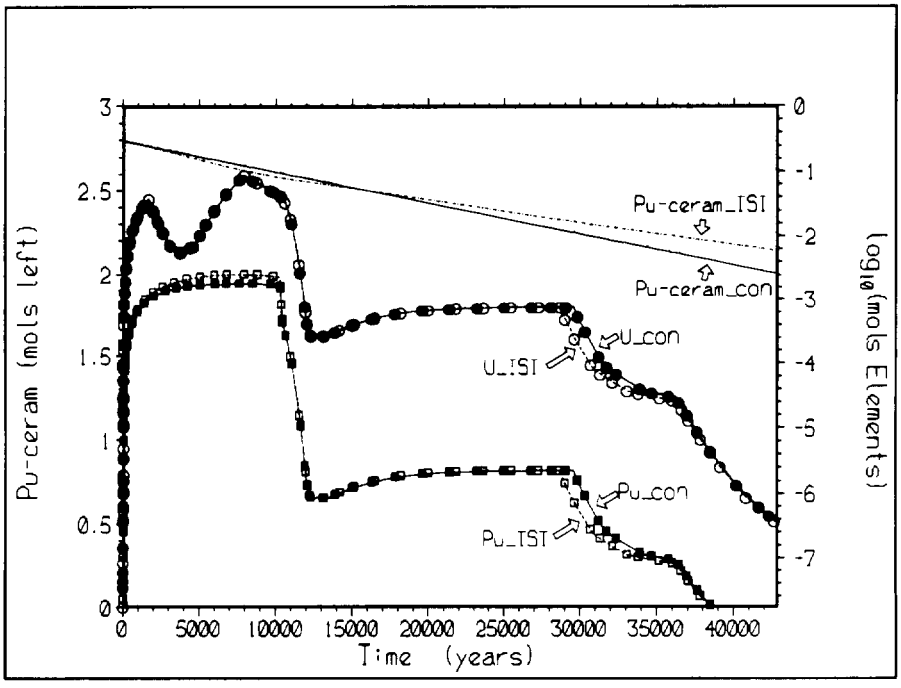

NOTE: Runs Pw2a1231 and Pw1a1231; TST= pH-dependent 50 °C rate for radiation-damaged ceramic; con= constant rate 8x10^{-15} cm^2/(s·mol), "mol" = 100 g. The mols elements are aqueous concentrations in WP.

Figure 5-9. Pu-ceramic Rates, pH-Dependent vs. Constant

5.3.2 Compositions and Rates for Invert Materials

The current EDA-II design (Ref. 17) specifies invert ballast material of crushed tuff. The tuff composition in Table 5-2 (leftmost two columns), serves as a basis for the calculations. The composition is converted into the moles of idealized minerals (for use as EQ6 reactants) shown on the right side of Table 5-2. The specific minerals chosen as idealized minerals are based on the main phenocrysts (large crystals) found in the Topopah Spring tuff (Ref. 31, p. F28), the host rock for the potential repository.

Table 5-2. Tuff Composition and Idealized Mineral Composition

Tuff Composition	
Oxide [a]	**Wt.%**
SiO_2	76.83
Al_2O_3	12.74
FeO	0.84
MgO	0.25
CaO	0.56
Na_2O	3.59
K_2O	4.93
TiO_2	0.1
P_2O_5	0.02
MnO	0.07
Total	99.93
Density [d] (g/cm^3)	2.543 3

EQ6 Minerals [b]	Mineral Formula	Mineral Molec. Wt. [c]	Moles Minerals in 100 g	wt %
Cristobalite (alpha)	SiO_2	60.0843	6.010E-01	36.1
Annite	$KFe_3AlSi_3O_{10}(OH)_2$	511.88	3.922E-03	2.0
Phlogopite	$KAlMg_3Si_3O_{10}(OH)_2$	417.26	2.081E-03	0.9
Anorthite	$CaAl_2(SiO_4)_2$	278.207	1.005E-02	2.8
Albite low	$NaAlSi_3O_8$	262.223	1.166E-01	30.6
Maximum Microcline	$KAlSi_3O_8$	278.332	9.934E-02	27.6

NOTE: [a] Original source is Ref. 31, pp. F32-F33. Six values were averaged (Ref. 13, p. 17) to give wt % listed here.
[b] These 6 minerals can account for 99.44% of tuff mass.
[c] Atomic weights of individual elements are from Ref. 34.
[d] Average particle density (without void space) of the hydrogeologic units TMN, TLL, TM2; Table 1 of Ref. 26 (DTN: MO9708RIB00040.000).

The invert is assumed (Assumption 3.13) to be filled with crushed tuff with 1-cm average grain diameter. The invert design is still hypothetical, but aggregate size of ~1 cm has been assumed (Assumption 3.16). However, it is probable that only the smaller fines will be sifted (< 200 mesh), so the effective surface area may be much larger than the geometric surface area calculated for a uniform, cm-sized aggregate. In addition, the tuff is probably microporous. It is conservative to overestimate the specific surface area, since contact between actinide-bearing solutions and tuff can induce precipitation by the mechanisms discussed below. Hence for all the calculations herein, the surface area was taken as corresponding to cm-sized cubes, multiplied by an area scaling factor of 10 to 100, with the factor 10 effectively corresponding to mm-sized cubes.

Potential mechanisms that would cause precipitation of actinides in the invert include the following:

- Loss of dissolved carbonate and the concomitant destabilization of aqueous Pu and U carbonate complexes, which could result from conversion of calcium silicates to calcite ($CaCO_3$)

- Reduction of Pu and U to highly insoluble Pu(IV) and U(IV), e.g., PuO_2 and UO_2, via oxidation of Fe(II) to Fe(III)

- Precipitation of uranium silicates caused by the release of silica from cristobalite and other silicates in the tuff.

For EQ6 reactants, all tuff Ca is assigned to anorthite ($CaAl_2Si_2O_8$), all Fe is assigned to annite ($KFe_3AlSi_3O_{10}(OH)_2$) as Fe(II), all Mg is assigned to phlogopite ($KAlMg_3Si_3O_{10}(OH)_2$), all Na is assigned to albite ($NaAlSi_3O_8$), and the remaining K is assigned to microcline ($KAlSi_3O_8$). Any remaining SiO_2 is then assigned to cristobalite (alpha). This process accounts for over 96% of the Al in the bulk analysis, and 99.44% of the bulk rock. The minor rock components (e.g., TiO_2) are ignored.

Dissolution rates for tuff minerals were cast in the TST formalism (Ref. 46, Section 3.3.3), using EQ6 mode **nrk=2**. The quartz dissolution rate was taken from Ref. 5. The rate of cristobalite dissolution was taken as three times the quartz rate; the reasoning behind the factor three is as follows. In Ref. 36 (Table 4, p. 1690), the rates for precipitation of all SiO_2 polymorphs are approximately the same. Microscopic reversibility implies the ratio (cristobalite rate) / (quartz rate) ~ (cristobalite solubility) / (quartz solubility) ~ $10^{(\log 10K\_crist - \log 10K\_quartz)} \sim 10^{(-3.4488 - -3.9993)} \sim 3.55$ at 25 °C and ~ $10^{(-2.9921 - -3.4734)} \sim 3.029$ at 60 °C, where the $\log_{10}K$ values are taken from database p0c. The average solubility ratio was rounded to 3, given the large uncertainties in the rate data and in the effective surface areas. The feldspar dissolution rates were taken as equal to the quartz solubility rates, per the observations in Ref. 4 that quartz and feldspar rates are approximately equal. Mica dissolution rates were taken from Ref. 6.

It is recognized that there is uncertainty in the rates for silicate dissolution, and in the effective surface areas of the silicates. Since the total rate is the product of the surface area and the fundamental reaction rate (EQ6 **rk1**), our interest is really in the uncertainty of the product. In particular, the effect of the rate product on U-silicate precipitation is of interest, since U accumulation may be limited by the availability of dissolved silica. To this end, a simple sensitivity study was performed for root file names **Px2a0a0j** (surface area multiplier of 1), **Px2a0a2j** (surface area multiplier of 10, the default), and **Px2a0a!j** (surface area multiplier of 100; all files available on electronic media, Attachment II, Disk 1, "Case 1,2,4,5" folder). The case with area multiplier=1 deposited 0.0216 mols U per liter void space; the default case with area multiplier =10 deposited 0.0174 mols U per liter void space; and the case with area multiplier=100 deposited 0.0059 mols U per liter void space (taken from the respective ***.min_info.txt** files). Thus the default area multiplier of 10 is actually conservative compared to a multiplier of 100, and only slightly different from using the pure geometric surface area (multiplier=1). While silica dissolution is indeed necessary for U-silicate precipitation, the higher surface area also increases the dissolution of alkaline

components (e.g., albite feldspar), which increases the pH and therefore stabilizes aqueous U-carbonate complexes. Thus, the intuitive result that higher surface area would increase U deposition proved incorrect, and the overall effect of the surface area proved remarkably small. It follows that within this order of magnitude uncertainty, the exact rates of tuff silicate mineral dissolution are not that important.

The quantity of magnetite formed from steel in the invert was calculated in spreadsheet **Invert_EQ6_122299.xls**, sheet **'Norm for EQ6 input'** (Attachment II). The dimensions of the steel I-beams came from Ref. 1. The degradation rate for magnetite was set to consume all the magnetite in 10^3 y after breach. The calculations are not very sensitive to magnetite rates varying between complete consumption in 10^2 and 10^4 years. This insensitivity occurs because the diffusion rate of O_2 through the saturated invert is too small to effect a rise in fO_2 until all the magnetite is consumed, and in the reductive scenarios, the U and Pu deposition occurs early after WP breach. To be very conservative, it is assumed that all of the iron in the drift (in EBS materials) is available for this precipitation reaction (Assumption 3.17).

5.4 WATER FLUENCE FOR WP AND DILUTION RATES IN INVERT

In previous EQ6 calculations of WP degradation (e.g. Ref. 15, Assumption 3.12), it was assumed that all water dripping on the WP entered the WP, and was available for reaction with the waste forms; this assumption was conservative for internal criticality. The drip rate onto the package was then varied from 0.0015 m^3/y to 0.5 m^3/y (Ref. 15, Section 5.1.1.3).

For the present calculation, a different approach is required for two reasons. First, it is necessary to start with the defined drip rates from Ref. 15 (Table 6-1). Second, the conditions that are conservative for internal criticality are not necessarily those that are conservative for external criticality. External to the WP, dilution (and consequent lowering of pH and ionic strength) becomes a possible contributor to accumulation of actinides in the invert. It is necessary to specify the dilutions of the water that drains from within the WP by water that flows around the WP. The water flowing around the WP will have a composition much like the in-dripping (J-13-like) water, and will likely be of modest pH and low ionic strength.

The default approach used in this calculation is motivated by the VA (Ref. 9, Section 6.5.2). In the VA modeling, only a small fraction of the water dripping on the package is considered likely to enter the package. Figure 6-51 in Ref. 9 shows only ~1% of the on-dripping water enters the package in breaches before $5x10^4$ y; the remainder is largely diverted down the package sides.

For the calculations presented in Section 6, the default included an equal, diluting flow of J-13-like water in the invert. A sensitivity study was used to determine the effects of varying the amount of diluting flow by factors of 10 and 100.

5.5 NORMALIZATION OF INVERT CALCULATIONS FOR EQ6

All EQ6 invert calculations are normalized to $V_w \equiv 1$ liter, where V_w is the volume of water involved in the EQ6 calculations. This simplifies passage of aqueous compositions from one calculation to the next. The liter of aqueous phase, and the corresponding mass of initial tuff, are referred to as the sample system or subsystem. The volume V_{min} (in cm^3) of all tuff minerals in the subsystem is:

$$V_{min} = (1000\ cm^3/liter)*(1-\phi)/(\phi \cdot S) \quad \text{(Eq. 4)}$$

where ϕ is the fractional porosity (taken as 0.35; Ref. 3, Figure 9.4.9, gives ~30 to 40% for average sorting, from sand to cobbles), and S is the fractional saturation of the pore space. In this calculation, S is either 1.0 (complete saturation) or 0.1; the latter gives water contents that are comparable to the irreducible water content of average sands (Ref. 3, Figure 9.4.9). The cross-sectional area A, which the subsample presents to the dripping water, is given by:

$$A = V_w / (L \cdot \phi \cdot S), \quad \text{(Eq. 5)}$$

where L is the depth of the invert, taken as 72.1· cm. The average grain (or particle) density of the minerals in the subsample is taken as 2.5433 g/cm^3 (Ref. 26; Table 1, DTN: MO9708RIB00040.000), so the mass of minerals in the subsample is either 4.72 or 47.2 kg (for S of 1 and 0.1, respectively). For ease of use, the moles of deposited actinides in Table 6-1 were all converted to 4.72 kg mineral in the subsample.

For the EQ6 calculations, the drip rate into the subsample must be converted to a rate constant **rk1** (in moles/cm^2/s) for the "**DISPLACER**" reactant. To simplify the EQ6 calculations, a "mole" of the **DISPLACER** fluid is defined as 1000 g ~ 1000 cm^3. The **rk1** is then calculated as:

$$\mathbf{rk1}\ (\text{for } \mathbf{DISPLACER}) = (DR \cdot V_w \cdot f)/(FP \cdot L \cdot S \cdot \phi) \quad \text{(Eq. 6)}$$

where DR is the drip rate in liters/s (i.e., the drip rate in m^3/yearx1000/(seconds per year)), FP is the WP footprint in cm^2, and f is a focus factor (taken as 1 or 10) that allows investigation of the effects of focussing the drips from the WP through an area smaller than the FP. Thus, f=1 implies the water dripping out of the package is spread out uniformly over the area beneath the package, while f=10 implies the flow is focussed onto $1/10^{th}$ the footprint. For the displacer reactant, the surface area **sk** in the EQ6 file is set to 1.0 cm^2.

5.6 IMPLEMENTATION OF DIFFUSING REACTANTS

Diffusion-controlled oxygen access was used in all cases for which the sixth character of the root file name was not "**a**." These cases involve the existence of a reducing material at the bottom of the drift (magnetite from corrosion of steel), and oxidizing conditions at the top of the invert. The redox state at the invert bottom is then controlled by three principal factors: (1) the rate of reaction of the reduced material with coexisting aqueous solutions and gases; (2) the

transport of comparatively oxidized species (e.g. Pu(VI), HCO_3^-, SO_4^{2-}) in the percolating water; and (3) the diffusion of oxygen from above.

The diffusion control was implemented by creating a EQ6 special reactant called **O2_Water_diff**. The EQ6 **rk1** rate for this reactant is calculated in spreadsheet **Invert_EQ6_122299.xls**, on sheet **'Norm for EQ6 input'**. Steady-state diffusion along a linear concentration gradient, between the top and middle of the invert, is implicit in this calculation. Because the formal oxygen concentration in the reduced zone will be very low, the concentration gradient is taken as the concentration at the top of the invert divided by half the invert depth. One can calculate gaseous diffusion through air-filled pores or aqueous diffusion of O_2 through water-saturated pores; however, diffusion through air-filled pores is so fast that it immediately eliminates reducing conditions, so only the water-filled case is considered here. Thus the **rk1** in the EQ6 input files can be given a value:

$$\mathbf{rk1} = A \cdot D_m \cdot (\phi / \tau) \cdot (\Delta C)/(L/2) \qquad \text{(Eq. 7)}$$

where A is the cross-sectional area (perpendicular to the direction of drip travel), $L/2$ is the half-thickness of the invert, ΔC is the concentration difference expressed in moles/cm^3 (~2 (moles O_2) /cm^3 water at air saturation; the aqueous O_2 concentration is calculated as part of each EQ6 run, and is approximately constant for fO_2 ~0.2 atm), D_m is the molecular diffusion coefficient of O_2 in water, and τ is the tortuosity. Bear (Ref. 3 p. 111) recommends $\tau \sim 1/0.56$ to 1/0.8. We conservatively pick high τ~2 and ϕ ~0.35 to slow the rate of oxygen access and enhance actinide precipitation by reduction. The diffusion coefficient is estimated as ~2×10^{-5} cm^2/s; Ref. 42 (pp. F-61 and F-62) gives 1.77×10^{-5} cm^2/s for H_2S (which has a molecular weight similar to O_2) in water, and shows that the diffusion coefficients of small molecules in water are in the range of 1×10^{-5} to 4×10^{-5} cm^2/s. Reduction of sulfate virtually presumes bacterial mediation; however, bacteria that reduce sulfate and simultaneously oxidize steel are ubiquitous. (Ref. 8, Section 4.2.1.3.3).

5.7 FILENAME CODES

Nearly all of the conditions used for an EQ6 WP or invert run are encoded in the 8-character root file name; any other special conditions are described in the file header, and the file header is the ultimate source for the description of conditions. However, the following guide to file naming is provided as a convenience for the reader. All root file names begin with "P" for Pu-ceramic. All WP source term files follow the basic format indicated in Ref. 15 (Section 5.4.2); for the WP source terms used in this calculation, the second character in the name is **e**, **w**, or **^**; the "**^**" character is used only for a few source terms with pre-decay of Pu in the ceramic. When the second character is **e**, the ceramic rates are taken from the previous WP degradation study (Ref. 15, Table 5-3), as described in Section 5.3.1.2. When the second character is **w**, the ceramic rates are taken calculated as described in Section 5.3.1.2, using the newer, lower rates from LLNL (Ref. 38, Section 6).

For all invert file names, the second character is either **t** or **x**. Invert file names that have **t** as the second character pick up WP source terms that use the older Pu-ceramic degradation rates

(Section 5.3.1.2). Invert file names with **x** as the second character pick up WP source terms that use the newer LLNL Pu-ceramic degradation rates (Section 5.3.1.2). The remainder of the file name is encoded as follows.

The third character represents the revision number of the file.

The fourth character is **a**, **c**, **n**, **s**, **t**, or **u**, and represents the database used, as indicated in Section 5.1.1.

The fifth character distinguishes the WP source term used, and is usually a number from **0** to **9**.

The sixth character describes the oxidation state controls in place, and is **a** (fO_2 fixed at 0.2 bars), **n** (magnetite in invert, thin boundary layer) or **o** (magnetite in invert, boundary layer equals one half invert depth).

The seventh character is *SAF*, a combination code of *S* (saturation), *A* (invert mineral surface area multiplier), and *F* (flow focus factor). To encode these conditions in one number, the digits 0 through 7 correspond to *S,A,F* combinations of (0,0,0), (0,0,1), (0,1,0), (0,1,1), (1,0,0), (1,0,1), (1,1,0) and (1,1,1), respectively. The *S* code of 0 corresponds to 100% saturation, and the *S* code of 1 corresponds to 10% saturation; the *A* code of 0 indicates geometric surface area of tuff, while the *A* code of 1 indicates a factor 10 multiplier (the default); and an *F* code of 0 means a focus factor of 1 (no focussing), whereas an *F* code of 1 indicates a factor ten focussing. In one case (**Px2a0a!j**, a sensitivity study), the seventh character is "!"; for that case is like *SAF*=2, except the BET factor is increased to 100.

The eighth character indicates other special conditions, such as presence of a diluting flow of J-13-like water.

For any invert calculation, the corresponding WP source term is identified by the "special conditions" block at the bottom of the ***.min_info.txt** file. For example, the invert EQ6 file **px2u0a2j.6i** has an associated file **px2u0a2j.min_info.txt**, which contains the block:

```
===SPECIAL CONDITIONS======
mwtmax= 0.0000E+00 (0=not active)
Variable displacer USED:
|EQ6 input file name= pw2u1231.6i                                          |
|Description= React J-13 water with materials in ceramic waste package.|
Decay pairs:
Parent Daughter     Years Halflife
Pu     U            2.4100E+04
===END SPECIAL CONDITIONS======
```

The "variable displacer" **pw2u1231.6i** is the WP source term file.

6. RESULTS

This document may be affected by technical product input information that requires confirmation. Any changes to the document that may occur as a result of completing the confirmation activities will be reflected in subsequent revisions. The status of the input information quality may be confirmed by review of the Document Input Reference System database.

Section 6.1 summarizes the results in Table 6-1. Section 6.2 examines, in detail, several cases from Table 6-1. Section 6.3 examines the plausibility of maintaining oxidizing conditions in a WP "bathtub."

6.1 SUMMARY OF RESULTS

Table 6-1 summarizes results of the core accumulation calculations. The cases listed in Table 6-1 test the sensitivity of accumulation calculations to several primary factors. With the exception of the case codes beginning with the number 3, all cases allowed decay of Pu to U, using a half-life of 2.41×10^4 y. The decay begins after breach of the WP, not after emplacement, with the exception of case 6, which predecays the Pu by one halflife before breach of the WP.) The primary factors are indicated by the numbers 1-10 at the beginning of the case code in the first column of the table. The other characters in the case code provide a minimal shorthand for distinguishing factors in the filenames (such as the database or O_2 control; Section 5.7). A summary of the results in the table follows, broken down by the primary "code"; i.e., the number (1 through 10) that begins the Case Code in column 1 of Table 6-1.

Code 1: This group (1a, 1c, 1s, and 1u) tests the effects of database choice for scenarios with oxidizing conditions in the WP and in the invert. The flow out of the WP is not focussed; that is, it is spread evenly over the footprint of the WP (defined as variable **FP**= 76558 cm^2 in spreadsheet **Invert_EQ6_122299.xls**). For a true bathtub scenario, oxidizing conditions in the WP are unlikely, as shown in Section 6.3. All cases yield very low Pu accumulation, and cases 1a,1c, and 1s yield approximately the same U accumulation, despite the precipitation of different solubiliy-controlling phases (haiweeite and soddyite for 1a and 1c, and Na boltwoodite for 1s) and significant differences in the U silicate thermodynamic data. Case 1u produces ~2 times the U accumulation, apparently due to the "improved" ionic strength corrections (Section 5.1.2).

Code 2: This group (2a, 2s, and 2u) tests the effects of database choice for scenarios with oxidizing conditions in the WP, and reducing conditions in the invert. The flow out of the WP is not focussed; that is, it is spread evenly over the footprint of the WP. To maintain reducing conditions in the invert, the pore spaces must stay saturated with water for most of the time before breach of the WP; else the remnants of the carbon steel girders would oxidize and become inert. Pu and U accumulations are much greater than for Code 1 (oxidizing conditions in invert), but database effects are relatively unimportant.

Table 6-1. Summary of Invert U and Pu Accumulations

Case Code	Invert Case Root Name	Max Pu mols / liter Void[a]	Max U mols / liter Void[a]	Comments
1a	Px2a0a2j	5e-5	0.0174	This group tests effects of different thermodynamic data files (p0a, p0c, p0s, p0u). Oxidizing conditions in WP and invert, outlet fluence spread over entire shadow of WP. 1a and 1c produce haiweeite and soddyite as principal U solids; 1s and 1u produce Na boltwoodite (reported U adjusted for formula unit).
1c	Px2c0a2j	4e-5	0.0140	
1s	Px2s0a2j	3.9e-4	0.0152	
1u	Px2u0a2j	4.9e-4	0.0356	
2a	Px2a0o2j	0.0104	0.264	Baseline "reducing" cases. All have Fe_3O_4 that degrades over 10^3 years. O_2 diffuses in from drift. Requires constant saturation (all pore space filled with water), which is improbable.
2s	Px2s0o2j	0.0109	0.298	
2u	Px2u0o2j	0.0112	0.223	
3aa	pt1a1a2_	4e-5	1.7e-4	Group 3 is the only group in table to use a WP source term (pe1?1222) with higher water fluence (0.015 m^3/y, as opposed to 0.0015 m^3/y in remainder of table). One reduced case. Shows dramatic effect of lowering pH and ionic strength of WP solutions, by flushing system more rapidly.
3sa	pt1s1a2_	4e-5	3e-5	
3ua	pt1u1a2_	6.6e-5	4e-5	
3an	pt1a1n2_	0.0016	0.034	
4aa	Px2a0a3j[b]	1.3e-4	0.231	Test effects of focussing flow through $1/10^{th}$ of the WP footprint. Two reduced cases (o in sixth character place), one to test database effects. Compare to 1a, 2a, and 2u.
4ao	Px2a0o3j	0.104	0.370	
4uo	Px2u0o3j	0.112	0.564	
5	Px2n0o3j	0.105	0.186	Estimates the fraction of U deposited that is from HLW (~50%), by using HLW with all U replaced by Np. Compare with 4ao.
6	Px2ado3j	0.053	0.329	Test effect of pre-decaying system by one ^{239}Pu halflife. Compare with 4ao.
7ho	Px2aHo3j	0.123	ND[c]	Effects of varying solubility from base case. H and L in fifth character are for high (default EQ6 "Lemire" $Pu(OH)_4$) and low (PuO_2) solubility controls. S in fifth place means $SiO_{2(aq)}$ controlled by cristobalite (not chalcedony). Compare with 4ao and 4aa.
7lo	Px2aLo3j	0.0902	ND	
7ha	Px2aHa3j	0[d]	ND	
7la	Px2aLa3j	0.031	ND	
7sa	Px2aSa3j	1.2e-4	~0.2[e]	
8	Px2a0a6k	4e-6	0.0192	Effects of varying saturation to 10% of pore space. Compare with 1a.
9o6^	Px2a6o3^	0.246	≥ 0.59	Pu-ceramic corrosion rate sensitivity. "6" in fifth character is for source term Pw6a1231, with 5 times base case rate; "7" has 10 times base case rate, "8" has 100 times base case rate. 9o6^ pre-decays ^{239}Pu one halflife. Compare with 4ao.
9o6	Px2a6o3j	0.488	≥ 0.67	
9o7	Px2a7o3j	0.941	ND	
9o8	Px2a8o3j	2.02	ND	
10a!	Px2u0a2!	3.5e-5	0.0223	Test effects of increasing J-13-like side-fluence from default of 1x WP fluence (j or k ending) to 10x (! Ending) and 100x (@ ending). Compare with 1u (for 10a!) and 2u (for 10o! and 10o@). Effect is insignificant.
10o!	Px2u0o2!	0.0112	0.236	
10o@	Px2u0o2@	0.0112	0.228[f]	

NOTES: [a] Per 4.72 kg tuff (2.86 liters tuff, including 35% void space). The cases with "n" or "o" as the sixth character in root name have an additional 1.21 kg Fe (1.67 kg as Fe_3O_4). The number of significant digits reflects the precision to which mineral peak heights were read from plots. The moles of U for the different cases reflect varying levels of enrichment at various times. The selection of specific values used for criticality calculations is explained in Ref. 2.

[b] Focussed cases (with a 3 as seventh character) contact a volume of invert that is 72.1 cm deep by 7655.8 cm^2, or 5520 liters = 5.52 m^3. All other cases have deposition in full shadow of WP (76558 cm^2).

[c] Not determined; test did not achieve steady state for U-silicates because as the Pu decays to U, the quantity of U-silicates continues to increase.

[d] No Pu solids precipitated in invert.

[e] Case 7sa did not pass 17,000 years in 3 runs, so steady-state U accumulation is not known. However, U versus time trend is extremely close to 4aa, so final U accumulation is estimated to be about the same.

[f] U silicates begin precipitation as boltwoodite, but convert to uranophane at peak.

Code 3: This is the only group in the table (3aa, 3sa, 3ua, and 3na) to use a source term with higher fluence of in-dripping water (0.015 m^3, versus 0.0015 m^3 for the rest of the groups). The flow out of the WP is not focussed; that is, it is spread evenly over the footprint of the WP. It is also the only group without decay of Pu to U. The source term (**Pe??1222**) used the "average" Pu-ceramic rate from Ref. 15 (Section 5-3), which is ~1.4 times the default rate used in the rest of the groups. Yet, deposition is much lower in group 3, essentially because the higher fluence of in-dripping water flushes out dissolved HLW components (which lowers pH and dissolved carbonate), thus greatly reducing the solubility of the actinides.

Code 4: This group (4aa, 4ao, and 4uo) tests the effects of focussing the flow through $1/10^{th}$ the footprint under the WP. Compared to Cases 1a, 2a, and 2u, the deposition of U and Pu is increased, by factors ranging from ~2.6 to ~16. However, the deposition is only within a volume of ~0.55 m^3.

Code 5: This single case (5) is used to estimate the fraction of U that originates from HLW, versus the Pu-ceramic. The flow out of the WP is focussed through $1/10^{th}$ the footprint under the WP. The estimate is made by replacing all the UO_2 in the HLW with chemically similar NpO_2. By comparison with case 4ao, it is estimated that approximately 50% of the U originates from the HLW, for the reduced, focussed-flow cases with the baseline Pu-ceramic degradation rate.

Code 6: This single case (6) tests the effects of pre-decaying the Pu in the ceramic by one halflife of ^{239}Pu (2.41×10^4 y; Ref. 34). The flow out of the WP is focussed through $1/10^{th}$ the footprint under the WP. The Pu deposition is reduced by ~1/2; this result is not surprising, since no stable Pu solid forms in the WP during the time of Pu deposition in the invert, so the Pu concentration in the WP is determined almost entirely by the competition between the ceramic degradation rate and the fluence of water from within the WP.

Code 7: This group (7ho, 7lo, 7ha, 7la) tests the effects of varying the stability constants of the Pu solubility-controlling phases (either $Pu(OH)_4$ or PuO_2; see Section 5.1.3) and the dominant silica polymorph (7sa). The flow out of the WP is focussed through $1/10^{th}$ the footprint under the WP. For the reduced cases (7ho and 7lo), the effect is stunningly small; this is expected, for two reasons. First, there is no stable Pu solid in the WP at the time of highest aqueous Pu, so the Pu concentration entering the invert is independent of the stability constants; and second, the reduced invert is so far from equilibrium with the oxidized WP solutions, that even soluble Pu solids are adequate to cause precipitation. For the oxidized cases (7ha and 7la), the low-solubility PuO_2 (7la) produces ~238 as much deposition; however, the amount of deposited Pu is still quite small. Case 7sa shows that the effects of assuming cristobalite saturation, instead of chalcedony saturation are quite small. This result may seem remarkable, given that the precipitation of U-silicates depends heavily on the dissolved silica concentration, and cristobalite engenders a much higher dissolved silica; however, the silica concentration in these runs is actually controlled by other silicates (clays, zeolites or Ni_2SiO_4) during the times of greatest U-silicate deposition.

Code 8: This single case (8) tests the effect of changing the saturation to only 10% of the void space (all other cases assume 100% saturation). The flow out of the WP is not focussed; that

is, it is spread evenly over the footprint of the WP. Effectively, this case increases the mass and surface area of invert minerals seen by the fluid that passes through the invert. However, it also decreases the residence time of the fluid in the invert. Compared to 1a, Pu deposition is reduced by a factor ~8, but U deposition in the invert is approximately the same.

Code 9: This group (9o6^, 9o6, 9o7, and 9o8) provides a sensitivity study on the importance of the Pu-ceramic corrosion rate; it can be compared with case 4ao. The case 9o6^ pre-decays the Pu to U over one halflife of ^{239}Pu. The flow out of the WP is focussed through $1/10^{th}$ the footprint under the WP, and the conditions are reducing. For these conditions, the increase in Pu deposition varies almost linearly with the ceramic corrosion rate, up to a factor 10 increase in the corrosion rate; at higher corrosion rates, the aqueous Pu concentration in the WP source term becomes mass-limited. These results are not unexpected; as outlined above, the Pu concentration in the WP source term is expected to vary almost linearly with ceramic corrosion rate (since no Pu solid precipitates in the WP during the time of peak Pu loss), and the invert conditions are so out of equilibrium with the source term, almost every bit of Pu that enters the invert precipitates.

Code 10: This group tests the effects of increasing the amount of diluting J-13-like water added to the invert (by diversion around the WP, as discussed in Section 5.4); the cases may be compared with 2u. The flow out of the WP is not focussed; that is, it is spread evenly over the footprint of the WP. The effect of increasing the dilution by a factor of 100 is small.

6.2 DETAILS OF CASES 4AO, 7SA, 9O7, AND 9O8

In all but one of the EQ6 runs, all SiO_2 polymorphs with solubilities lower than that of chalcedony (e.g., quartz) are suppressed. Thus in many calculations, chalcedony precipitates and polymorphs with higher solubility (e.g., cristobalite) do not. However, cristobalite exists in the YMP tuffs (Ref. 31, p. F27), and the concentration of dissolved silica in J-13 well water is substantially above chalcedony saturation. Since the solubilities of uranium silicates such as haiweeite, soddyite and Boltwoodite-Na are controlled partly by the concentration of aqueous silica, it is important to determine if higher aqueous SiO_2 contents, determined by cristobalite saturation, would enhance precipitation of U-silicates. A pair of WP-Invert runs, forced to cristobalite saturation (Pw2a123S and Px2aSa3j; Table 6-1), were used to test this hypothesis.

Figure 6-1 compares the results of the runs with soluble (cristoblite) and comparatively insoluble (chalcedony) SiO_2 solids. The Px2aSa3j series (Code 7sa in Table 6-1) could not be carried out to steady state because of small step size; however, it is clear from the figure that the cristobalite case tracks the default chalcedony case very closely, causing no enhancement of the U-silicate precipitation. The likely cause is that for most of the runs in the WP and invert, aqueous SiO_2 is controlled not by the silica polymorphs, but by other silicates (e.g. clays).

Figure 6-2 shows the effects of varying the Pu-ceramic degradation rate above the base case rate of $8x10^{-15}$ mols/(cm^2·s), where a "mol" is defined as 100 g of ceramic. The base case rate is an average value for 50 °C, which includes a conservative factor 30 multiplier for radiation damage (see Section 5.3.1.2). The higher rates might correspond to large increases in the

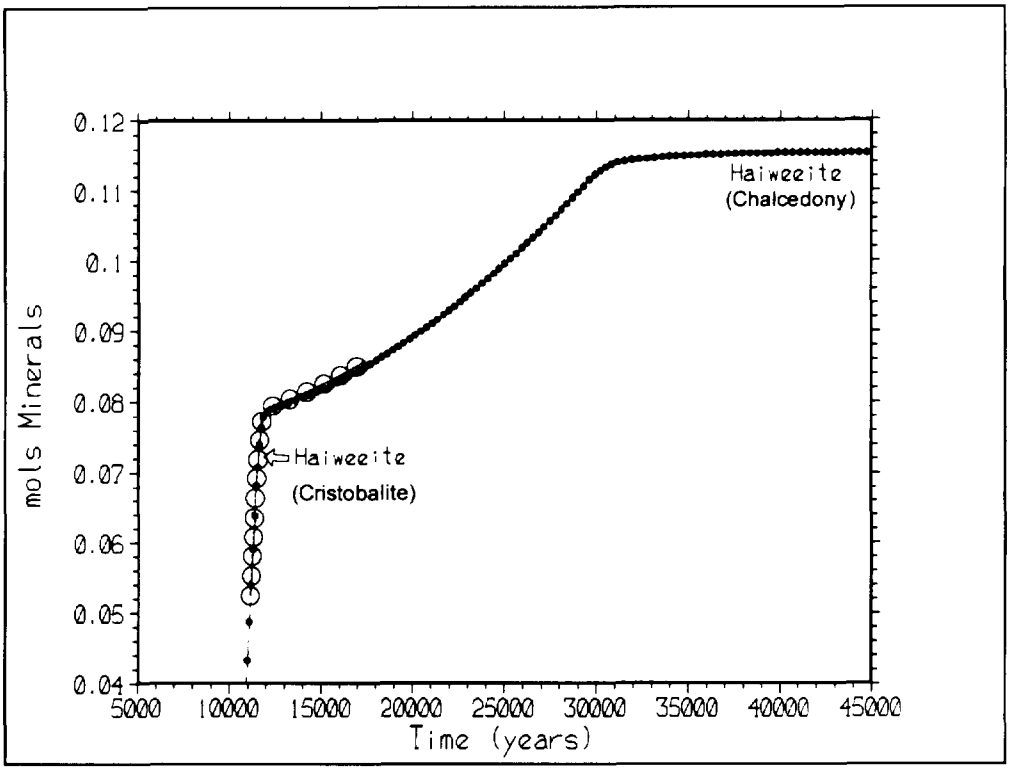

NOTE: Open circles denote cristobalite case. Small solid circles denote chalcedony case.

Figure 6-1. Effect of SiO_2 Control on U-Silicate Precipitation

effective surface area, due to fracturing of the pucks during manufacturing or excessive connected pore space. The units of "mols" on the left axis of the figure are per liter of void space in the invert, which corresponds to per ~4.72 kg tuff.

6.3 OXYGEN AND CO_2 FUGACITIES IN WP DETERMINED BY DIFFUSION AND DEGRADATION RATES

In this calculation, and in most previous EQ6 calculations associated with the YMP, it has been assumed that the fluids inside the WP are well mixed by convection, and an oxidizing atmosphere is thus sustained by communication with the atmosphere external to the WP. However, it is instructive to consider the likelihood of maintaining an oxidizing environment in the WP, which contains large masses of reduced materials (steels and the UO_2 component of the ceramic).

The `Pela1231` source term (hereafter referred to as wp0 source term), produces high Pu and U loss because it is oxidizing, and because the rapid degradation of the HLW, combined with the fixed fCO_2, yields an alkaline carbonate solution. In addition, the rapid degradation of the ceramic exposes the actinides to these hostile conditions. (This run was performed early in the preparation of this calculation, and used the "high" rate of ~3.47×10^{-13} mols/(cm^2·s) from

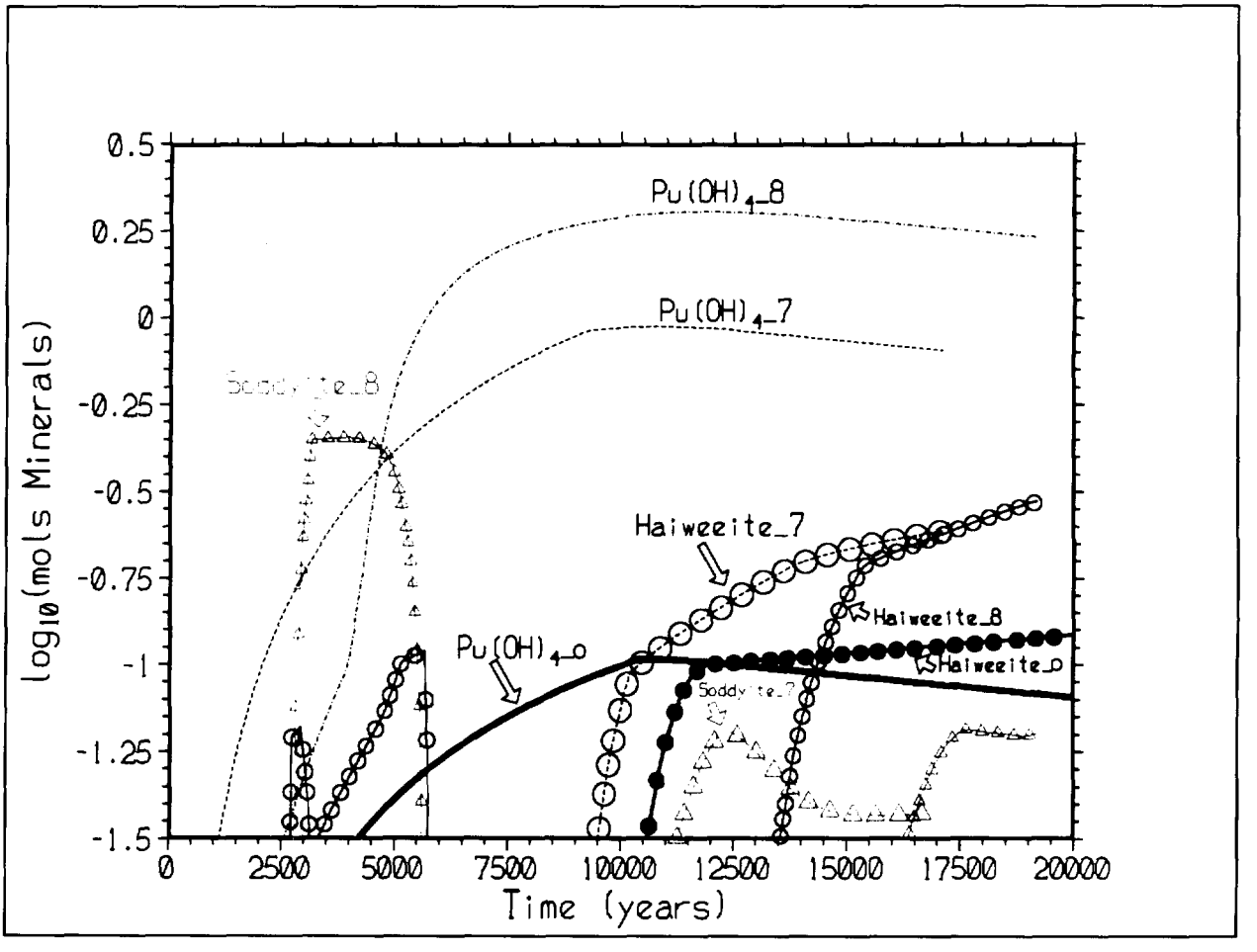

NOTE: Reducing conditions: "_o" endings for Case 4ao, with base case rate; "_7" endings for case 9o7, 10 times base case rate; "_8" endings for Case 9o8, 100 times base case rate.

Figure 6-2. Pu-Ceramic Degradation Rate Sensitivity, Accumulation in Invert

Table 5-3 of Ref. 15.) However, the rapid degradation rates imply the accumulation of substantial degradation products in the form of hematite and smectite clays. The wp0 source term generates minerals amounting to 20% of the WP void volume within ~$2x10^3$ years; and 50% of the void volume within ~$5x10^3$ years. These calculated volumes do not include the water entrapped among the particles (or porosity), which can cause the actual volume of corrosion products to exceed twice the volume of the particles. Thus, with the degradation rates assumed in the wp0 source term, the WP should rapidly fill with corrosion products and alteration minerals, which will mantle the degrading WP materials. There may well be convection cells within more open spaces of the package, but transport of oxygen to most "fresh" WP materials will be limited by diffusion through the water-filled pores of the mud. It is, thus, likely that there will be substantial variations of fO_2 within the system; since the Pu-ceramic itself is reducing, the local environment of the ceramic is also likely to be reducing.

Three source term runs were used to test the effects of diffusion-controlled O_2 access: wp2, wp3 and wp4 (corresponding to files **Pe2a1231.6i**, **Pe3a1231.6i**, and **Pe4a1231.6i** on the electronic media, Attachment II, Disk 1, "Diffuse Oxygen" folder). For wp2, the O_2 diffusion was limited by a 1-cm diffusive boundary layer, but CO_2 addition was controlled only by the dissolved carbonate in the in-dripping, J-13-like water. As with the wp0 source term, all the components of the WP were assumed to be exposed and available for reaction with the water at the same time. Run wp3 is the same as wp2, except CO_2 diffusion control was added. This control is achieved with a reactant, analogous to the O_2 diffusive reactant described in Section 5.6, with an **rk1** proportional to both the ambient CO2 fugacity (10^{-3} bars) and the Henry's Law constant for CO_2 (aq) / CO_2 (g) (The Henry's Law constant, $10^{(6.3447-7.8136)}$, is determined by the $\log_{10}K$ values in database p0a). Figure 6-3 compares the Pu and U aqueous concentrations for runs wp2 and wp3; except for a brief spike of U concentration in the latter run, there is comparatively little difference in the calculated concentrations.

It could be argued that source terms wp2 and wp3 are not conservative because they assume a boundary layer (1 cm thick) exists from the inception of the run, whereas a significant mantling with rust and altered glass would not exist for the first few hundred years of water influx. In addition, runs wp2 and wp3 do not model the fill period, before the WP reaches the "overflowing bathtub" state. Run wp4 addresses these shortcomings by splitting the calculation into two stages. The first stage fills the WP without allowing water to escape, and fixes the fO_2 at 0.2 bars; the stage ends when the carbon steel support structure (referred to as the "outer web" in Ref. 15) is completely degraded. The second stage begins the flow-through (SCFT) mode, and allows the fO_2 to be determined by the competition between diffusion and reaction. The boundary layer is taken as 10 cm in thickness.

The source term wp2 and wp3 cases can be eliminated from further consideration because they produce aqueous concentrations that are too low, or of too short duration, to produce significant accumulations of U or Pu in the invert. For example, the aqueous Pu peak in Figure 6-4 endures for ~$2x10^4$ years, and has a maximum concentration of ~$3x10^{-7}$ molal (molality is ~molarity for this case). The maximum Pu that can leave the package to be deposited in the invert or fractured tuff is, thus, ($2x10^4$ years) x (1.5 liters/year) x ($3x10^{-7}$ moles/liter) = 0.009 moles ~ 2.2 g, which is not a fissionable mass in any configuration.

The source term wp4 case generates initial high aqueous U and Pu concentrations. These high aqueous concentrations are due entirely to the presumption of oxidizing conditions and exposure of the ceramic in the first "filling" stage. When the fO_2 is allowed to drift in the second stage (that is, to be determined by the competition between O_2 diffusion and consumption of the steel and ceramic), the Pu and U concentrations plummet. The Pu spike is so brief, about two years duration, it does not even appear on the truncated scale of Figure 6-5; however, the U spike reaches ~0.03 M for $2x10^2$ years., for ~9 moles or ~2 kg U released for a single WP. This amount will also not constitute a fissile mass by itself, particularly since it will consist primarily of depleted U from HLW and Pu-ceramic degradation.

Figure 6-6 compares the invert Pu and U accumulations for run **Pt1a4n3_** (which uses the wp4 source term, discussed in the previous paragraph), and run **Pt1a0n3_** (which uses the

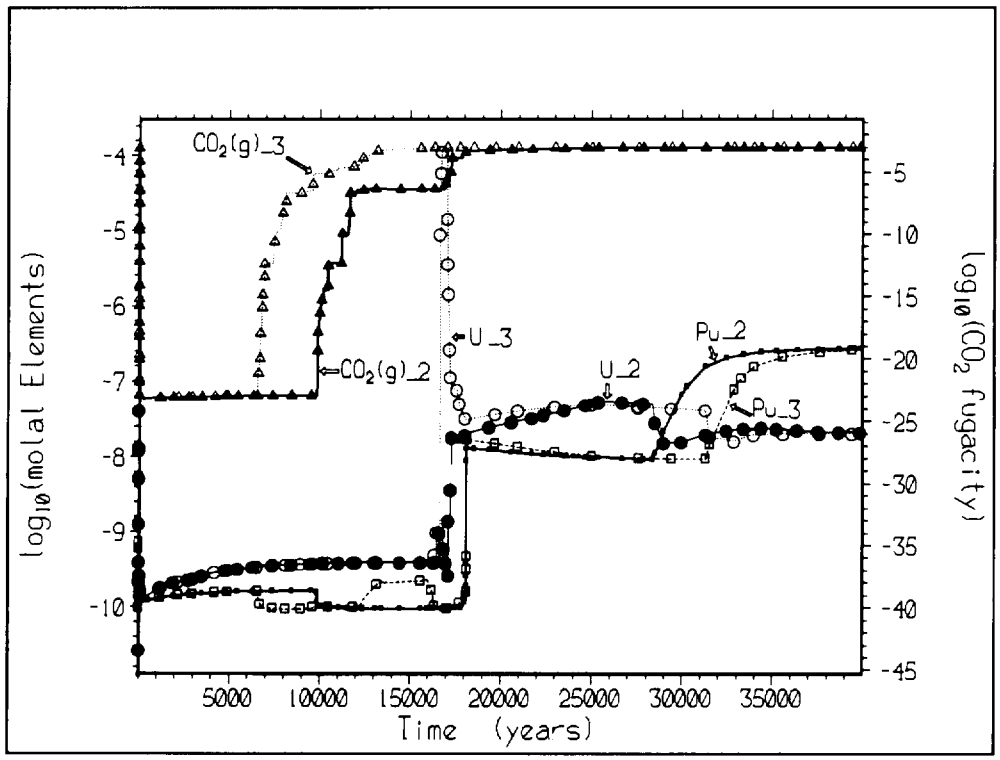

NOTE: Run wp2 [filled symbols and "_2" endings] has CO_2 determined by in-dripping water; run wp3 [open symbols and "_3" endings] also has diffusion control for CO_2

Figure 6-3. In-WP Reducing Conditions with and without CO_2 Diffusion

default oxidizing source term from wp0) (Attachment II, Disk 1, "Diffuse Oxygen" folder). The deposition of U and Pu is greatly lowered in the run with the low-fO_2 source term; in fact, there is no actinide accumulation after ~$6x10^3$ years. The maximum uraninite (UO_2) accumulation is ~0.041 mols / (liter void space); in this scenario, where the flow is focussed in $1/10^{th}$ the area under the WP, the total deposited U mols, in ~193 liters void space (**Invert_EQ6_122299.xls**, sheet '**Norm for EQ6 Input**') is ~8 mols. That is, most or all of the U lost from the package was deposited in the focussed flow zone.

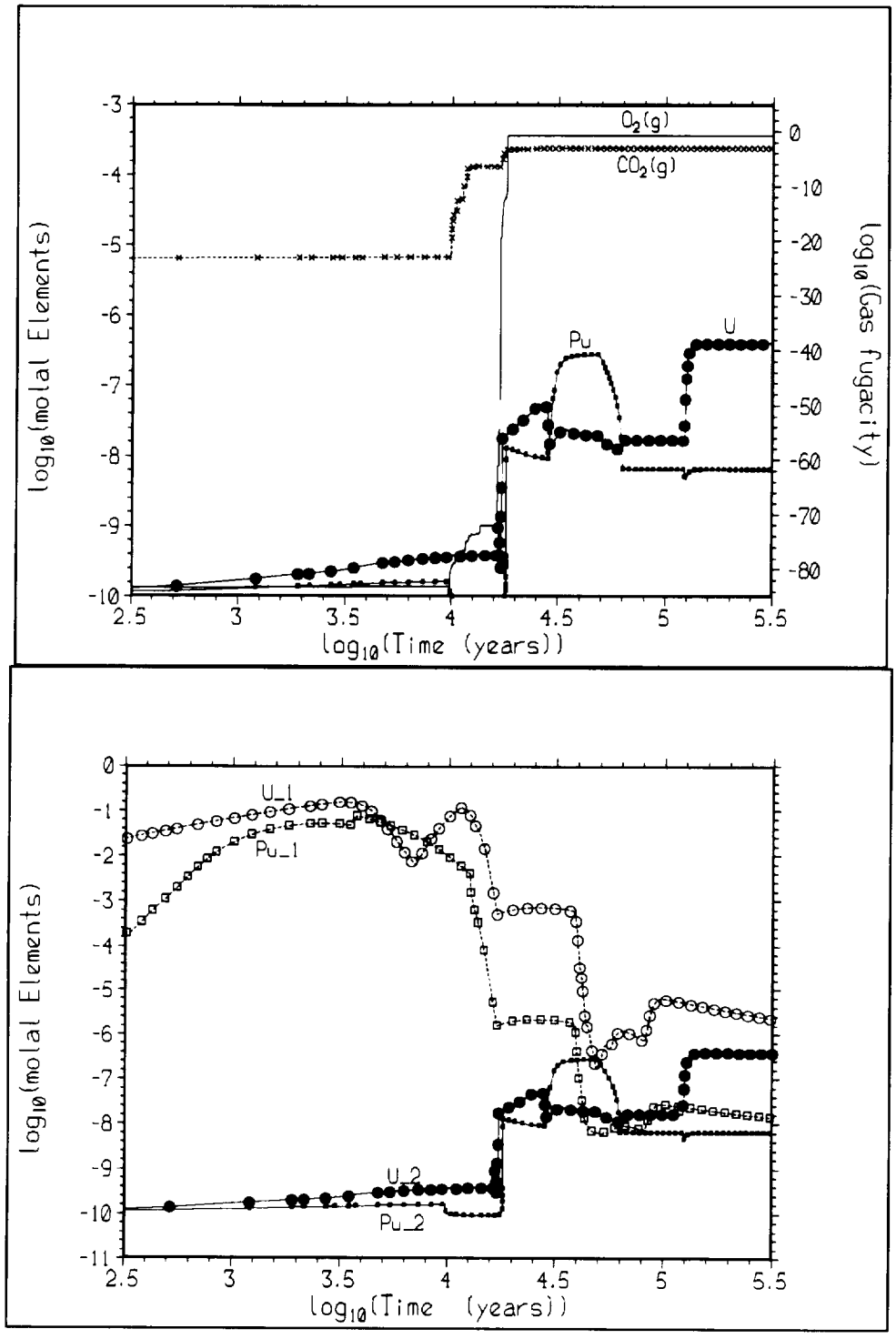

NOTE: Top plot gives gas fugacities and aqueous U and Pu for wp2; bottom plot compares aqueous U and Pu for wp2 (U_2 and Pu_2) against aqueous U and Pu for base case Pe1a1231 (U_1 and Pu_1).

Figure 6-4. In-WP, Source Term wp2, Reducing Conditions

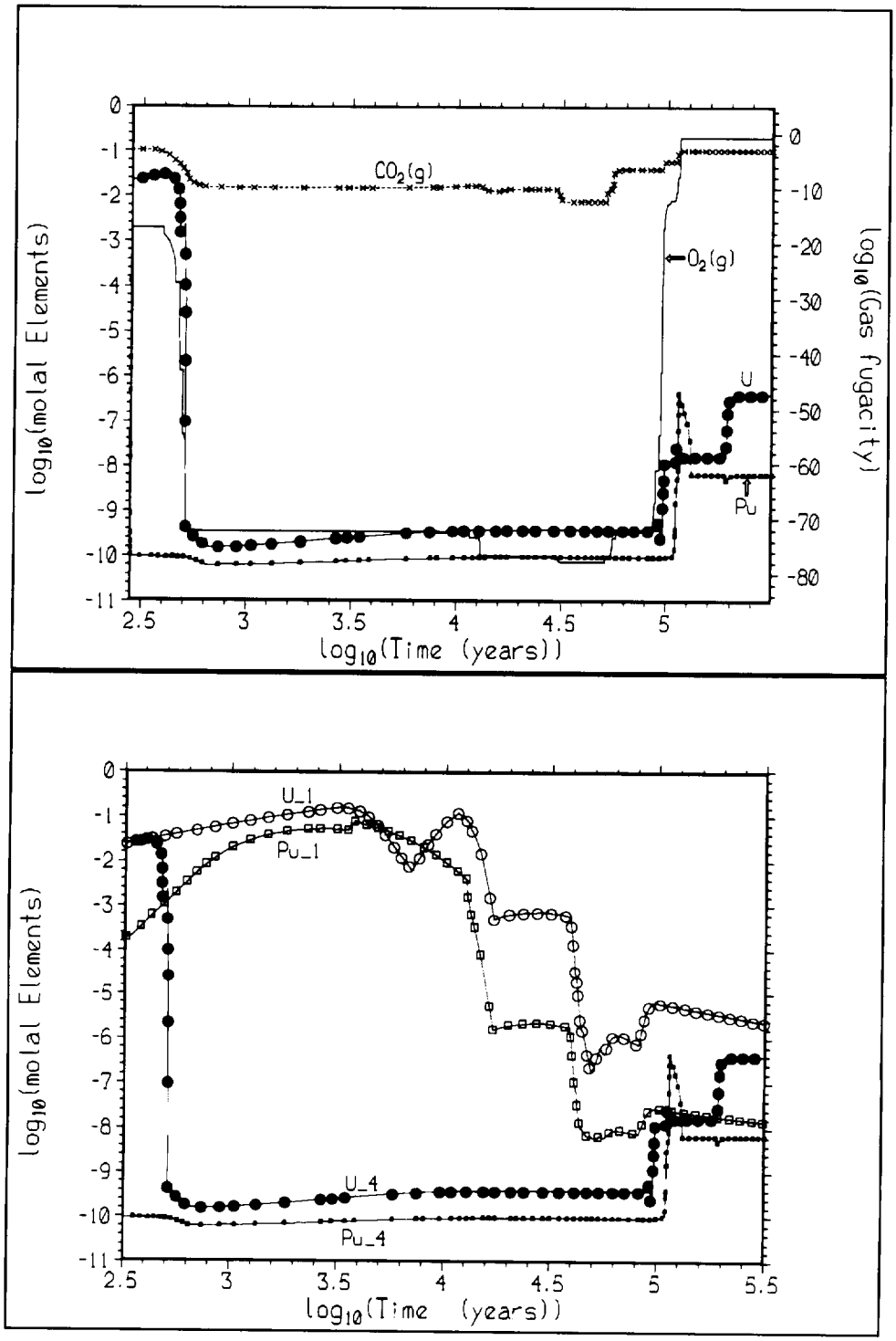

NOTE: Top plot gives gas fugacities and aqueous U and Pu for wp2; bottom plot compares aqueous U and Pu for wp4 (U_4 and Pu_4) against aqueous U and Pu for base case Pe1a1231 (U_1 and Pu_1.

Figure 6-5. In-WP, Source Term wp4, Reducing Conditions

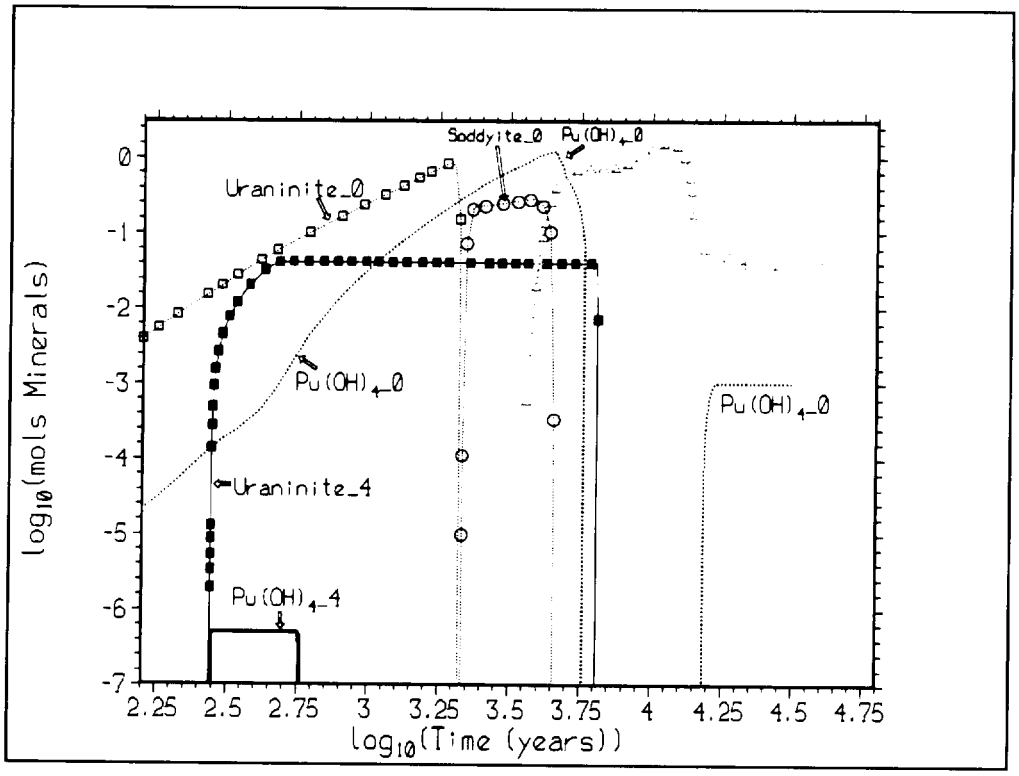

NOTE: Dashed lines, open symbols and "_4" ending on names for Pt1a4n3_; unbroken lines, filled symbols and "_0" ending for Pt1a0n3_.

Figure 6-6. Invert Pu and U Accumulation Compared for Pt1a4n3_ and Pt1a0n3_

7. REFERENCES

1. AISC (American Institute of Steel Construction) 1991. *Manual of Steel Construction, Allowable Stress Design.* 9th Edition. Chicago, Illinois: American Institute of Steel Construction. TIC: 4254.

2. CRWMS M&O 2000. *Probability of External Criticality of Plutonium Disposition Waste Forms.* CAL-EBS-NU-000011 REV 00. Las Vegas, Nevada: CRWMS M&O. ACC: MOL.20000920.0164.

3. Bear, J. 1988. *Dynamics of Fluids in Porous Media.* New York, New York: Dover Publications. TIC: 217568.

4. Brady, P.V and Walther, J.V. 1989. "Controls on Silicate Dissolution Rates in Neutral and Basic pH Solutions at 25° C Modeling." *Geochimica et Cosmochimica Acta, 53,* 2823-2830. New York, New York: Pergamon Press. TIC: 235216.

5. Brady, P.V. and Walther, J.V. 1990. "Kinetics of Quartz Dissolution at Low Temperatures." *Chemical Geology, 82,* 253-264. Amsterdam, The Netherlands: Elsevier Science Publishers B.V. TIC: 235349.

6. Knauss, K.G. and Wolery, T.J. 1989. "Muscovite Dissolution Kinetics as a Function of pH and Time at 70°C." *Geochimica et Cosmochimica Acta, 53,* 1493-1501. Elmsford, New York: Pergamon Press. TIC: 236215.

7. CRWMS M&O 1996. *Second Waste Package Probabilistic Criticality Analysis: Generation and Evaluation of Internal Criticality Configurations.* BBA000000-01717-2200-00005 REV 00. Las Vegas, Nevada: CRWMS M&O. ACC: MOL.19960924.0193.

8. CRWMS M&O 1998. "Near-Field Geochemical Environment." Chapter 4 of *Total System Performance Assessment-Viability Assessment (TSPA-VA) Analyses Technical Basis Document.* B00000000-01717-4301-00004 REV 01. Las Vegas, Nevada: CRWMS M&O. ACC: MOL.19981008.0004.

9. CRWMS M&O 1998. "Waste Form Degradation, Radionuclide Mobilization, and Transport Through the Engineered Barrier System." Chapter 6 of *Total System Performance Assessment-Viability Assessment (TSPA-VA) Analyses Technical Basis Document.* B00000000-01717-4301-00006 REV 01. Las Vegas, Nevada: CRWMS M&O. ACC: MOL.19981008.0006.

10. CRWMS M&O 1998. "Waste Package Degradation Modeling and Abstraction." Chapter 5 of *Total System Performance Assessment-Viability Assessment (TSPA-VA) Analyses Technical Basis Document.* B00000000-01717-4301-00005 REV 01. Las Vegas, Nevada: CRWMS M&O. ACC: MOL.19981008.0005.

11. CRWMS M&O 1998. *EQ6 Calculations for Chemical Degradation of Fast Flux Test Facility (FFTF) Waste Packages.* BBA000000-01717-0210-00028 REV 00. Las Vegas, Nevada: CRWMS M&O. ACC: MOL.19981229.0081.

12. CRWMS M&O 1998. *EQ6 Calculations for Chemical Degradation of Pu-Ceramic Waste Packages.* BBA000000-01717-0210-00018 REV 00. Las Vegas, Nevada: CRWMS M&O. ACC: MOL.19980918.0004.

13. CRWMS M&O 1997. *Evaluation of the Potential for Deposition of Uranium/Plutonium from Repository Waste Packages.* BBA000000-01717-0200-00050 REV 00. Las Vegas, Nevada: CRWMS M&O. ACC: MOL.19980216.0001.

14. CRWMS M&O 1998. *Software Qualification Report (SQR) Addendum to Existing LLNL Document UCRL-MA-110662 PT IV: Implementation of a Solid-Centered Flow-Through Mode for EQ6 Version 7.2B.* CSCI: UCRL-MA-110662 V 7.2b. SCR: LSCR198. Las Vegas, Nevada: CRWMS M&O. ACC: MOL.19990920.0169.

15. CRWMS M&O 1999. *EQ6 Calculation for Chemical Degradation of Pu-Ceramic Waste Packages: Effects of Updated Materials Composition and Rates.* CAL-EDC-MD-000003 REV 00. Las Vegas, Nevada: CRWMS M&O. ACC: MOL.19990928.0235.

16. CRWMS M&O 2000. *Invert Configuration and Drip Shield Interface.* TDR-EDS-ST-000001 REV 00. Las Vegas, Nevada: CRWMS M&O. ACC: MOL.20000505.0232.

17. CRWMS M&O 2000. *Monitored Geologic Repository Project Description Document.* TDR-MGR-SE-000004 REV 01 ICN 02. Las Vegas, Nevada: CRWMS M&O. Submit to RPC URN-0529

18. CRWMS M&O 1999. *One (1) Compact Diskette for Electronic Data for EQ6 Calculation for Chemical Degradation of Pu-Ceramic Waste Packages: Effects of Updated Materials Composition and Rates.* CAL-EDC-MD-000003 REV 00. Las Vegas, Nevada: CRWMS M&O. ACC: MOL.19990923.0238.

19. CRWMS M&O 2000. *Water Diversion Model.* ANL-EBS-MD-000028 REV 00. Las Vegas, Nevada: CRWMS M&O. ACC: MOL.20000107.0329.

20. CRWMS M&O 2000. Process Control Evaluation for Supplement V: "In-Drift Accumulation of Fissile Material From Waste Package Containing Plutonium Disposition Waste Forms (21019074M1)". Las Vegas, Nevada: CRWMS M&O. ACC: MOL.20000828.0122.

21. CRWMS M&O 2000. *Defense High Level Waste Glass Degradation.* ANL-EBS-MD-000016 REV 00. Las Vegas, Nevada: CRWMS M&O. ACC: MOL.20000329.1183.

22. CRWMS M&O 2000. *Validation Test Report for EQ6 V7.2bLV.* SDN: 10075-VTR-7.2bLV-00. Las Vegas, Nevada: CRWMS M&O. ACC: MOL.20000124.0135.

23. Daveler, S.A. and Wolery, T.J. 1992. *EQPT, A Data File Preprocessor for the EQ3/6 Software Package. User's Guide, and Related Documentation (Version 7.0).* UCRL-MA-110662 PT II. Livermore, California: Lawrence Livermore National Laboratory. TIC: 205240.

24. DOE (U.S. Department of Energy) 1998. *Total System Performance Assessment.* Volume 3 of *Viability Assessment of a Repository at Yucca Mountain.* DOE/RW-0508. Washington, D.C.: U.S. Department of Energy, Office of Civilian Radioactive Waste Management. ACC: MOL.19981007.0030.

25. Efurd, D.W.; Runde, W.; Banar, J.C.; Janecky, D.R.; Kaszuba, J.P.; Palmer, P.D.; Roensch, F.R.; and Tait, D. 1998. "Neptunium and Plutonium Solubilities in a Yucca Mountain Groundwater. "*Environmental Science & Technology, 32,* (24), 3893-3900. Easton, Pennsylvania: Environmental Science & Technology. TIC: 243857.

26. MO9708RIB00040.000. RIB Item #40/Rev. 0: Hydrologic Characteristics: Hydrogeologic Unit Characteristics. Submittal date: 08/29/1997. Submit to RPC URN-0534 .

27. Grenthe, I.; Ferri, D.; Salvatore, F; and Riccio, G. 1984. "Studies on Metal Carbonate Equilibria. Part 10.† A Solubility Study of the Complex Formation in the Uranium (VI)-Water-Carbon Dioxide (g) System at 25 Degrees C." *Journal of the Chemical Society, Dalton Transactions,* 2439-2443. London, England: Royal Society of Chemistry. TIC: 236325.

28. Grenthe, I.; Fuger, J.; Konings, R.J.M.; Lemire, R.J.; Muller, A.B.; Nguyen-Trung, C.; and Wanner, H. 1992. *Chemical Thermodynamics of Uranium.* Volume 1 of *Chemical Thermodynamics.* Wanner, H. and Forest, I., eds. Amsterdam, The Netherlands: North-Holland Publishing Company. TIC: 224074.

29. Harrar, J.E.; Carley, J.F.; Isherwood, W.F.; and Raber, E. 1990. *Report of the Committee to Review the Use of J-13 Well Water in Nevada Nuclear Waste Storage Investigations.* UCID-21867. Livermore, California: Lawrence Livermore National Laboratory. ACC: NNA.19910131.0274.

30. LA9912WR831372.004. EQ Database for Np, Pu, and Tc Solubility Calculations. Submittal date: 12/09/1999.

31. Lipman, P.W.; Christiansen, R.L.; and O'Connor, J.T 1966. *A Compositionally Zoned Ash-Flow Sheet in Southern Nevada.* Professional Paper 524-F. Washington, D.C.: U.S. Geological Survey. TIC: 219972.

32. LLNL (Lawrence Livermore National Laboratory) 1998. *Plutonium Immobilization Project Data for Yucca Mountain Total Systems Performance Assessment, Rev. 1.* PIP 98-012. Livermore, California: Lawrence Livermore National Laboratory. ACC: MOL.19980818.0349.

33. NRC (U.S. Nuclear Regulatory Commission) 1999. *Issue Resolution Status Report Key Technical Issue: Radionuclide Transport.* Rev. 1. Washington, D.C.: U.S. Nuclear Regulatory Commission. ACC: MOL.19991214.0621.

34. Parrington, J.R.; Knox, H.D.; Breneman, S.L.; Baum, E.M.; and Feiner, F. 1996. *Nuclides and Isotopes, Chart of the Nuclides.* 15th Edition. San Jose, California: General Electric Company and KAPL, Inc. TIC: 233705.

35. Rai, D. and Ryan, J.L. 1982. "Crystallinity and Solubility of Pu(IV) Oxide and Hydrous Oxide in Aged Aqueous Suspensions. "*Radiochimica Acta, 30,* 213-216. Munchen, Germany: R. Oldenbourg Verlag. TIC: 219107.

36. Rimstidt, J.D. and Barnes, H.L 1980. "The Kinetics of Silica-Water Reactions. "*Geochimica et Cosmochimica Acta, 44,* 1683-1699. Oxford, England: Pergamon Press. TIC: 219975.

37. Roberts, W.L.; Rapp, G.R., Jr.; and Weber, J. 1974. *Encyclopedia of Minerals.* 1st Edition. New York, New York: Van Nostrand Reinhold Company. TIC: 241917.

38. Shaw, H., ed. 1999. *Plutonium Immobilization Project Input for Yucca Mountain Total Systems Performance Assessment.* PIP-99-107. Livermore, California: Lawrence Livermore National Laboratory. TIC: 245437.

39. Spahiu, K. and Bruno, J. 1995. *A Selected Thermodynamic Database for REE to be Used in HLNW Performance Assessment Exercises.* SKB Technical Report 95-35. Stockholm, Sweden: Swedish Nuclear Fuel and Waste Management Company. TIC: 225493.

40. Stockman, H.W. 1994. *PP: A Graphics Post-Processor for the EQ6 Reaction Path Code.* SAND94-1955. Albuquerque, New Mexico: Sandia National Laboratories. TIC: 241246.

41. SN9908T0872799.004. Tabulated In-Drift Geometric and Thermal Properties Used in Drift-Scale Models for TSPA-SR (Total System Performance Assessment-Site Recommendation). Submittal date: 08/30/1999.

42. Weast, R.C. and Astle, M.J., eds. 1978. *CRC Handbook of Chemistry and Physics.* 59th Edition. pp. D-265, D-299, D-300, -304 , F-61 and F-62. Boca Raton, Florida: CRC Press. TIC: 246395.

43. Wilson, C.N. and Bruton, C.J. 1989. *Studies on Spent Fuel Dissolution Behavior Under Yucca Mountain Repository Conditions.* PNL-SA-16832. Richland, Washington: Pacific Northwest Laboratory. ACC: HQX.19890918.0047.

44. Wolery, T.J. 1992. *EQ3/6, A Software Package for Geochemical Modeling of Aqueous Systems. Package Overview and Installation Guide (Version 7.0).* UCRL-MA-110662 PT I. Livermore, California: Lawrence Livermore National Laboratory. TIC: 205087.

45. Wolery, T.J. 1992. *EQ3NR, A Computer Program for Geochemical Aqueous Speciation-Solubility Calculations. Theoretical Manual, User's Guide, and Related Documentation*

(Version 7.0). UCRL-MA-110662 PT III. Livermore, California: Lawrence Livermore National Laboratory. TIC: 205154.

46. Wolery, T.J. and Daveler, S.A. 1992. *EQ6, A Computer Program for Reaction Path Modeling of Aqueous Geochemical Systems: Theoretical Manual, User's Guide, and Related Documentation (Version 7.0).* UCRL-MA-110662 PT IV. Livermore, California: Lawrence Livermore National Laboratory. TIC: 205002.

47. YMP (Yucca Mountain Site Characterization Project) 1998. *Disposal Criticality Analysis Methodology Topical Report.* YMP/TR-004Q, Rev. 0. Las Vegas, Nevada: Yucca Mountain Site Characterization Office. ACC: MOL.19990210.0236.

48. CRWMS M&O 1998. "Disruptive Events." Chapter 10 of *Total System Performance Assessment-Viability Assessment (TSPA-VA) Analyses Technical Basis Document.* B00000000-01717-4301-00010 REV 01. Las Vegas, Nevada: CRWMS M&O. ACC: MOL.19981008.0010.

49. CRWMS M&O 1999. *User's Manual for EQ6 V7.2bLV.* SDN: 10075-ITP-7.2bLV-00. Las Vegas, Nevada: CRWMS M&O. ACC: MOL.20000126.0158.

50. Runde, W. 1999. "Letter Report on Uranyl(VI) Silicate Thermodynamic Database." Memorandum from W. Runde (LANL) to P. Dixon (LANL), May 27, 1999, LA-CST-TIP-88-004, with attachment. ACC: MOL.20000223.0499.

51. CRWMS M&O 2000. *Far-Field Accumulation of Fissile Material from Waste Packages Containing Plutonium Disposition Waste Forms.* CAL-EDC-GS-000002 REV 00. Las Vegas, Nevada: CRWMS M&O. Submit to RPC URN-0544.

52. CRWMS M&O 2000. *Waste Package Related Impacts of Plutonium Disposition Waste Forms in a Geologic Repository.* TDR-EBS-MD-000003 REV 01 ICN 01. Las Vegas, Nevada: CRWMS M&O. ACC: MOL.20000510.0163.

53. AP-3.12Q, Rev.0, ICN 2. *Calculations.* Washington, D.C.: U.S. Department of Energy, Office of Civilian Radioactive Waste Management. ACC: MOL.20000620.0068.

54. CRWMS M&O 1999. *FY 1999 Plutonium Disposition Waste Package Criticality Tasks.* TDP-DDC-MD-000001 REV 00. Las Vegas, Nevada: CRWMS M&O. ACC: MOL.19990729.0059.

55. AP-SI.1Q, Rev. 2, ICN 4. *Software Management.* Washington, D.C.: U.S. Department of Energy, Office of Civilian Radioactive Waste Management. ACC: MOL.20000223.0508.

56. CRWMS M&O 1999. *DOE SRS HLW Glass Chemical Composition.* BBA000000-01717-0210-00038 REV 00. Las Vegas, Nevada: CRWMS M&O. ACC: MOL.19990215.0397.

57. MO0006J13WTRCM.000. Recommended Mean Values of Major Constituents in J-13 Well Water. Submittal date: 06/07/2000. Submit to RPC URN-0532 .

58. AP-SV.1Q, Rev. 0, ICN 2. *Control of the Electronic Management of Information.* Washington, D.C.: U.S. Department of Energy, Office of Civilian Radioactive Waste Management. ACC: MOL.20000831.0065.

8. ATTACHMENTS

Attachment I. Listing of Files on Compact Disks (16 pages)

Attachment II. Two Compact Disks

Attachment I. Listing of Files on Compact Disks

This attachment contains the MS-DOS directory for files placed on the electronic media (Attachment II, two compact disks). The files are of various types:

1) Excel files (extension = xls), called out in the text and tables are found in folder "Excel".
2) EQ3/6 input files (extensions = 3i or 6i).
3) EQ6 output files (text, extension = 6o).
4) Tab-delimited text files (extension = txt), with names p???????.elem????.txt. These contain total aqueous moles (*.elem_aqu.txt), total moles in minerals and aqueous phase (*.elem_m_a.txt), total moles in minerals, aqueous phase, and remain special reactants (*.elem_tot.txt), and the total moles in minerals alone (*.elem_min.txt). The *.elem_tot.txt and *.elem_min.txt also have the volume in cm^3 of the minerals and total solids (including special reactants) in the system.
5) EQ6 text data files used for the calculations, with names data0.p0* and data1.p0*.
6) Selected binary files (bin extension), created by EQ6, used for plotting.

Table I-1 provides the listing of cases from Table 6-1 and the location of the files on the electronic media.

Table I-1. Location of Files on the Electronic Media for Cases Listed in Table 6-1

Case Code	Invert Case Root Name	Location of Invert Files		WP Case Root Name	Location of WP Files	
		Disk	Folder		Disk	Folder
1a	Px2a0a2j	2	Case 1,2,4,5	pw2a1231	1	WP 1,2,4,5,8,10
1c	Px2c0a2j	2	Case 1,2,4,5	pw2c1231	1	WP 1,2,4,5,8,10
1s	Px2s0a2j	2	Case 1,2,4,5	pw2s1231	1	WP 1,2,4,5,8,10
1u	Px2u0a2j	2	Case 1,2,4,5	pw2u1231	1	WP 1,2,4,5,8,10
2a	Px2a0o2j	2	Case 1,2,4,5	pw2a1231	1	WP 1,2,4,5,8,10
2s	Px2s0o2j	2	Case 1,2,4,5	pw2s1231	1	WP 1,2,4,5,8,10
2u	Px2u0o2j	2	Case 1,2,4,5	pw2u1231	1	WP 1,2,4,5,8,10
3aa	pt1a1a2_	2	Case 3	Pe1a1222	1	WP 3
3sa	pt1s1a2_	2	Case 3	Pe1s1222	1	WP 3
3ua	pt1u1a2_	2	Case 3	Pe1u1222	1	WP 3
3an	pt1a1n2_	2	Case 3	Pe1a1222	1	WP 3
4aa	Px2a0a3j[b]	2	Case 1,2,4,5	pw2a1231	1	WP 1,2,4,5,8,10
4ao	Px2a0o3j	2	Case 1,2,4,5	pw2a1231	1	WP 1,2,4,5,8,10
4uo	Px2u0o3j	2	Case 1,2,4,5	pw2u1231	1	WP 1,2,4,5,8,10
5	Px2n0o3j	2	Case 1,2,4,5	pw1n1231	1	WP 1,2,4,5,8,10
6	Px2ado3j	2	Case 6	pwda1231	1	WP 6
7ho	Px2aHo3j	2	Case 7	pw2a123H	1	WP 7
7lo	Px2aLo3j	2	Case 7	pw2a123L	1	WP 7
7ha	Px2aHa3j	2	Case 7	pw2a123H	1	WP 7
7la	Px2aLa3j	2	Case 7	pw2a123L	1	WP 7
7sa	Px2aSa3j	2	Case 7	pw2a123S	1	WP 7
8	Px2a0a6k	1	Case 8	pw2a1231	1	WP 1,2,4,5,8,10
9o6^	Px2a6o3^	1	Case 9	p^6a1231	1	WP 9
9o6	Px2a6o3j	1	Case 9	pw6a1231	1	WP 9
9o7	Px2a7o3j	1	Case 9	pw7a1231	1	WP 9
9o8	Px2a8o3j	1	Case 9	pw8a1231	1	WP 9
10a!	Px2u0a2!	1	Case 10	pw2u1231	1	WP 1,2,4,5,8,10
10o!	Px2u0o2!	1	Case 10	pw2u1231	1	WP 1,2,4,5,8,10
10o@	Px2u0o2@	1	Case 10	pw2u1231	1	WP 1,2,4,5,8,10

Table I-2 provides the location of files for the sensitivity cases that are discussed in the text.

Table I-2. Location of Files on the Electronic Media for the Sensitivity Cases

Sensitivity Case	Invert Case Root Name	Location of Invert Files		WP Case Root Name	Location of WP Files	
		Disk	Folder		Disk	Folder
Source Term	N/A	N/A	N/A	Pe0a1231 Pe1a1222 P00_1231 Pw2a1231	1 1 1 1	Previous WP 3 Ref. 15 WP 1,2,4,5,8,10
Diffusion controlled Oxygen in WP	N/A	N/A	N/A	Pe1a1231 Pe2a1231 Pe3a1231 Pe41231	1 1 1 1	Ref. 15 Diffuse Oxygen Diffuse Oxygen Diffuse Oxygen
Average waste form degradation rate	N/A	N/A	N/A	Pw1a1231	1	WP 1,2,4,5,8,10
Surface Area	Px2a0a0j Px2a0a2j Px2a0a!j	2 2 2	Case 1,2,4,5 (subfolder SurfArea) Case 1,2,4,5 Case 1,2,4,5 (subfolder SurfArea)	Pw2a1231	1	WP 1,2,4,5,8,10

Below are listed the contents of the DOS directories within the electronic attachment:

The first column is the DOS file name.
The second column lists <DIR> if it is a folder or gives the file size (bytes) if it is a file.
The third and fourth columns are the date and time of the last update.
The fifth column is the file name.

```
Directory of Disk 1 (puextnew1)

DOS FILE NAME    SIZE (IF A FILE)    DATE      TIME   FILE NAME
CASE10~5         <DIR>               09-12-00  5:24p  Case 10
CASE8~7          <DIR>               09-12-00  4:33p  Case 8
CASE9~9          <DIR>               09-12-00  4:34p  Case 9
DATAB~11         <DIR>               09-12-00  4:38p  databases
DIFFU~13         <DIR>               09-12-00  4:41p  Diffuse Oxygen
EBERT~15         <DIR>               09-12-00  4:55p  Ebert glass
EXCEL            <DIR>               09-12-00  4:55p  Excel
IONIC~19         <DIR>               09-12-00  4:55p  Ionic Strength
J13              <DIR>               09-12-00  4:55p  J13
PP               <DIR>               09-12-00  4:57p  pp
PREVIOUS         <DIR>               09-12-00  4:57p  previous
WP1_2~27         <DIR>               09-12-00  4:57p  WP 1,2,4,5,8,10
WP3~29           <DIR>               09-12-00  5:04p  WP 3
WP6~31           <DIR>               09-12-00  5:22p  WP 6
WP7~33           <DIR>               09-12-00  4:31p  WP 7
WP9~35           <DIR>               09-12-00  5:28p  WP 9

Directory of puextnew1\Case 10

DECAYE~6 241              10  01-25-00 11:23a decay.eq6.24100
```

```
ELEM0A~8 AW2        19,516  01-25-00  4:49p elem0aqu.bin.aw2
ELEM0~10 UW2        18,336  01-25-00  5:45p elem0aqu.bin.uw2
PX2U0~12 BAT         1,501  01-30-00  6:13p px2u0_2!-@.bat
PX2U0_2! BAT         1,009  01-19-00  1:40p px2u0_2!.bat
PX2U0A2! 6I         44,635  01-19-00 11:50a px2u0a2!.6i
PX2U0A2! 6O      7,766,552  01-31-00  1:35p px2u0a2!.6o
PX2U0A2! BAT           782  01-19-00  1:40p px2u0a2!.bat
PX2U0~44 TXT        60,996  01-31-00  1:35p px2u0a2!.elem_aqu.txt
PX2U0~46 TXT        57,211  01-31-00  1:35p px2u0a2!.elem_min.txt
PX2U0~48 TXT        57,224  01-31-00  1:35p px2u0a2!.elem_tot.txt
PX2U0~50 TXT       137,244  01-31-00  1:35p px2u0a2!.min_info.txt
PX2U0O2! 6I         47,196  01-19-00 11:51a px2u0o2!.6i
PX2U0O2! 6O      8,039,340  01-31-00 12:49p px2u0o2!.6o
PX2U0~80 TXT        68,696  01-31-00 12:49p px2u0o2!.elem_aqu.txt
PX2U0~84 TXT        64,431  01-31-00 12:49p px2u0o2!.elem_min.txt
PX2U0~86 TXT        64,444  01-31-00 12:49p px2u0o2!.elem_tot.txt
PX2U0~88 TXT       192,456  01-31-00 12:49p px2u0o2!.min_info.txt
PX2U0O2@ 6I         47,273  01-19-00  3:43p px2u0o2@.6i
PX2U0O2@ 6O      7,487,829  02-01-00  6:15p px2u0o2@.6o
PX2U0O2@ BAT           900  01-31-00  8:11p px2u0o2@.bat
PX2U~118 TXT        62,536  02-01-00  6:15p px2u0o2@.elem_aqu.txt
PX2U~120 TXT        58,655  02-01-00  6:15p px2u0o2@.elem_min.txt
PX2U~122 TXT        58,668  02-01-00  6:15p px2u0o2@.elem_tot.txt
PX2U~124 TXT       150,854  02-01-00  6:15p px2u0o2@.min_info.txt
        25 file(s)     24,508,294 bytes

Directory of puextnew1\Case 8

DECAYE~6 241            10  01-25-00 11:23a decay.eq6.24100
ELEM0A~8 AW2        19,516  01-25-00  4:49p elem0aqu.bin.aw2
PX2A0A6J 6I         44,881  01-17-00  3:56p px2a0a6j.6i
PX2A0A6J BAT           472  01-17-00  4:01p px2a0a6j.bat
PX2A0~14 TXT        34,431  01-17-00  4:29p px2a0a6j.elem_aqu.txt
PX2A0~16 TXT        32,302  01-17-00  4:29p px2a0a6j.elem_min.txt
PX2A0~18 TXT        32,315  01-17-00  4:29p px2a0a6j.elem_tot.txt
PX2A0A6K 6I         44,956  01-17-00  5:43p px2a0a6k.6i
PX2A0A6K 6O      8,321,895  02-01-00  7:54p px2a0a6k.6o
PX2A0A6K BAT           590  02-01-00  6:53p px2a0a6k.bat
PX2A0~50 TXT        62,151  02-01-00  7:53p px2a0a6k.elem_aqu.txt
PX2A0~54 TXT        58,294  02-01-00  7:53p px2a0a6k.elem_min.txt
PX2A0~56 TXT        58,307  02-01-00  7:53p px2a0a6k.elem_tot.txt
PX2A0~58 TXT       147,041  02-01-00  7:53p px2a0a6k.min_info.txt
        14 file(s)      8,857,161 bytes

Directory of puextnew1\Case 9

DECAYE~6 241            10  01-25-00 11:23a decay.eq6.24100
ELEM0A~8 AW6        22,112  01-30-00  5:11p elem0aqu.bin.aw6
ELEM0~10 AW6        22,112  01-30-00  5:34p elem0aqu.bin.aw6d
ELEM0~12 AW7        20,224  01-30-00  4:24p elem0aqu.bin.aw7
ELEM0~14 AW8        19,280  01-30-00  4:47p elem0aqu.bin.aw8
PX2A6~16 BAT         1,632  01-30-00  5:53p px2a6-8o3j.bat
PX2A6O3^ 6I         47,187  01-20-00  9:38a px2a6o3^.6i
PX2A6O3^ 6O      6,951,605  01-30-00 10:36p px2a6o3^.6o
PX2A6~44 TXT        53,681  01-30-00 10:36p px2a6o3^.elem_aqu.txt
PX2A6~46 TXT        50,352  01-30-00 10:36p px2a6o3^.elem_min.txt
PX2A6~48 TXT        50,365  01-30-00 10:36p px2a6o3^.elem_tot.txt
PX2A6~50 TXT       140,819  01-30-00 10:36p px2a6o3^.min_info.txt
PX2A6O3J 6I         47,035  01-20-00  9:35a px2a6o3j.6i
```

```
PX2A6O3J 6O      6,770,968  01-30-00  9:34p px2a6o3j.6o
PX2A6O3J BAT         1,109  01-20-00  9:42a px2a6o3j.bat
PX2A6~78 TXT        50,986  01-30-00  9:34p px2a6o3j.elem_aqu.txt
PX2A6~80 TXT        47,825  01-30-00  9:34p px2a6o3j.elem_min.txt
PX2A6~82 TXT        47,838  01-30-00  9:34p px2a6o3j.elem_tot.txt
PX2A6~84 TXT       133,195  01-30-00  9:34p px2a6o3j.min_info.txt
PX2A7~86 BAT           983  01-15-00  1:03p px2a7-8o3j.bat
PX2A7O3J 6I         46,958  01-15-00  2:28p px2a7o3j.6i
PX2A7O3J 6O      6,262,777  01-30-00  7:08p px2a7o3j.6o
PX2A7O3J BAT           701  01-15-00  2:29p px2a7o3j.bat
PX2A~112 TXT        45,981  01-30-00  7:08p px2a7o3j.elem_aqu.txt
PX2A~114 TXT        43,132  01-30-00  7:08p px2a7o3j.elem_min.txt
PX2A~116 TXT        43,145  01-30-00  7:08p px2a7o3j.elem_tot.txt
PX2A~118 TXT       117,549  01-30-00  7:08p px2a7o3j.min_info.txt
PX2A8O3J 6I         46,884  01-15-00  1:11p px2a8o3j.6i
PX2A8O3J 6O      7,226,374  01-30-00  8:27p px2a8o3j.6o
PX2A~146 TXT        55,606  01-30-00  8:27p px2a8o3j.elem_aqu.txt
PX2A~148 TXT        52,157  01-30-00  8:27p px2a8o3j.elem_min.txt
PX2A~150 TXT        52,170  01-30-00  8:27p px2a8o3j.elem_tot.txt
PX2A~152 TXT       146,127  01-30-00  8:27p px2a8o3j.min_info.txt
        33 file(s)     28,618,879 bytes

Directory of puextnew1\databases

DATA0    P0A     2,305,725  12-23-99 12:01a data0.p0a
DATA0    P0C     2,190,829  12-07-99 12:27p data0.p0c
DATA0    P0N     2,304,092  01-18-00  8:55p data0.p0n
DATA0    P0S     2,305,129  01-18-00  5:56p data0.p0s
DATA0    P0T     2,305,480  12-01-99 12:22p data0.p0t
DATA0    P0U     2,305,614  12-01-99 12:26p data0.p0u
DATA1    P0A       794,677  12-23-99 12:01a data1.p0a
DATA1    P0C       706,807  12-07-99 12:28p data1.p0c
DATA1    P0N       807,003  01-17-00  5:50p data1.p0n
DATA1    P0S       793,796  12-01-99  2:55p data1.p0s
DATA1    P0T       794,300  12-01-99  2:55p data1.p0t
DATA1    P0U       794,552  12-01-99  2:55p data1.p0u
        12 file(s)     18,408,004 bytes

Directory of puextnew1\Diffuse Oxygen

ELEM0A~6 A3D        49,488  01-25-00 10:56p elem0aqu.bin.a3diff
ELEM0A~8 A4D        33,204  01-25-00 11:29p elem0aqu.bin.a4diff
ELEM0~10 A_D        52,320  01-25-00 10:04p elem0aqu.bin.a_diff
PE2-4~12 BAT         1,684  01-25-00  8:46p Pe2-4a1231.bat
PE2A1231 6I         41,903  12-22-99  5:55p pe2a1231.6i
PE2A1231 6O      9,791,192  01-25-00 10:05p pe2a1231.6o
PE2A1231 BAT           331  12-22-99  3:40p Pe2a1231.bat
PE2A1~50 TXT        85,251  01-25-00 10:04p pe2a1231.elem_aqu.txt
PE2A1~52 TXT        79,954  01-25-00 10:04p pe2a1231.elem_min.txt
PE2A1~54 TXT        79,967  01-25-00 10:04p pe2a1231.elem_tot.txt
PE2A1~56 TXT       348,278  01-25-00 10:04p pe2a1231.min_info.txt
PE3A1231 6I         43,435  12-25-99  5:23p pe3a1231.6i
PE3A1231 6O      9,067,232  01-25-00 10:57p pe3a1231.6o
PE3A1231 BAT           339  12-22-99  4:27p Pe3a1231.bat
PE3A1~92 TXT        80,631  01-25-00 10:56p pe3a1231.elem_aqu.txt
PE3A1~94 TXT        75,622  01-25-00 10:56p pe3a1231.elem_min.txt
PE3A1~96 TXT        75,635  01-25-00 10:56p pe3a1231.elem_tot.txt
PE3A1~98 TXT       324,034  01-25-00 10:56p pe3a1231.min_info.txt
PE4A1231 6I         42,574  01-06-00  6:22p pe4a1231.6i
```

```
PE4A1231 6O      5,899,116  01-25-00 11:29p pe4a1231.6o
PE4A1231 BAT           511  12-23-99  5:58p Pe4a1231.bat
PE4A~124 TXT        54,066  01-25-00 11:29p pe4a1231.elem_aqu.txt
PE4A~126 TXT        50,713  01-25-00 11:29p pe4a1231.elem_min.txt
PE4A~128 TXT        50,726  01-25-00 11:29p pe4a1231.elem_tot.txt
PE4A~130 TXT       198,860  01-25-00 11:29p pe4a1231.min_info.txt
PE4FILL1 6I         41,622  12-25-99  8:39a pe4fill1.6i
PE4FILL1 6O        936,874  01-25-00 11:00p pe4fill1.6o
PE4FILL1 BAT           431  12-23-99  5:33p Pe4fill1.bat
PE4F~142 TXT         9,406  01-25-00 11:00p pe4fill1.elem_aqu.txt
PE4F~144 TXT         8,837  01-25-00 11:00p pe4fill1.elem_min.txt
PE4F~146 TXT         8,850  01-25-00 11:00p pe4fill1.elem_tot.txt
PE4F~148 TXT        21,424  01-25-00 11:00p pe4fill1.min_info.txt
PT1A0N3_ 6I         43,045  12-07-99  9:29p pt1a0n3_.6i
PT1A4N3  BAT           470  12-25-99  8:12p pt1a4n3.bat
PT1A4N3_ 6I         43,700  01-07-00 12:11p pt1a4n3_.6i
PT1A4N3_ 6O      5,025,169  01-26-00 10:47a pt1a4n3_.6o
PT1A4N3_ BIN    53,050,368  01-26-00 10:47a pt1a4n3_.bin
PT1A~330 TXT        42,901  01-26-00 10:47a pt1a4n3_.elem_aqu.txt
PT1A~332 TXT        40,244  01-26-00 10:47a pt1a4n3_.elem_min.txt
PT1A~334 TXT        40,257  01-26-00 10:47a pt1a4n3_.elem_tot.txt
PT1A~338 TXT       120,801  01-26-00 10:47a pt1a4n3_.min_info.txt
        41 file(s)     85,961,465 bytes

Directory of puextnew1\Ebert glass

PEEA1231 6I         41,063  07-19-00  9:37a peEa1231.6i
         1 file(s)          41,063 bytes

Directory of puextnew1\Excel

BDOT     XLS        44,544  09-08-00  2:01p bdot.xls
DIR      TXT           660  09-12-00  2:14p dir.txt
EBERT~10 XLS        15,872  09-08-00  1:11p Ebert_glass.xls
GLASS~12 XLS        61,952  09-08-00  1:09p Glass_rates_110999.xls
INVER~14 XLS       840,704  09-08-00 10:38a Invert_EQ6_122299.xls
RATE_~18 XLS        15,360  09-08-00 10:53a Rate_avg_Pw1a1231.xls
         6 file(s)        979,092 bytes

Directory of puextnew1\Ionic Strength

EXP3IP1C TXT           159  01-25-00  8:08a Exp3Ip1C.txt
U!CARB4B 6I         22,063  11-16-99  7:00p U!carb4B.6i
U@CARB4B 6I         22,075  11-17-99  2:36p U@carb4B.6i
U_CARB00 3I         10,722  11-15-99 12:58p U_carb00.3i
U_CARB01 3I         10,871  11-15-99  4:31p U_carb01.3i
U_CARB02 3I         11,018  11-15-99  5:12p U_carb02.3i
U_CARB03 3I         11,166  11-15-99  6:22p U_carb03.3i
U_CARB04 3I         11,314  11-16-99 12:13p U_carb04.3i
U_CARB4A 6I         24,616  11-16-99 12:25p U_carb4A.6i
U_CARB4B 6I         21,915  11-17-99  2:33p U_carb4B.6i
U_CARB4C TMP         1,068  11-16-99  6:54p U_CARB4C.TMP
U_CARB_A 6I         22,371  12-30-99 10:51a U_carb_a.6i
U_CARB_A 6O         71,335  12-30-99 10:54a u_carb_a.6o
U_CARB_A BIN        74,656  02-22-00  5:42p U_carb_a.bin
U_CAR~36 BAT           373  12-30-99 10:37a U_carb_DB.bat
U_CARB_T 6I         22,371  12-30-99 10:53a U_carb_t.6i
U_CARB_T 6O         81,319  12-30-99 10:54a u_carb_t.6o
U_CARB_T BIN        76,688  02-22-00  5:42p U_carb_t.bin
```

```
U_CARB_U 6I          22,371  12-30-99 10:53a U_carb_u.6i
U_CARB_U 6O          80,724  12-30-99 10:54a u_carb_u.6o
U_CARB_U BIN         72,104  02-22-00  5:43p U_carb_u.bin
U_CARBAA 6I          23,260  11-15-99  4:37p U_carbAA.6i
U_CARBAB 6I          23,672  11-15-99  5:40p U_carbAB.6i
U_CARBAC 6I          20,583  11-15-99  6:03p U_carbAC.6i
U_CARBBB 6I          23,948  11-16-99 12:18p U_carbBB.6i
U_CARBBC 6I          20,879  11-15-99  6:34p U_carbBC.6i
U_CARBCC 6I          21,027  11-15-99  6:48p U_carbCC.6i
U_CARNBC 6I          20,731  11-15-99  6:27p U_carnBC.6i
WUCARB_A 000         44,268  12-30-99 11:42a WUCARB_A.000
WUCARB_T 000         44,388  12-30-99 11:38a WUCARB_T.000
WUCARB_U 000         44,208  12-30-99 11:47a WUCARB_U.000
WUCARB_U 001         44,098  12-30-99 11:49a WUCARB_U.001
        32 file(s)      1,002,361 bytes

Directory of puextnew1\J13

J13NC30P 3I          12,808  02-16-00  4:22p j13nc30p.3i
J13NC30P 3O         113,596  02-16-00  4:22p j13nc30p.3o
J13NC30P 3P          10,252  02-16-00  4:22p j13nc30p.3p
J13WSF   6I          28,425  08-04-99  3:03p j13wsf.6i
J13WSF_  6I          28,499  08-04-99  7:57p j13wsf_.6i
J13WSF_  6O       1,103,716  02-22-00  6:08p j13wsf_.6o
J13WSF_A BIN      3,925,384  02-22-00  6:03p j13wsf_a.bin
J13WS~34 TXT         18,905  02-22-00  6:03p j13wsf_a.elem_aqu.txt
J13WSF_C BIN      4,083,880  02-22-00  6:08p j13wsf_c.bin
J13WS~50 TXT         18,905  02-22-00  6:08p j13wsf_c.elem_aqu.txt
J13WSFCO 6I          28,924  08-04-99  5:13p J13WSFCO.6I
J13WSFHI 6I          28,863  08-04-99  4:26p j13wsfhi.6i
J13WSFHI 6O       1,157,617  02-22-00  5:58p j13wsfhi.6o
J13WSFHI BIN      3,977,240  02-22-00  5:58p j13wsfhi.bin
J13WS~76 TXT         19,374  02-22-00  5:58p j13wsfhi.elem_aqu.txt
J13WSFRE 6I          28,579  08-05-99  2:00p j13wsfre.6i
J13WSFVH 6I          28,943  08-04-99  5:40p j13wsfvh.6i
        17 file(s)     14,613,910 bytes

Directory of puextnew1\pp

HELP_PP              50,724  03-31-98  6:04p HELP_PP
PP       EXE        308,609  10-10-98  4:15p PP.EXE
PREFER   PP              62  01-20-99 10:25a PREFER.PP
         3 file(s)        359,395 bytes

Directory of puextnew1\previous

PE0_1231 BAT          1,032  12-04-99  6:20p PE0_1231.BAT
PE0A1231 6I          41,128  12-01-99  2:53p pe0a1231.6i
PE0A1231 BAT            424  01-06-00 11:04a pe0a1231.bat
PE0A1~12 TXT         34,416  12-01-99  3:58p pe0a1231.elem_aqu.txt
PE0A1~14 TXT         32,575  12-01-99  3:58p pe0a1231.elem_min.txt
PE0A1~16 TXT         32,588  12-01-99  3:58p pe0a1231.elem_tot.txt
PE0A1~18 TXT         75,676  12-01-99  3:58p pe0a1231.min_info.txt
PE0S1231 6I          41,274  12-01-99  3:27p pe0s1231.6i
PE0S1~22 TXT         34,416  12-04-99  7:03p pe0s1231.elem_aqu.txt
PE0S1~24 TXT         32,575  12-04-99  7:03p pe0s1231.elem_min.txt
PE0S1~28 TXT         32,588  12-04-99  7:03p pe0s1231.elem_tot.txt
PE0S1~30 TXT         76,012  12-01-99  4:20p pe0s1231.min_info.txt
PE0T1231 6I          41,495  12-01-99  6:56p pe0t1231.6i
```

```
PE0T1231 BAT           225  12-01-99  6:23p pe0t1231.bat
PE0T1~36 TXT        14,836  12-01-99  7:05p pe0t1231.elem_aqu.txt
PE0T1~38 TXT        14,051  12-01-99  7:05p pe0t1231.elem_min.txt
PE0T1~40 TXT        14,064  12-01-99  7:05p pe0t1231.elem_tot.txt
PE0T1~42 TXT        29,194  12-01-99  7:05p pe0t1231.min_info.txt
PE0U1231 6I         41,424  12-01-99  3:31p pe0u1231.6i
PE0U1~46 TXT        31,746  12-04-99  7:28p pe0u1231.elem_aqu.txt
PE0U1~48 TXT        30,049  12-04-99  7:28p pe0u1231.elem_min.txt
PE0U1~50 TXT        30,062  12-04-99  7:28p pe0u1231.elem_tot.txt
PE0U1~52 TXT        69,868  12-01-99  6:10p pe0u1231.min_info.txt
PE1T1231 6I         40,447  12-01-99  7:07p pe1t1231.6i
PE1T1231 BAT           225  12-01-99  7:08p pe1t1231.bat
PE1T1~58 TXT        20,176  12-01-99  7:22p pe1t1231.elem_aqu.txt
PE1T1~60 TXT        19,103  12-01-99  7:22p pe1t1231.elem_min.txt
PE1T1~62 TXT        19,116  12-01-99  7:22p pe1t1231.elem_tot.txt
PE1T1~64 TXT        45,274  12-01-99  7:22p pe1t1231.min_info.txt
        29 file(s)        896,059 bytes

Directory of puextnew1\WP 1,2,4,5,8,10

DECAYE~6 241            10  01-25-00 11:23a decay.eq6.24100
ELEM0A~8 AN         20,224  01-25-00  7:33p elem0aqu.bin.an
ELEM0~10 AW         19,044  01-13-00 11:20a elem0aqu.bin.aw
ELEM0~12 AW2        19,516  01-25-00  4:49p elem0aqu.bin.aw2
ELEM0~14 CW2        27,068  01-25-00  7:08p elem0aqu.bin.cw2
ELEM0~18 SW2        19,516  01-25-00  5:16p elem0aqu.bin.sw2
ELEM0~20 UW2        18,336  01-25-00  5:45p elem0aqu.bin.uw2
PW1A1231 6I         40,713  01-13-00 10:45a pw1a1231.6i
PW1A1231 6O      3,623,007  01-13-00 12:40p pw1a1231.6o
PW1A1231 BAT           455  01-13-00 10:51a PW1a1231.bat
PW1A1~38 TXT        30,966  01-13-00 11:20a pw1a1231.elem_aqu.txt
PW1A1~40 TXT        29,053  01-13-00 11:20a pw1a1231.elem_min.txt
PW1A1~42 TXT        29,066  01-13-00 11:20a pw1a1231.elem_tot.txt
PW1N1231 &6I        40,989  01-25-00  2:56p PW1N1231.&6I
PW1N1231 &6O        39,806  01-25-00  2:54p PW1N1231.&6O
PW1N1231 6I         40,989  01-25-00  3:01p pw1n1231.6i
PW1N1231 6O      3,827,593  01-25-00  7:33p pw1n1231.6o
PW1N1231 6P      3,525,732  01-25-00  7:33p pw1n1231.6p
PW1N1231 BAT           504  01-25-00  2:40p PW1n1231.bat
PW1N1~78 TXT        32,891  01-25-00  7:33p pw1n1231.elem_aqu.txt
PW1N1~80 TXT        30,858  01-25-00  7:33p pw1n1231.elem_min.txt
PW1N1~82 TXT        30,871  01-25-00  7:33p pw1n1231.elem_tot.txt
PW1N1~84 TXT        84,998  01-25-00  7:33p pw1n1231.min_info.txt
PW2_1231 &BA         1,412  01-25-00 11:13a PW2_1231.&BA
PW2_1231 BAT         1,958  01-25-00  4:15p PW2_1231.bat
PW2A1231 6I         42,423  01-13-00 12:35p pw2a1231.6i
PW2A1231 6O      3,756,365  01-25-00  4:49p pw2a1231.6o
PW2A1231 6P      3,417,842  01-25-00  4:49p pw2a1231.6p
PW2A1231 BAT           760  01-13-00 12:39p PW2a1231.bat
PW2A~120 TXT        31,736  01-25-00  4:49p PW2a1231.elem_aqu.txt
PW2A~122 TXT        29,775  01-25-00  4:49p PW2a1231.elem_min.txt
PW2A~124 TXT        29,788  01-25-00  4:49p PW2a1231.elem_tot.txt
PW2A~126 TXT        81,108  01-25-00  4:49p PW2a1231.min_info.txt
PW2A~128 TXT        29,788  01-25-00 11:57a PW2as1231.elem_tot.txt
PW2C1231 6I         42,593  01-17-00  9:13p pw2c1231.6i
PW2C1231 6O      6,536,435  01-25-00  7:08p pw2c1231.6o
PW2C1231 6P      4,801,270  01-25-00  7:08p pw2c1231.6p
PW2C1231 BAT           852  01-17-00  6:26p pw2c1231.bat
PW2C~172 TXT        44,056  01-25-00  7:08p PW2c1231.elem_aqu.txt
```

```
PW2C~174 TXT        41,327  01-25-00  7:08p PW2c1231.elem_min.txt
PW2C~176 TXT        41,340  01-25-00  7:08p PW2c1231.elem_tot.txt
PW2C~178 TXT       114,694  01-25-00  7:08p PW2c1231.min_info.txt
PW2S1231 6I         42,497  01-14-00 10:34a pw2s1231.6i
PW2S1231 6O      3,747,172  01-25-00  5:16p pw2s1231.6o
PW2S1231 6P      3,433,422  01-25-00  5:17p pw2s1231.6p
PW2S~208 TXT        31,736  01-25-00  5:16p PW2s1231.elem_aqu.txt
PW2S~210 TXT        29,775  01-25-00  5:16p PW2s1231.elem_min.txt
PW2S~212 TXT        29,788  01-25-00  5:16p PW2s1231.elem_tot.txt
PW2S~214 TXT        82,142  01-25-00  5:16p PW2s1231.min_info.txt
PW2U1231 6I         42,497  01-14-00 10:36a pw2u1231.6i
PW2U1231 6O      3,543,756  01-25-00  5:45p pw2u1231.6o
PW2U1231 6P      3,225,648  01-25-00  5:45p pw2u1231.6p
PW2U~242 TXT        29,811  01-25-00  5:45p PW2u1231.elem_aqu.txt
PW2U~244 TXT        27,970  01-25-00  5:45p PW2u1231.elem_min.txt
PW2U~246 TXT        27,983  01-25-00  5:45p PW2u1231.elem_tot.txt
PW2U~248 TXT        77,022  01-25-00  5:45p PW2u1231.min_info.txt
        56 file(s)     44,948,946 bytes

Directory of puextnew1\WP 3

ELEM0A~6 A          18,336  12-05-99  6:43a elem0aqu.bin.a
ELEM0A~8 A_1        38,868  01-26-00 12:08p elem0aqu.bin.a_1222
ELEM0~12 A_S        17,628  12-28-99  1:06p elem0aqu.bin.a_SiO2
ELEM0~14 S          18,336  12-05-99  6:59a elem0aqu.bin.s
ELEM0~16 S_1        40,992  01-26-00  1:02p elem0aqu.bin.s_1222
ELEM0~18 U          16,684  12-05-99  7:15a elem0aqu.bin.u
ELEM0~20 U_1        40,284  01-26-00  2:00p elem0aqu.bin.u_1222
PE1_1222 &BA           816  01-26-00 11:15a PE1_1222.&BA
PE1_1222 BAT           847  01-26-00 11:16a Pe1_1222.bat
PE1_1231 BAT         1,032  12-05-99  6:22a Pe1_1231.bat
PE1A1222 6I         40,822  12-07-99 10:46a pe1a1222.6i
PE1A1222 6O      8,064,438  01-26-00 12:08p pe1a1222.6o
PE1A1222 BIN    89,236,656  01-26-00 12:08p pe1a1222.bin
PE1A~318 TXT        63,306  01-26-00 12:08p pe1a1222.elem_aqu.txt
PE1A~320 TXT        59,377  01-26-00 12:08p pe1a1222.elem_min.txt
PE1A~322 TXT        59,390  01-26-00 12:08p pe1a1222.elem_tot.txt
PE1A~324 TXT       164,122  01-26-00 12:08p pe1a1222.min_info.txt
PE1A1231 6I         40,617  12-13-99 12:10p pe1a1231.6i
PE1A~330 TXT        29,811  12-05-99  6:43a pe1a1231.elem_aqu.txt
PE1A~332 TXT        27,970  12-05-99  6:43a pe1a1231.elem_min.txt
PE1A~334 TXT        27,983  12-05-99  6:43a pe1a1231.elem_tot.txt
PE1A123S 6I         41,039  12-07-99  4:44p pe1a123S.6i
PE1A123S BAT           407  12-28-99 12:51p Pe1a123S.bat
PE1A~340 TXT        28,656  12-28-99  1:06p pe1a123S.elem_aqu.txt
PE1A~342 TXT        26,887  12-28-99  1:06p pe1a123S.elem_min.txt
PE1A~344 TXT        26,900  12-28-99  1:06p pe1a123S.elem_tot.txt
PE1N1231 6I         40,841  01-14-00  1:33a pe1n1231.6i
PE1S1222 6I         40,896  12-07-99 10:48a pe1s1222.6i
PE1S1222 6O      8,426,222  01-26-00  1:02p pe1s1222.6o
PE1S~376 TXT        66,771  01-26-00  1:02p pe1s1222.elem_aqu.txt
PE1S~378 TXT        62,626  01-26-00  1:02p pe1s1222.elem_min.txt
PE1S~382 TXT        62,639  01-26-00  1:02p pe1s1222.elem_tot.txt
PE1S~384 TXT       180,374  01-26-00  1:02p pe1s1222.min_info.txt
PE1S1231 6I         40,837  12-05-99  6:25a pe1s1231.6i
PE1S~388 TXT        29,811  12-05-99  6:59a pe1s1231.elem_aqu.txt
PE1S~390 TXT        27,970  12-05-99  6:59a pe1s1231.elem_min.txt
PE1S~392 TXT        27,983  12-05-99  6:59a pe1s1231.elem_tot.txt
PE1U1222 6I         40,896  12-07-99 10:48a pe1u1222.6i
```

```
PE1U1222 6O      8,331,841  01-26-00  2:01p pe1u1222.6o
PE1U~422 TXT        65,616  01-26-00  2:00p pe1u1222.elem_aqu.txt
PE1U~424 TXT        61,543  01-26-00  2:00p pe1u1222.elem_min.txt
PE1U~428 TXT        61,556  01-26-00  2:00p pe1u1222.elem_tot.txt
PE1U~430 TXT       176,870  01-26-00  2:00p pe1u1222.min_info.txt
PE1U1231 6I         40,987  12-05-99  6:27a pe1u1231.6i
PE1U~434 TXT        27,116  12-05-99  7:15a pe1u1231.elem_aqu.txt
PE1U~436 TXT        25,443  12-05-99  7:15a pe1u1231.elem_min.txt
PE1U~438 TXT        25,456  12-05-99  7:15a pe1u1231.elem_tot.txt
        47 file(s)    115,996,498 bytes

Directory of puextnew1\WP 6

DECAYE~6 241            10  01-25-00 11:23a decay.eq6.24100
ELEM0A~8 AWD        14,088  02-02-00 11:11a elem0aqu.bin.awd
PWDA1231 6I         42,573  01-15-00  4:50p pwda1231.6i
PWDA1231 6O      2,544,552  02-02-00 11:11a pwda1231.6o
PWDA1231 BAT           878  02-02-00 10:56a PWda1231.bat
PWDA1231 BIN    12,553,568  02-02-00 11:11a PWda1231.bin
PWDA1~62 TXT        22,881  02-02-00 11:11a PWda1231.elem_aqu.txt
PWDA1~64 TXT        21,472  02-02-00 11:11a PWda1231.elem_min.txt
PWDA1~68 TXT        21,485  02-02-00 11:11a PWda1231.elem_tot.txt
PWDA1~70 TXT        55,357  02-02-00 11:11a PWda1231.min_info.txt
        10 file(s)     15,276,864 bytes

Directory of puextnew1\WP 7

DECAYE~6 241            10  01-25-00 11:23a decay.eq6.24100
ELEM0A~8 AW2        21,640  01-30-00 10:03a elem0aqu.bin.aw2H
ELEM0~10 AW2        21,404  01-30-00 12:17p elem0aqu.bin.aw2L
ELEM0~12 AW2        17,628  01-31-00  7:11p elem0aqu.bin.aw2S
PW2A123H 6I         42,610  01-16-00  1:17p pw2a123H.6i
PW2A123H 6O      4,314,765  01-30-00 10:03a pw2a123h.6o
PW2A123H BAT           601  01-16-00 12:38p PW2a123H.bat
PW2A1~32 TXT        35,201  01-30-00 10:03a PW2a123H.elem_aqu.txt
PW2A1~34 TXT        33,024  01-30-00 10:03a PW2a123H.elem_min.txt
PW2A1~36 TXT        33,037  01-30-00 10:03a PW2a123H.elem_tot.txt
PW2A1~38 TXT        90,576  01-30-00 10:03a PW2a123H.min_info.txt
PW2A123L 6I         42,571  01-16-00  2:24p pw2a123L.6i
PW2A123L 6O      4,203,523  01-30-00 12:17p pw2a123l.6o
PW2A123L BAT           653  01-30-00 11:45a PW2a123L.bat
PW2A1~58 TXT        34,816  01-30-00 12:17p PW2a123L.elem_aqu.txt
PW2A1~62 TXT        32,663  01-30-00 12:17p PW2a123L.elem_min.txt
PW2A1~64 TXT        32,676  01-30-00 12:17p PW2a123L.elem_tot.txt
PW2A1~66 TXT        89,480  01-30-00 12:17p PW2a123L.min_info.txt
PW2A1~68 BAT           917  01-30-00  9:28a PW2a123LH.bat
PW2A123S 6I         42,868  01-17-00  4:08p pw2a123S.6i
PW2A123S 6O      3,340,890  01-31-00  7:11p pw2a123s.6o
PW2A123S BAT         1,034  01-31-00 12:00p PW2a123S.bat
PW2A1~86 TXT        28,656  01-31-00  7:11p PW2a123S.elem_aqu.txt
PW2A1~88 TXT        26,887  01-31-00  7:11p PW2a123S.elem_min.txt
PW2A1~90 TXT        26,900  01-31-00  7:11p PW2a123S.elem_tot.txt
PW2A1~92 TXT        74,555  01-31-00  7:11p PW2a123S.min_info.txt
        26 file(s)     12,589,585 bytes

Directory of puextnew1\WP 9

DECAYE~6 241            10  01-25-00 11:23a decay.eq6.24100
ELEM0A~8 AW6        22,112  01-30-00  5:11p elem0aqu.bin.aw6
```

```
ELEM0~10 AW6         22,112  01-30-00  5:34p elem0aqu.bin.aw6d
ELEM0~12 AW7         20,224  01-30-00  4:24p elem0aqu.bin.aw7
ELEM0~14 AW8         19,280  01-30-00  4:47p elem0aqu.bin.aw8
P^6A1231 6I          42,827  01-20-00  8:45a p^6a1231.6i
P^6A1231 6O       4,263,896  01-30-00  5:34p p^6a1231.6o
P^6A1~34 TXT         35,971  01-30-00  5:34p P^6a1231.elem_aqu.txt
P^6A1~36 TXT         33,746  01-30-00  5:34p P^6a1231.elem_min.txt
P^6A1~38 TXT         33,759  01-30-00  5:34p P^6a1231.elem_tot.txt
P^6A1~40 TXT         94,006  01-30-00  5:34p P^6a1231.min_info.txt
PW6-8~42 BAT          1,821  01-30-00  3:41p PW6-8a1231.bat
PW6A1231 6I          42,737  01-20-00  8:42a pw6a1231.6i
PW6A1231 6O       4,266,589  01-30-00  5:11p pw6a1231.6o
PW6A1231 BAT          1,328  01-20-00  8:48a PW6a1231.bat
PW6A1~62 TXT         35,971  01-30-00  5:11p PW6a1231.elem_aqu.txt
PW6A1~64 TXT         33,746  01-30-00  5:11p PW6a1231.elem_min.txt
PW6A1~66 TXT         33,759  01-30-00  5:11p PW6a1231.elem_tot.txt
PW6A1~68 TXT         94,054  01-30-00  5:11p PW6a1231.min_info.txt
PW7-8~70 BAT          1,180  01-15-00 11:37a PW7-8a1231.bat
PW7A1231 6I          42,603  01-15-00 11:55a pw7a1231.6i
PW7A1231 6O       3,907,621  01-30-00  4:24p pw7a1231.6o
PW7A1231 BIN     31,786,688  01-30-00  4:24p PW7a1231.bin
PW7A~182 TXT         32,891  01-30-00  4:24p PW7a1231.elem_aqu.txt
PW7A~186 TXT         30,858  01-30-00  4:24p PW7a1231.elem_min.txt
PW7A~188 TXT         30,871  01-30-00  4:24p PW7a1231.elem_tot.txt
PW7A~190 TXT         85,958  01-30-00  4:24p PW7a1231.min_info.txt
PW8A1231 6I          42,576  01-15-00 11:55a pw8a1231.6i
PW8A1231 6O       3,700,279  01-30-00  4:47p pw8a1231.6o
PW8A1231 BIN     30,636,112  01-30-00  4:47p PW8a1231.bin
PW8A~298 TXT         31,351  01-30-00  4:47p PW8a1231.elem_aqu.txt
PW8A~300 TXT         29,414  01-30-00  4:47p PW8a1231.elem_min.txt
PW8A~302 TXT         29,427  01-30-00  4:47p PW8a1231.elem_tot.txt
PW8A~304 TXT         78,616  01-30-00  4:47p PW8a1231.min_info.txt
        34 file(s)     79,564,393 bytes

Total files listed:
       386 file(s)    452,621,969 bytes
        48 dir(s)

Directory of Disk 2 (puextnew2)

CASE1_~5       <DIR>          08-16-00  3:46p Case 1,2,4,5
CASE3~7        <DIR>          08-16-00  3:39p Case 3
CASE6~9        <DIR>          08-16-00  3:25p Case 6
CASE7~11       <DIR>          08-16-00  4:47p Case 7

Directory of puextnew2\Case 1,2,4,5

DECAYE~6 241            10  01-25-00 11:23a decay.eq6.24100
ELEM0A~8 AN          20,224  01-25-00  7:33p elem0aqu.bin.an
ELEM0~10 AW          19,044  01-13-00 11:20a elem0aqu.bin.aw
ELEM0~12 AW2         19,516  01-25-00  4:49p elem0aqu.bin.aw2
ELEM0~14 CW2         27,068  01-25-00  7:08p elem0aqu.bin.cw2
ELEM0~16 SW2         19,516  01-25-00  5:16p elem0aqu.bin.sw2
ELEM0~18 UW2         18,336  01-25-00  5:45p elem0aqu.bin.uw2
PX1A0N3J 6I          45,817  01-13-00 11:46a px1a0n3j.6i
PX1A0N3J BAT            461  01-13-00 11:37a px1a0n3j.bat
PX1A0~24 TXT         42,131  01-13-00 12:22p px1a0n3j.elem_aqu.txt
PX1A0~26 TXT         39,522  01-13-00 12:22p px1a0n3j.elem_min.txt
PX1A0~28 TXT         39,535  01-13-00 12:22p px1a0n3j.elem_tot.txt
```

```
PX2_0_2J BAT          2,369  01-26-00  7:17p px2_0_2j.bat
PX2_0_3J BAT          1,422  01-28-00 10:05a px2_0_3j.bat
PX2_0A2J BAT          1,500  01-26-00  7:12p px2_0a2j.bat
PX2_0O2J BAT          1,200  01-15-00  9:11a px2_0o2j.bat
PX2A0A2J 6I          44,559  01-15-00  2:18a px2a0a2j.6i
PX2A0A2J 6O       3,322,636  01-26-00  7:39p px2a0a2j.6o
PX2A0A2J BAT            822  02-02-00  8:40a px2a0a2j.bat
PX2A0A2J BIN     23,901,720  01-26-00  7:39p px2a0a2j.bin
PX2A~126 TXT         27,501  01-26-00  7:39p px2a0a2j.elem_aqu.txt
PX2A~128 TXT         25,804  01-26-00  7:39p px2a0a2j.elem_min.txt
PX2A~130 TXT         25,817  01-26-00  7:39p px2a0a2j.elem_tot.txt
PX2A~132 TXT         64,019  01-26-00  7:39p px2a0a2j.min_info.txt
PX2A0A3J 6I          44,712  01-14-00  1:52p px2a0a3j.6i
PX2A0A3J 6O       8,187,921  01-28-00 11:07a px2a0a3j.6o
PX2A0A3J BAT            586  01-14-00  1:20p px2a0a3j.bat
PX2A0A3J BIN     89,205,368  01-28-00 11:07a px2a0a3j.bin
PX2A~428 TXT         61,381  01-28-00 11:07a px2a0a3j.elem_aqu.txt
PX2A~430 TXT         57,572  01-28-00 11:07a px2a0a3j.elem_min.txt
PX2A~432 TXT         57,585  01-28-00 11:07a px2a0a3j.elem_tot.txt
PX2A~434 TXT        146,883  01-28-00 11:07a px2a0a3j.min_info.txt
PX2A0O2J 6I          46,955  01-15-00  9:01a px2a0o2j.6i
PX2A0O2J 6O       3,932,373  01-26-00  9:09p px2a0o2j.6o
PX2A0O2J BIN     30,083,192  01-26-00  9:09p px2a0o2j.bin
PX2A~542 TXT         36,356  01-26-00  9:09p px2a0o2j.elem_aqu.txt
PX2A~544 TXT         34,107  01-26-00  9:09p px2a0o2j.elem_min.txt
PX2A~546 TXT         34,120  01-26-00  9:09p px2a0o2j.elem_tot.txt
PX2A~548 TXT         99,717  01-26-00  9:09p px2a0o2j.min_info.txt
PX2A0O2J ZIP     26,614,169  04-13-00  9:50a Px2a0o2j.zip
PX2A0O3J 6I          46,807  01-14-00  2:06a px2a0o3j.6i
PX2A0O3J 6O       8,261,944  01-28-00 12:12p px2a0o3j.6o
PX2A0O3J BAT            520  01-13-00  2:25p px2a0o3j.bat
PX2A~662 TXT         69,466  01-28-00 12:12p px2a0o3j.elem_aqu.txt
PX2A~664 TXT         65,153  01-28-00 12:12p px2a0o3j.elem_min.txt
PX2A~666 TXT         65,166  01-28-00 12:12p px2a0o3j.elem_tot.txt
PX2A~668 TXT        187,457  01-28-00 12:12p px2a0o3j.min_info.txt
PX2C0A2J 6I          44,559  01-15-00  3:26a px2c0a2j.6i
PX2C0A2J 6O       3,409,309  01-26-00  8:44p px2c0a2j.6o
PX2C0A2J BAT            669  01-15-00  3:27a px2c0a2j.bat
PX2C~686 TXT         27,886  01-26-00  8:44p px2c0a2j.elem_aqu.txt
PX2C~688 TXT         26,165  01-26-00  8:44p px2c0a2j.elem_min.txt
PX2C~690 TXT         26,178  01-26-00  8:44p px2c0a2j.elem_tot.txt
PX2C~692 TXT         65,355  01-26-00  8:44p px2c0a2j.min_info.txt
PX2N0O3J 6I          46,971  01-14-00  2:05a px2n0o3j.6i
PX2N0O3J 6O       7,799,758  01-28-00  1:11p px2n0o3j.6o
PX2N0O3J BAT            584  01-14-00  2:10a px2n0o3j.bat
PX2N~724 TXT         63,306  01-28-00  1:10p px2n0o3j.elem_aqu.txt
PX2N~726 TXT         59,377  01-28-00  1:10p px2n0o3j.elem_min.txt
PX2N~728 TXT         59,390  01-28-00  1:10p px2n0o3j.elem_tot.txt
PX2N~730 TXT        167,783  01-28-00  1:10p px2n0o3j.min_info.txt
PX2S0A2J 6I          44,559  01-15-00  2:17a px2s0a2j.6i
PX2S0A2J 6O       3,638,919  01-26-00  8:02p px2s0a2j.6o
PX2S~748 TXT         30,196  01-26-00  8:02p px2s0a2j.elem_aqu.txt
PX2S~750 TXT         28,331  01-26-00  8:02p px2s0a2j.elem_min.txt
PX2S~752 TXT         28,344  01-26-00  8:02p px2s0a2j.elem_tot.txt
PX2S~754 TXT         69,385  01-26-00  8:02p px2s0a2j.min_info.txt
PX2S0O2J 6I          47,194  01-15-00  9:05a px2s0o2j.6i
PX2S0O2J 6O       4,192,030  01-26-00  9:36p px2s0o2j.6o
PX2S~774 TXT         39,051  01-26-00  9:35p px2s0o2j.elem_aqu.txt
PX2S~776 TXT         36,634  01-26-00  9:35p px2s0o2j.elem_min.txt
```

```
PX2S~778 TXT        36,647  01-26-00  9:35p px2s0o2j.elem_tot.txt
PX2S~780 TXT       107,751  01-26-00  9:35p px2s0o2j.min_info.txt
PX2U0A2J 6I         44,559  01-15-00  2:17a px2u0a2j.6i
PX2U0A2J 6O      3,328,453  01-26-00  8:22p px2u0a2j.6o
PX2U~796 TXT        27,501  01-26-00  8:22p px2u0a2j.elem_aqu.txt
PX2U~798 TXT        25,804  01-26-00  8:22p px2u0a2j.elem_min.txt
PX2U~800 TXT        25,817  01-26-00  8:22p px2u0a2j.elem_tot.txt
PX2U~802 TXT        63,105  01-26-00  8:22p px2u0a2j.min_info.txt
PX2U0O2J 6I         47,120  01-15-00  8:59a px2u0o2j.6i
PX2U0O2J 6O      4,077,560  01-26-00 10:02p px2u0o2j.6o
PX2U0O2J BIN    31,127,280  01-26-00 10:02p px2u0o2j.bin
PX2U~914 TXT        37,511  01-26-00 10:02p px2u0o2j.elem_aqu.txt
PX2U~916 TXT        35,190  01-26-00 10:02p px2u0o2j.elem_min.txt
PX2U~918 TXT        35,203  01-26-00 10:02p px2u0o2j.elem_tot.txt
PX2U~920 TXT       103,967  01-26-00 10:02p px2u0o2j.min_info.txt
PX2U0O3J 6I         46,972  01-14-00 12:05p px2u0o3j.6i
PX2U0O3J 6O      7,969,066  01-28-00  2:11p px2u0o3j.6o
PX2U0O3J BAT           581  01-14-00 12:05p px2u0o3j.bat
PX2U~952 TXT        65,231  01-28-00  2:11p px2u0o3j.elem_aqu.txt
PX2U~954 TXT        61,182  01-28-00  2:11p px2u0o3j.elem_min.txt
PX2U~956 TXT        61,195  01-28-00  2:11p px2u0o3j.elem_tot.txt
PX2U~958 TXT       179,629  01-28-00  2:11p px2u0o3j.min_info.txt
SURFAREA       <DIR>        08-16-00  4:26p SurfArea
        93 file(s)    262,509,316 bytes

Directory of puextnew2\Case 1,2,4,5\SurfArea

PX2A0A!J 6I         44,874  02-01-00  8:35p px2a0a!j.6i
PX2A0A!J 6O      3,639,388  02-02-00  1:47p px2a0a!j.6o
PX2A0A!J BAT           821  02-01-00  8:38p px2a0a!j.bat
PX2A0A!J BIN    31,985,696  02-02-00  1:47p px2a0a!j.bin
PX2A~118 TXT        29,426  02-02-00  1:47p px2a0a!j.elem_aqu.txt
PX2A~120 TXT        27,609  02-02-00  1:47p px2a0a!j.elem_min.txt
PX2A~122 TXT        27,622  02-02-00  1:47p px2a0a!j.elem_tot.txt
PX2A~124 TXT        67,457  02-02-00  1:47p px2a0a!j.min_info.txt
PX2A~128 BAT         1,112  02-02-00 12:52p px2a0a0-!j.bat
PX2A0A0J 6I         44,699  02-02-00  9:10a px2a0a0j.6i
PX2A0A0J 6O      6,331,990  02-02-00  3:18p px2a0a0j.6o
PX2A0A0J BAT           819  02-02-00  7:57a px2a0a0j.bat
PX2A0A0J BIN    89,193,992  02-02-00  3:18p px2a0a0j.bin
PX2A~416 TXT        41,361  02-02-00  3:18p px2a0a0j.elem_aqu.txt
PX2A~418 TXT        38,800  02-02-00  3:18p px2a0a0j.elem_min.txt
PX2A~420 TXT        38,813  02-02-00  3:18p px2a0a0j.elem_tot.txt
PX2A~422 TXT        97,307  02-02-00  3:18p px2a0a0j.min_info.txt
        17 file(s)    131,611,786 bytes

Directory of puextnew2\Case 3

ELEM0A~6 A          18,336  12-05-99  6:43a elem0aqu.bin.a
ELEM0A~8 A_1        38,868  01-26-00 12:08p elem0aqu.bin.a_1222
ELEM0~12 S          18,336  12-05-99  6:59a elem0aqu.bin.s
ELEM0~14 S_1        40,992  01-26-00  1:02p elem0aqu.bin.s_1222
ELEM0~16 U          16,684  12-05-99  7:15a elem0aqu.bin.u
ELEM0~18 U_1        40,284  01-26-00  2:00p elem0aqu.bin.u_1222
PEN1231O 6I         43,911  07-31-99  7:18p peN1231o.6i
PET1231A 6I         40,737  12-04-99 10:41p peT1231A.6i
PT0A0A2_ 6I         41,538  12-05-99  1:53p pt0a0a2_.6i
PT1_0A2  BAT           777  12-05-99 10:37p pt1_0a2.bat
PT1_0N2  BAT           777  12-05-99 10:39p pt1_0n2.bat
```

```
PT1_1A2  BAT         1,000  01-26-00  2:00p pt1_1a2.bat
PT1A0_3  BAT           615  12-07-99  9:33p pt1a0_3.bat
PT1A0A2_ 6I         41,787  12-05-99  7:53p pt1a0a2_.6i
PT1A0~36 TXT        19,031  12-05-99  8:15p pt1a0a2_.elem_aqu.txt
PT1A0~38 TXT        17,862  12-05-99  8:15p pt1a0a2_.elem_min.txt
PT1A0~40 TXT        17,875  12-05-99  8:15p pt1a0a2_.elem_tot.txt
PT1A0A2J 6I         44,547  12-13-99 12:12p pt1a0a2j.6i
PT1A0A2J BAT           406  12-13-99 12:14p pt1a0a2j.bat
PT1A0~46 TXT        19,416  12-13-99 12:28p pt1a0a2j.elem_aqu.txt
PT1A0~48 TXT        18,223  12-13-99 12:28p pt1a0a2j.elem_min.txt
PT1A0~50 TXT        18,236  12-13-99 12:28p pt1a0a2j.elem_tot.txt
PT1A0A2S 6I         42,267  12-07-99  4:48p pt1a0a2S.6i
PT1A0A2S BAT           475  12-07-99  4:52p Pt1a0a2S.bat
PT1A0~56 TXT        26,731  12-07-99  5:33p pt1a0a2S.elem_aqu.txt
PT1A0~58 TXT        25,082  12-07-99  5:33p pt1a0a2S.elem_min.txt
PT1A0~60 TXT        25,095  12-07-99  5:33p pt1a0a2S.elem_tot.txt
PT1A0A3_ 6I         41,935  12-07-99  9:27p pt1a0a3_.6i
PT1A0~64 TXT        32,891  12-07-99 10:28p pt1a0a3_.elem_aqu.txt
PT1A0~66 TXT        30,858  12-07-99 10:28p pt1a0a3_.elem_min.txt
PT1A0~70 TXT        30,871  12-07-99 10:28p pt1a0a3_.elem_tot.txt
PT1A0A6  BAT           403  12-13-99 10:22a pt1a0a6.bat
PT1A0A6_ 6I         42,089  12-10-99  4:47p pt1a0a6_.6i
PT1A0~76 TXT        37,511  12-10-99  5:16p pt1a0a6_.elem_aqu.txt
PT1A0~78 TXT        35,190  12-10-99  5:16p pt1a0a6_.elem_min.txt
PT1A0~80 TXT        35,203  12-10-99  5:16p pt1a0a6_.elem_tot.txt
PT1A0A7  BAT           420  12-13-99 10:21a pt1a0a7.bat
PT1A0A7_ 6I         42,163  12-13-99 10:18a pt1a0a7_.6i
PT1A0~86 TXT        66,771  12-13-99 11:37a pt1a0a7_.elem_aqu.txt
PT1A0~88 TXT        62,626  12-13-99 11:37a pt1a0a7_.elem_min.txt
PT1A0~90 TXT        62,639  12-13-99 11:37a pt1a0a7_.elem_tot.txt
PT1A0N2! 6I         43,263  01-03-00 11:50a pt1a0n2!.6i
PT1A0N2! BAT         1,007  01-03-00 11:45a pt1a0n2!.bat
PT1A0~96 TXT        25,191  01-03-00 12:07p pt1a0n2!.elem_aqu.txt
PT1A0~98 TXT        23,638  01-03-00 12:07p pt1a0n2!.elem_min.txt
PT1A~100 TXT        23,651  01-03-00 12:07p pt1a0n2!.elem_tot.txt
PT1A0N2_ 6I         42,897  12-05-99 10:43p pt1a0n2_.6i
PT1A~104 TXT        27,116  12-05-99 11:06p pt1a0n2_.elem_aqu.txt
PT1A~106 TXT        25,443  12-05-99 11:06p pt1a0n2_.elem_min.txt
PT1A~108 TXT        25,456  12-05-99 11:06p pt1a0n2_.elem_tot.txt
PT1A0N3! 6I         43,533  01-03-00  5:45p pt1a0n3!.6i
PT1A0N3! BAT           475  01-03-00  4:18p pt1a0n3!.bat
PT1A~116 TXT        39,821  01-03-00  6:55p pt1a0n3!.elem_aqu.txt
PT1A~118 TXT        37,356  01-03-00  6:55p pt1a0n3!.elem_min.txt
PT1A~120 TXT        37,369  01-03-00  6:55p pt1a0n3!.elem_tot.txt
PT1A0N3_ 6I         43,045  12-07-99  9:29p pt1a0n3_.6i
PT1A~124 TXT        46,366  12-07-99 10:07p pt1a0n3_.elem_aqu.txt
PT1A~126 TXT        43,493  12-07-99 10:07p pt1a0n3_.elem_min.txt
PT1A~130 TXT        43,506  12-07-99 10:07p pt1a0n3_.elem_tot.txt
PT1A0N3K 6I         45,817  12-21-99  3:45p pt1a0n3K.6i
PT1A0N3K BAT           531  12-21-99  2:37p pt1a0n3K.bat
PT1A~136 TXT        67,156  12-21-99  3:35p pt1a0n3K.elem_aqu.txt
PT1A~138 TXT        62,987  12-21-99  3:35p pt1a0n3K.elem_min.txt
PT1A~140 TXT        63,000  12-21-99  3:35p pt1a0n3K.elem_tot.txt
PT1A0O2  BAT           498  12-10-99  4:51p pt1a0o2.bat
PT1A0O2_ 6I         43,051  12-10-99  4:41p pt1a0o2_.6i
PT1A~146 TXT        25,576  12-10-99  4:27p pt1a0o2_.elem_aqu.txt
PT1A~148 TXT        23,999  12-10-99  4:27p pt1a0o2_.elem_min.txt
PT1A~150 TXT        24,012  12-10-99  4:27p pt1a0o2_.elem_tot.txt
PT1A1A2_ 6I         41,888  12-07-99  1:14p pt1a1a2_.6i
```

```
PT1A1A2_ 6O       1,743,863  01-26-00  2:13p pt1a1a2_.6o
PT1A1A2_ BIN      9,271,096  01-26-00  2:13p pt1a1a2_.bin
PT1A~190 TXT         15,566  01-26-00  2:13p pt1a1a2_.elem_aqu.txt
PT1A~192 TXT         14,613  01-26-00  2:13p pt1a1a2_.elem_min.txt
PT1A~194 TXT         14,626  01-26-00  2:13p pt1a1a2_.elem_tot.txt
PT1A~196 TXT         33,669  01-26-00  2:13p pt1a1a2_.min_info.txt
PT1A1N2  &BA            362  01-26-00  3:38p PT1A1N2.&BA
PT1A1N2  BAT            415  01-26-00  3:38p pt1a1n2.bat
PT1A1N2_ 6I          42,972  12-07-99  8:47p pt1a1n2_.6i
PT1A1N2_ 6O       2,524,406  01-26-00  3:55p pt1a1n2_.6o
PT1A1N2_ BIN     16,975,160  01-26-00  3:55p pt1a1n2_.bin
PT1A~266 TXT         23,266  01-26-00  3:55p pt1a1n2_.elem_aqu.txt
PT1A~268 TXT         21,833  01-26-00  3:55p pt1a1n2_.elem_min.txt
PT1A~270 TXT         21,846  01-26-00  3:55p pt1a1n2_.elem_tot.txt
PT1A~272 TXT         57,741  01-26-00  3:55p pt1a1n2_.min_info.txt
PT1N0A2_ 6I          41,787  12-05-99  7:53p pt1n0a2_.6i
PT1N0A2_ BAT            509  12-09-99  1:34p Pt1n0a2_.bat
PT1S0A2_ 6I          41,880  12-05-99  7:55p pt1s0a2_.6i
PT1S~280 TXT         18,646  12-05-99  8:26p pt1s0a2_.elem_aqu.txt
PT1S~282 TXT         17,501  12-05-99  8:26p pt1s0a2_.elem_min.txt
PT1S~284 TXT         17,514  12-05-99  8:26p pt1s0a2_.elem_tot.txt
PT1S0N2! 6I          43,337  01-03-00 11:48a pt1s0n2!.6i
PT1S~288 TXT         22,881  01-03-00 12:25p pt1s0n2!.elem_aqu.txt
PT1S~290 TXT         21,472  01-03-00 12:25p pt1s0n2!.elem_min.txt
PT1S~292 TXT         21,485  01-03-00 12:25p pt1s0n2!.elem_tot.txt
PT1S0N2_ 6I          42,971  12-05-99 10:45p pt1s0n2_.6i
PT1S~296 TXT         25,576  12-05-99 11:25p pt1s0n2_.elem_aqu.txt
PT1S~298 TXT         23,999  12-05-99 11:25p pt1s0n2_.elem_min.txt
PT1S~300 TXT         24,012  12-05-99 11:25p pt1s0n2_.elem_tot.txt
PT1S1A2_ 6I          41,981  12-07-99  1:15p pt1s1a2_.6i
PT1S1A2_ 6O       1,797,841  01-26-00  2:28p pt1s1a2_.6o
PT1S~312 TXT         15,566  01-26-00  2:28p pt1s1a2_.elem_aqu.txt
PT1S~314 TXT         14,613  01-26-00  2:28p pt1s1a2_.elem_min.txt
PT1S~316 TXT         14,626  01-26-00  2:28p pt1s1a2_.elem_tot.txt
PT1S~318 TXT         34,173  01-26-00  2:28p pt1s1a2_.min_info.txt
PT1U0A2_ 6I          41,880  12-05-99  7:56p pt1u0a2_.6i
PT1U~322 TXT         16,721  12-05-99  8:36p pt1u0a2_.elem_aqu.txt
PT1U~324 TXT         15,696  12-05-99  8:36p pt1u0a2_.elem_min.txt
PT1U~326 TXT         15,709  12-05-99  8:36p pt1u0a2_.elem_tot.txt
PT1U0N2! 6I          43,337  01-03-00 11:49a pt1u0n2!.6i
PT1U~330 TXT         22,881  01-03-00 12:41p pt1u0n2!.elem_aqu.txt
PT1U~332 TXT         21,472  01-03-00 12:41p pt1u0n2!.elem_min.txt
PT1U~336 TXT         21,485  01-03-00 12:41p pt1u0n2!.elem_tot.txt
PT1U0N2_ 6I          42,971  12-05-99 10:46p pt1u0n2_.6i
PT1U~340 TXT         23,651  12-05-99 11:43p pt1u0n2_.elem_aqu.txt
PT1U~342 TXT         22,194  12-05-99 11:43p pt1u0n2_.elem_min.txt
PT1U~344 TXT         22,207  12-05-99 11:43p pt1u0n2_.elem_tot.txt
PT1U0N3  BAT            441  12-08-99  4:10a pt1u0n3.bat
PT1U0N3_ 6I          42,009  12-08-99  4:09a pt1u0n3_.6i
PT1U~350 TXT         30,581  12-08-99  4:31a pt1u0n3_.elem_aqu.txt
PT1U~352 TXT         28,692  12-08-99  4:31a pt1u0n3_.elem_min.txt
PT1U~354 TXT         28,705  12-08-99  4:31a pt1u0n3_.elem_tot.txt
PT1U1A2_ 6I          42,002  12-07-99  1:17p pt1u1a2_.6i
PT1U1A2_ 6O       1,834,409  01-26-00  2:39p pt1u1a2_.6o
PT1U~366 TXT         16,336  01-26-00  2:39p pt1u1a2_.elem_aqu.txt
PT1U~368 TXT         15,335  01-26-00  2:39p pt1u1a2_.elem_min.txt
PT1U~370 TXT         15,348  01-26-00  2:39p pt1u1a2_.elem_tot.txt
PT1U~372 TXT         35,981  01-26-00  2:39p pt1u1a2_.min_info.txt
       128 file(s)     37,556,446 bytes
```

```
Directory of puextnew2\Case 6

DECAYE~6 241            10  01-25-00 11:23a decay.eq6.24100
ELEM0A~8 AWD        14,088  02-02-00 11:11a elem0aqu.bin.awd
PX2ADO3J 6I         46,955  01-15-00  6:04p px2ado3j.6i
PX2ADO3J 6O      8,151,999  02-02-00  3:11p px2ado3j.6o
PX2ADO3J BAT          757  02-02-00 11:00a px2ado3j.bat
PX2ADO3J BIN    89,167,912  02-02-00  3:09p px2ado3j.bin
PX2A~302 TXT        67,926  02-02-00  3:09p px2ado3j.elem_aqu.txt
PX2A~304 TXT        63,709  02-02-00  3:09p px2ado3j.elem_min.txt
PX2A~306 TXT        63,722  02-02-00  3:09p px2ado3j.elem_tot.txt
PX2A~308 TXT       182,890  02-02-00  3:09p px2ado3j.min_info.txt
        10 file(s)     97,759,968 bytes

Directory of puextnew2\Case 7

DECAYE~6 241            10  01-25-00 11:23a decay.eq6.24100
ELEM0A~8 AW2        21,640  01-30-00 10:03a elem0aqu.bin.aw2H
ELEM0~10 AW2        21,404  01-30-00 12:17p elem0aqu.bin.aw2L
ELEM0~12 AW2        17,628  01-31-00  7:11p elem0aqu.bin.aw2S
PW2A123S 6I         42,868  01-17-00  4:08p pw2a123S.6i
PW2A123S BAT           986  01-17-00  4:13p PW2a123S.bat
PX2-4~18 BAT         1,377  01-31-00  6:52p px2-4asa3j.bat
PX2A0A3J 6I         44,712  01-14-00  1:52p px2a0a3j.6i
PX2AH~22 BAT         1,677  01-30-00 12:24p px2aH-L_3j.bat
PX2AH~24 BAT         1,007  01-30-00 12:21p px2aH-La3j.bat
PX2AHA3J 6I         44,862  01-16-00  2:33p px2aHa3j.6i
PX2AHA3J 6O      7,984,095  01-30-00  2:13p px2aha3j.6o
PX2AH~54 TXT        60,996  01-30-00  2:13p px2aHa3j.elem_aqu.txt
PX2AH~56 TXT        57,211  01-30-00  2:13p px2aHa3j.elem_min.txt
PX2AH~58 TXT        57,224  01-30-00  2:13p px2aHa3j.elem_tot.txt
PX2AH~60 TXT       142,557  01-30-00  2:13p px2aHa3j.min_info.txt
PX2AHO3J 6I         47,030  01-16-00  6:55p px2aHo3j.6i
PX2AHO3J 6O      6,740,116  01-30-00  3:01p px2aho3j.6o
PX2AHO3J BAT           718  01-16-00  6:56p px2aHo3j.bat
PX2AH~88 TXT        56,376  01-30-00  3:01p px2aHo3j.elem_aqu.txt
PX2AH~90 TXT        52,879  01-30-00  3:01p px2aHo3j.elem_min.txt
PX2AH~92 TXT        52,892  01-30-00  3:01p px2aHo3j.elem_tot.txt
PX2AH~94 TXT       150,879  01-30-00  3:01p px2aHo3j.min_info.txt
PX2ALA3J 6I         44,862  01-16-00  2:35p px2aLa3j.6i
PX2ALA3J 6O      8,036,248  01-30-00  1:19p px2ala3j.6o
PX2A~124 TXT        61,381  01-30-00  1:18p px2aLa3j.elem_aqu.txt
PX2A~126 TXT        57,572  01-30-00  1:18p px2aLa3j.elem_min.txt
PX2A~130 TXT        57,585  01-30-00  1:18p px2aLa3j.elem_tot.txt
PX2A~132 TXT       146,919  01-30-00  1:18p px2aLa3j.min_info.txt
PX2ALO3J 6I         46,957  01-16-00  6:05p px2aLo3j.6i
PX2ALO3J 6O      6,559,681  01-30-00  3:52p px2alo3j.6o
PX2ALO3J BAT           718  01-16-00  5:05p px2aLo3j.bat
PX2A~160 TXT        55,606  01-30-00  3:52p px2aLo3j.elem_aqu.txt
PX2A~162 TXT        52,157  01-30-00  3:52p px2aLo3j.elem_min.txt
PX2A~164 TXT        52,170  01-30-00  3:52p px2aLo3j.elem_tot.txt
PX2A~166 TXT       147,629  01-30-00  3:52p px2aLo3j.min_info.txt
PX2ASA3J 6I         45,308  01-18-00  7:51a px2aSa3j.6i
PX2ASA3J 6O      5,757,963  01-31-00  9:35p px2asa3j.6o
PX2ASA3J BAT           733  01-17-00  5:10p px2aSa3j.bat
PX2A~192 TXT        37,896  01-31-00  9:35p px2aSa3j.elem_aqu.txt
PX2A~194 TXT        35,551  01-31-00  9:35p px2aSa3j.elem_min.txt
PX2A~196 TXT        35,564  01-31-00  9:35p px2aSa3j.elem_tot.txt
```

```
PX2A~198 TXT        88,574  01-31-00  9:35p px2aSa3j.min_info.txt
PX3ASA3J 6I         46,837  01-18-00  9:43a Px3aSa3j.6i
PX3ASA3J 6O      4,929,364  01-31-00 10:35p px3asa3j.6o
PX3ASA3J BAT           795  01-18-00  9:58a px3aSa3j.bat
PX3A~220 TXT        29,426  01-31-00 10:35p px3aSa3j.elem_aqu.txt
PX3A~222 TXT        27,609  01-31-00 10:35p px3aSa3j.elem_min.txt
PX3A~224 TXT        27,622  01-31-00 10:35p px3aSa3j.elem_tot.txt
PX3A~226 TXT        44,916  01-31-00 10:35p px3aSa3j.min_info.txt
PX4ASA3J 6I         47,461  01-18-00 11:49a px4asa3j.6i
PX4ASA3J 6O      5,125,493  01-31-00 11:16p px4asa3j.6o
PX4ASA3J BAT           824  01-18-00 11:48a px4asa3j.bat
PX4A~250 TXT        29,811  01-31-00 11:16p px4aSa3j.elem_aqu.txt
PX4A~252 TXT        27,970  01-31-00 11:16p px4aSa3j.elem_min.txt
PX4A~254 TXT        27,983  01-31-00 11:16p px4aSa3j.elem_tot.txt
PX4A~256 TXT        55,626  01-31-00 11:16p px4aSa3j.min_info.txt
        57 file(s)     47,343,955 bytes

Total files listed:
305 file(s)    576,781,471 bytes
15 dir(s)
```

MOL.20010116.0004 MB010116/2

OFFICE OF CIVILIAN RADIOACTIVE WASTE MANAGEMENT
SPECIAL INSTRUCTION SHEET

1. QA: QA

Page: 1 of: 2

10.16.00

Complete Only Applicable Items

This is a placeholder page for records that cannot be scanned or microfilmed

2. Record Date	3. Accession Number
09/28/2000	ATT-TO MOL.20010116.0008
4. Author Name(s)	**5. Author Organization**
HARLAN W. STOCKMAN	N/A

6. Title
IN-DRIFT ACCUMULATION OF FISSLE MATERIAL FROM WASTE PACKAGE CONTAINING PLUTONIUM DISPOSITION WASTE FORMS (ATTACHMENT II, TWO CD-ROMS)

7. Document Number(s)	8. Version
CAL-EDC-GS-000001	REV. 00
9. Document Type	**10. Medium**
DATA	CD-ROM

11. Access Control Code
PUB

12. Traceability Designator
DC #22013

13. Comments
THESE ARE SPECIAL PROCESS CD-ROMS, AND CAN BE LOCATED THROUGH THE RPC

NOTE: PER AP-17.1Q, REV.1, ICN 2. (ELECTRONIC FILES), THE ELECTRONIC INFORMATION ON THIS CD-ROM IS LOCATED AS AN ATTACHMENT TO THIS PAGE

DC# 22013

OFFICE OF CIVILIAN RADIOACTIVE WASTE MANAGEMENT
ELECTRONIC SOURCE FILE VERIFICATION

QA: N/A

2 OF 2

1. DOCUMENT TITLE:	
In-Drift Accumulation of Fissile Material from Waste Packages Containing Plutonium Disposition Waste Forms	
2. DOCUMENT IDENTIFIER: CAL-EDC-GS-000001	3. REVISION DESIGNATOR: 00

ELECTRONIC SOURCE FILE INFORMATION

4. ELECTRONIC SOURCE FILE NAME WITH FILE EXTENSION PROVIDED BY THE SOFTWARE: pu_inv_rev00.doc		
5. DATE LAST MODIFIED: 9/28/00	6. ELECTRONIC SOURCE FILE APPLICATION: (I.E., EXCEL, WORD, CORELDRAW) WORD	7. FILE SIZE IN KILOBYTES: 2,621
8. FILE LINKAGE INSTRUCTIONS/INFORMATION: The file is compressed into a self-extracting file (*.exe). Double click on file and it will expand to the location specified by the user.		
9. FILE CUSTODIAN: (I.E., DC, OR DC APPROVED CUSTODIAN) DC	10. FILE LOCATION FOR DC APPROVED CUSTODIAN (I.E., SERVER, DIRECTORY) N/A	
11. PRINTER SPECIFICATION (i. e., HP4SI) INCLUDING POSTSCRIPT INFORMATION (I.E., PRINTER DRIVER) AND PRINTING PAGE SETUP (I.E., LANDSCAPE, 11 X 17 PAPER) HP Color LaserJet 5/5M for pages 17-21, 24, 29, 40, 41, 43-46; HP LaserJet 5Si for the remaining pages		
12. COMPUTING PLATFORM USED: (I.E., SUN) Windows 95	13. OPERATING EQUIPMENT USED: (I.E., UNIX, SOLARIS) N/A	
14. ADDITIONAL HARDWARE/SOFTWARE REQUIREMENT USED TO CREATE FILE(S): N/A	15. ACCESS RESTRICTIONS: (IF ANY) N/A	

COMMENTS/SPECIAL INSTRUCTIONS

16. N/A

CERTIFICATION

17. NAME (Print and Sign) Susan LeStrange	Susan LeStrange		18. DATE: 9/28/00
19. ORGANIZATION M&O/SAIC	20. DEPARTMENT Waste Package	21. LOCATION/MAIN STOP 1032H	22. PHONE 295-5006

DC USE ONLY

23. DATE RECEIVED: 9/29/2000	24. DATE REVIEWED: 9/29/2000	25. DATE FILES TRANSFERRED: 9/29/2000
26. NAME (Print and Sign): Teri McCoy		27. DATE: 10/13/2000